NOVEL GLAZING TECHNOLOGY FOR BUILDING ENVELOPES: evaluation of the energy performance and its influence on the thermal control

Sara Vanzo

October 2014 - March 2015

Supervisors: Dr. Andreas Schüler

Dr. André Kostro

Pr. Marco Perino

"Iniziare un nuovo cammino spaventa,

ma dopo ogni passo che percorriamo

ci rendiamo conto

di quanto fosse pericoloso rimanere fermi."

Roberto Benigni

Acknowledgments

Foremost, I would like to thank my supervisor Professor Marco Perino, that gave me the opportunity to develop abroad my master thesis.

At the same time, I would like to express my gratitude to Dr. Andreas Schüler for hosting me in the Laboratory of Solar Energy and Building Physics (LESO) at EPFL, as a project student and for the precious help during these months.

Furthermore, I'm thankful to André Kostro for introducing me to the topic, as well for the support on the way. His constructive help and his constant availability during all the period I passed in Lausanne were a key element. I am sincerely grateful to Olivia Bouvard to teach me how to manage in the laboratory and to all the colleagues at LESO for the extremely friendly atmosphere, sharing discussions, ideas and experiences together every day. They made me feel part of a team from the first day.

Special thanks to Federico for his support and trust; he has been always present in my life during these months, despite the distance.

I'm grateful to those who supported me throughout this period abroad, first of all my brother and my family.

I want also to thank Fabbri family for the hospitality they gave me at the beginning of this experience. I would like to thank Martina, Eleonora and all of my friends who encouraged me to during these years at University. Finally a thank to Monica, Francesco, Alessandro, Martina and Claudia and all the other friends of a lifetime, always ready to dedicate to me free time.

Abstract

Residential and commercial buildings currently account for almost 40% of total final energy consumption in Europe [BPIE ,2011], nearly from 20% to 60% of which is attributed to the envelope [IEA, 2013]. Moreover, both the expansion of the building sector and the global warming phenomenon are contributing to increase the energy consumption. The increase of the mean monthly temperatures and of the global horizontal irradiance has been detected in different geographical areas since the mid-twentieth century. The last decades have been marked by a global warming of the Earth with a temperature increase between 0,6°C and 0,9°C [Le Treut, 2003]. The policies to improve the energy efficiency of buildings are becoming increasingly stringent. The European Council emphasises the need to improve energy efficiency so as to achieve the objective of reducing by 20% the energy consumption by 2020. Therefore, an accurate action plan is needed, in order to promote the use of renewable energy and identify the technologies that potentially allow to reach significant energy savings. Among all the building components, fenestration systems have a relevant influence on the heating and air conditioning requirements because they are responsible for about 40% of the heat losses in a typical building envelope. The fenestration system design affects the management of solar gains, thermal losses, daylighting and glare. Consequently, an improvement in the glazing envelope efficiency can have a significant impact on the cooling and heating consumption.

The selection of the glazing envelope for a building is a critical decision, especially when the glazed area is large (more than 50% of the external walls). It can affect both the visual comfort and the energy consumption of lighting and of the heating and cooling system. The framework of this research work offers different variety of innovative technologies as solution to this problem. The insulated glass units are quite spread in the market and they can reduce cooling loads in buildings. Incorporated Grätzel cells in transparent modules could be combined with other conventional glazing in the building façade, in order to yield an aesthetic appearance and at the same time provide electricity. For the optical characterization of these glazing technologies, the experimental set up available in the Solar Energy and Building Physics Laboratory (LESO) has been used.

The last analysed glazing technology is a particular typology of Complex Fenestration System (CFS), such as embedded microstructures, that can significantly contribute to reduce the energy consumption, through the smart management of the annual thermal loads. In order to evaluate the thermal performance of this novel glazing envelope, a parametric approach has been carried out. Optical microstructures found to be a valid solution to increase energy savings up to 20%, depending on the geometric configuration of the micro-mirrors and on the location, when compared with a conventional glazing.

Contents

List of tables

List of figures

Acronyms

AM	Air Mass
ASTM	American Society for Testing and Materials
BIPV	Building Integrated Photovoltaic Market
BTDF	Bidirectional Transmission Distribution Function
CFS	Complex Fenestration System
COP	Coefficient of Performance
DSSC	Dye Sensitized Solar Cell
ELC	Energy Load Coefficient
EPA	Environmental Protection Agency
EPDM	Ethylene, Propylene, Diene Monomer
GSHP	Ground Source Heat Pump
HVAC	Heating Ventilation and Air Conditioning
IPCC	Intergovernmental Panel on Climate Change
IR	Infra Red
IUG	Insulating Glass Unit
LCP	Laser Cut Panel
NHE	Normal Hydrogen Electrode
PIB	Polyisobutylene
PMMA	Polymethylmethacrylate
PV	Photovoltaic
PVD	Physical Vapour Deposition
UHI	Urban Heat Island
UV	Ultra Violet
WMO	World Meteorological Organization
WWR	Window to Wall Ratio

1 Introduction

The present work deals with the role of the innovative glazing technology in buildings that could be an important element to improve energy efficiency from the point of view of the thermal control and of the visual comfort. The advantages that can be obtained from this strategy are first of all the possibility to have considerable energy savings during the overall year, both for heating and cooling, and secondly an improvement on the exploitation of the natural light, avoiding glare and increasing the daylight level in the indoor environment.

The final aim is to provide a set of different building design cases, discussing different innovative glazing technologies applications and their important influence on all the aspects just mentioned.

1.1 Motivation

Windows are becoming the major part of the building envelope, especially for aesthetic motivations in modern constructions, so the importance to focus on their role from the energetic point of view is growing. One of the essential parts of window is the glazing; selecting a window glazing is complicated when energy savings and daylighting aspects of a building have to be considered. The origin of this increase of attention for the energetic and visual performances of these glazed areas lies in two main necessities: the need to face global climate changes, promoting the environmental sustainability in the building design sector. On the other hand, the reduction of the energy consumption brings to an improvement of the indoor comfort of the occupants and to an economic advantage in terms of saving.

In the building sector, more energy efficient building envelopes and other low carbon and energy efficient building technologies are needed. Most of this technologies are commercially available, but are not widely deployed because of economic barriers, such as split incentives or lack of information, therefore the potential for energy efficiency improvements in buildings remains largely untapped. In fact about 20% to 60% of all energy used in buildings is affected by the design and the construction of the building envelope [*IEA, 2013*].

A deep analysis of the solar irradiance incident on the glazing surface during the year has to be set, in order to determine its influence on the thermal control system and on the daylight feature: during the winter, if windows have not a suitable insulation, the heat losses becomes quite high, while in the hot season there is the risk of overheating of the building with as consequence an increasing of the cooling demand.

Focusing on the background of the energy consumption in Switzerland, in recent years the increase of the energy consumption in most sectors occurred, for example for the heating and cooling systems and for lighting. The only sector that kept the energy consumption quite constant was the industry. From 2000 to 2013 the total energy consumption for space heating grew up of about 7,2%; for lighting the increase was of 5,2% but the most relevant percentage is related to the air conditioning and ventilation sector, with a rise of 18% [*Kemmler et al, 2013*].

In Figure 1.1 the distribution of the total energy consumption is shown referring to 2013, including the residential buildings demand and industrial one. The total consumption is dominated by the space heating (35%) and the transports (29%); however in recent years the sector of transports saw a lower increase of consumption, around +2,9% versus +7,9% of increase of space heating consumption. The lighting consumption in 2013 covered only 3% of the total energy consumption in the country [*Kemmler et al, 2013*].

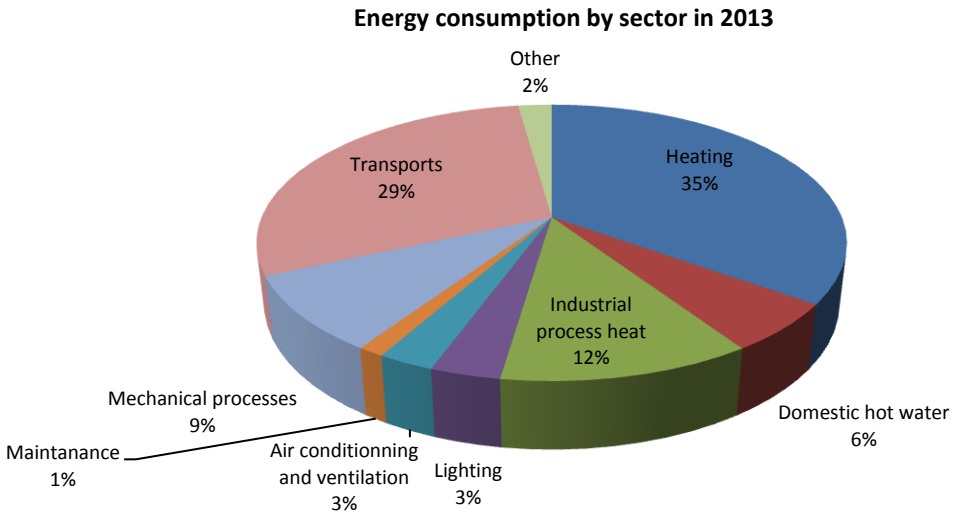

Fig. 1.1: percentages energy consumption by sector for the year 2013 in Switzerland [*Kemmler et al, 2013*].

Without considering the industrial sector, in Switzerland electric lighting, heating and air conditioning account all together for about 74,4% of total energy demand in residential and commercial buildings. Heating consumption dominates with 70,7%. Moreover, 56,6% of the overall Swiss electricity usage, is dominated by air conditioning and ventilation, followed by lighting with 24,2% and space heating with 7,3%.

Therefore, to face this relevant increase in consumption, which according to the previsions is going to grow in the future, a careful design of the buildings is required, in order to minimize the amount of heat losses in winter and the cooling demand in warm months.

Concerning residential buildings and offices, the weakest component among building envelopes are the windows. Previous studies show that a large part of the heat loss occurs through the glazed parts of the envelope. As it can be seen in Fig. 1.2, in northern climates, the heat loss related to windows can contribute over 40% of the total heat loss through the building envelope for a typical office (without considering the ventilation) [*Grynning, 2011*].

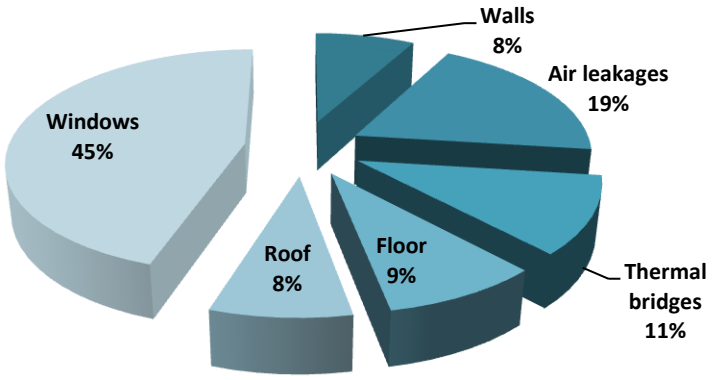

Fig. 1.2: percentage distribution of heat losses through the various building envelope parts of an office building in northern climates [*Grynning, 2011*].

Consequently, acting on the glazing envelopes of building façade is fundamental and can be effective to achieve these aims. Daylight affects lighting, heating and cooling demand of a building's energy system in a quantitative way. First, using the sun's natural light can displace indoor electric lighting during the day, but it has also potential benefits in heating and cooling applications.

1.2 Method

The presented framework in this thesis offers a series of possible solutions, not all currently available on the market, that are potentially able to improve the energy efficiency of the glazing envelope in buildings.

Different types of novel glazing technologies were analysed in this work. Firstly, the insulated glass units, quite spread on the market. Then, the dye sensitized solar cells, that, being a typology of photovoltaic panel, can partially provide electricity to the building. Concerning these glazing envelopes, the optical and energetic characterization of the modules was performed in the laboratory. Finally, a particular kind of Complex Fenestration System has been studied. It consists in an embedded microstructured polymer film, that allows the clear view towards the external ambient. Both the daylighting ant the thermal comfort can be improved using this complex fenestration system. The potential of this device is manifold because it could also ensure reduced energy consumption of the building. The second part of this thesis focuses on this thermal aspect, considering the possible energy savings that can be achieved using this novel technology. In order to perform this evaluation, several parametric studies have been carried out. The use of a suitable program that allows to perform simulations was necessary.

The evaluations on the glazing envelopes allow to assess the thermal performance of the device and to predict their potential success in the building sector, especially if the technology is not available in the market yet.

1.3 Thesis overview

Chapter 2 presents further context for the state of the art of novel glazing envelope technologies, on which the thesis is focused. It includes the description of the principle of operation of the device, the current availability and applications of the technology and an overview on the future perspectives.

Then, chapter 3 concerns the optical and thermal characterization of some insulated glass units and dye sensitized solar cells modules. The experiments were carried out in the Solar Energy and Building Physics Laboratory (LESO) at École Polytechnique Fédérale de Lausanne (EPFL). Firstly an overview on the optical and thermal properties of the glazing is presented. Secondly the description of the experimental set up and results are discussed.

After chapter 3, all the others analyse the novel glazing envelope technology, such as embedded microstructures. Chapter 4 is focused on the approach and research framework developed for evaluating and assessing the thermal performance of the studied Complex Fenestration System (CFS). It contains the motivation, the method, the hypothesis and the input data on which the parametric studies are based.

Concerning chapter 5, it contains the optimization of the geometric configuration of the embedded microstructures, depending on the location. Then, the thermal performance of the CFS have been analysed at different range of latitudes, maintaining the same building characteristics.

Chapter 6 is about the second parametric study, that presents the analysis of the microstructured glass performance, varying the geometric and thermal characteristics of the building.

Finally, chapter 7 contains the conclusions of the work. A summary of the achievements and the possible future developments are presented.

2 State of the art

In this chapter a general overview on the state of the art in the field of the novel glazing technology for building envelopes is presented. The initial part is about the most widespread installation of windows, that are the insulating glass units (IGU); then other particular solutions for the improvement of the performance of the glazed façades are discussed, such as Grätzel cell technology and the complex fenestration system applications. Usually windows are the cause of about 30% - 50% of the heat transmission losses through the building envelopes; improving the energetic performance of fenestration could save a significant amount of energy.

2.1 Insulating glass units IGU

The priority to reduce energy use and carbon emissions in the building and construction sector lead to the increase of the thermal performance of their envelopes. One of the way to reach this goal is to focus on the thermal transmittance (U-value) of the windows, in order to reduce the thermal losses, improving the insulation of the entire system. For example, in cold climates the aim should be to minimize heat transfer through the glazing, in order to reduce the heating demand and optimize the thermal comfort. This need leads to the study of better performed materials for the construction of windows, such as gas fillings, spacers or low emissivity coatings.

2.1.1 Physical structure and properties

The insulating glasses (IGU) are prefabricated units made of at least two glass panes (sometimes three) separated by dry air or an inert gas (such argon, krypton, xenon) to reduce the heat transfer between the outdoor and the indoor environment. Moreover, a large air space or the use of sulphur hexafluoride can improve the noise insulation quality, that is able to save from the exterior acoustic pollution.

The long term stability of the insulating glass unit is determined by the quality of the edge seal. The key function of the edge seal is to keep the glass panes separated at equal distances while providing a barrier to prevent infiltration of water vapour or exfiltration of air or gas fill between the panes. As it can be seen in Figure 2.1, the edge seal total width (w) varies from 8 to 12 *mm* and the thickness of the space between the panes (t) depends on the number of glass panes, the types of gas fill and the acoustical requirements [*Van Den Bergh at al., 2013*]:

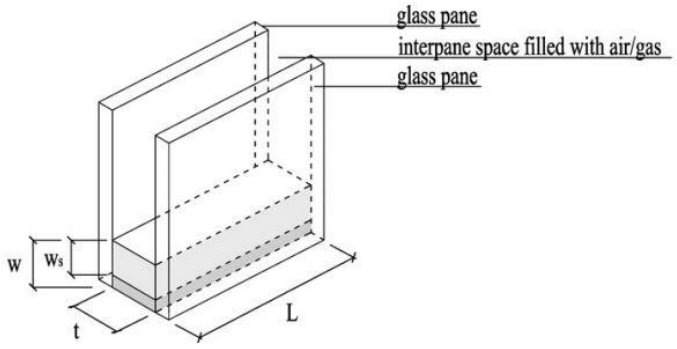

Fig. 2.1: edge seal geometry of a double IGU with edge seal thickness t, width w, spacer bar width w_s and length L [*Van Den Bergh at al., 2013*].

The components including the edge seal are [*Van Den Bergh at al., 2013*]:

a) the spacer bar: it holds the glass panes at a fixed distance from each other, establishing the size of the interpane space;

b) the sealant: it bonds the glass panes and spacer bar together while providing an high level of moisture vapour and gas diffusion resistance. There are two possible configurations: in dual sealed IG units both the primary and the secondary sealant contributes to perform this functions, while in the single sealed IG there is only the secondary sealant. Today the majority of IG units manufactured globally are dual sealed. In Figure 2.2 it is shown that the primary sealant, made of synthetic rubbers such as polyisobutylene (PIB), is applied between the spacer bar and the glass pane because its goal is to reduce water vapour and gas permeability through the glass area; the PIB only cannot guarantee the structural integrity of the IG because the strength of this material decreases rapidly with the increase of temperature, so a secondary sealant in silicone or polyurethane is required, that is applied around the perimeter of the glass;

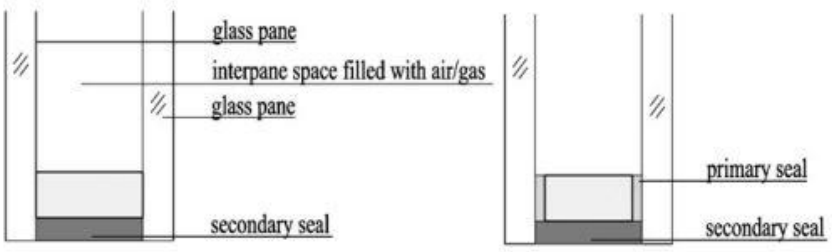

Fig. 2.2: single sealed IG unit (left) and double sealed IG unit (right) [*Van Den Bergh at al., 2013*].

c) the desiccant: it's used to prevent the inside glass surfaces from condensation of moisture vapour that may be in the interpane space. There are different ways in which moisture can be trapped in the inner space: during the manufacturing of the IG unit or during its use it can happen that some vapour permeate through the edge. Desiccant prolongs the window's service life by absorbing moisture and organic vapour. In the glass structure it's placed in integration with the edge seal design or as a fill in hollow spacer bars, that are perforated to allow the contact between the desiccant fill and the vapour. Commonly used desiccants in the IG industry are molecular sieves or a blend of a silica gel with molecular sieves [*Wolf, 1992*].

Concerning the service life, good properties for IG units are that the primary sealant must maintain its low gas and vapour permeability and the secondary sealant must preserve good adhesion when exposed to many external factors. IGU are exposed to different environmental factors, such as temperature and atmospheric pressure fluctuations, sunlight, wind loads, working loads and water that exert a negative influence on their life expectancy. During service, the edge seal is exposed to a microclimate and therefore it must have this following properties, all inversely proportional to the early degradation of the materials [*Wolf, 1992*]:

a) durability, i.e. the resistance against meteorological phenomena;
b) structural strength;
c) low moisture and gas permeability.

Improving edge seal thermal performance will significantly reduce the negative influence on the overall window U-value, that has to be as low as possible, in order to make the window well-insulated, reducing also the effect of thermal bridges.

2.1.2 Current technology and applications

Concerning the spacer bars, the current trend is the replacement of the traditional metal spacers, that having an high thermal conductivity, created a significant risk of condensation and a high heat flow through the edge of glass region with spacer bars made from non-metallic and low conductivity materials. Although the main structure of these latter is non-metallic, a metallized foil is often incorporated to ensure that the seal has low water vapour and gas permeability. The non-metal spacers are divided in three subgroups:

a) composite spacers: are constructed from several components such as highly insulated composite plastic or a flexible stabilizer, a moisture barrier membrane and a desiccant coating;
b) structural foam spacers: such a silicone foam or EPDM (ethylene, propylene, diene monomer);
c) thermoplastic spacers: made of PIB with integrated desiccant and it is extruded directly between the glass panes, creating a continuous and homogenous edge seal.

For the sealant, it has to be taken into consideration that the secondary sealant has a significant impact on fenestration products thermal performance and so the attention has to be paid on its thermal conductivity [*Van Den Bergh at al., 2013*].

IGU are used in a wide range of applications including the commercial and residential field: offices, hospitals, hotels, houses and buildings with heating or cooling requirements. They are also used in particular cases in which there is the need to respect some thresholds; for example to prevent condensation in airport control towers or for train windows and to protect from acoustic pollution some residential zones near highways or railways, thanks to their sound properties.

Most cold climate countries are making a significant effort to promote high performance windows, but triple-glazed windows have not achieved full market, because manufacturers were able to obtain comparable performance using double glazed and low-e coatings windows. This trend is changing and Austria, Germany and Switzerland have the highest market share for triple glazing (at 54% of total windows sales). Overall, the majority of windows installed in Europe are still double glazed. Worldwide, especially in certain regions, single glazed are used with clear glass and poorly insulated frames (the U-value is too high, around 4,5 W/m^2K). From the histogram below (Figure 2.3) it can be noticed the general overview of the market of windows in the world; triple glazed technology is still only a niche market but in the future it might spread in cold climates.

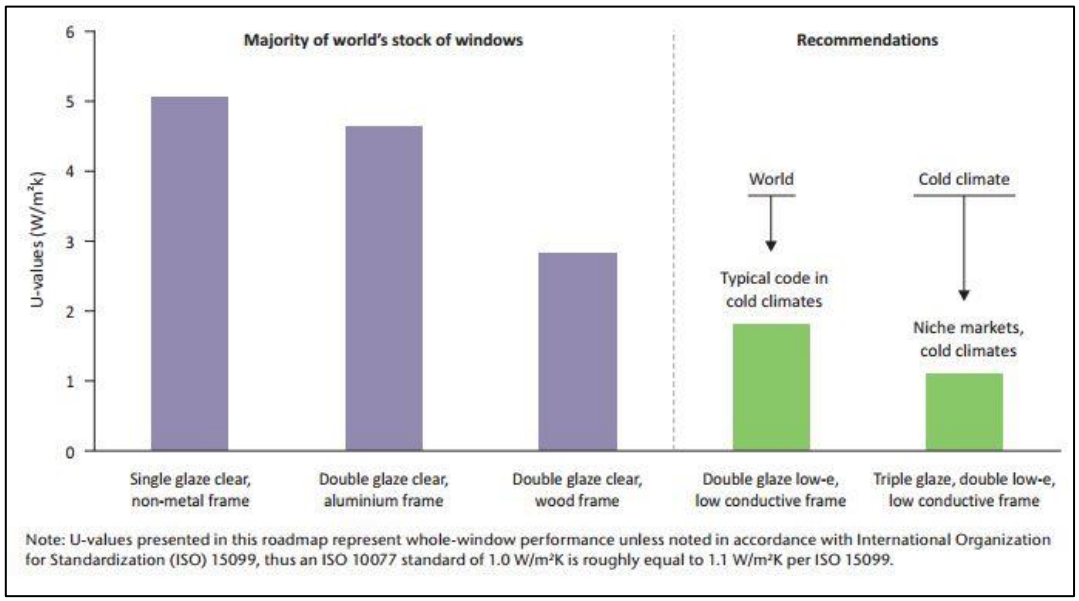

Fig. 2.3: most common types of windows in service and being sold today [*IEA, 2013*].

There has been a significant interest in developing highly insulating windows with grater passive heating benefits. The cost effectiveness of highly insulating windows depends significantly on heating requirements. For most cold regions is indicated a U-value around 1,1 $W/(m^2 K)$ or lower. However if the goal is to achieve zero energy buildings, a low U-value has to be coupled with a higher solar heat gain coefficient, to provide the best energy balance [*IEA, 2013*].

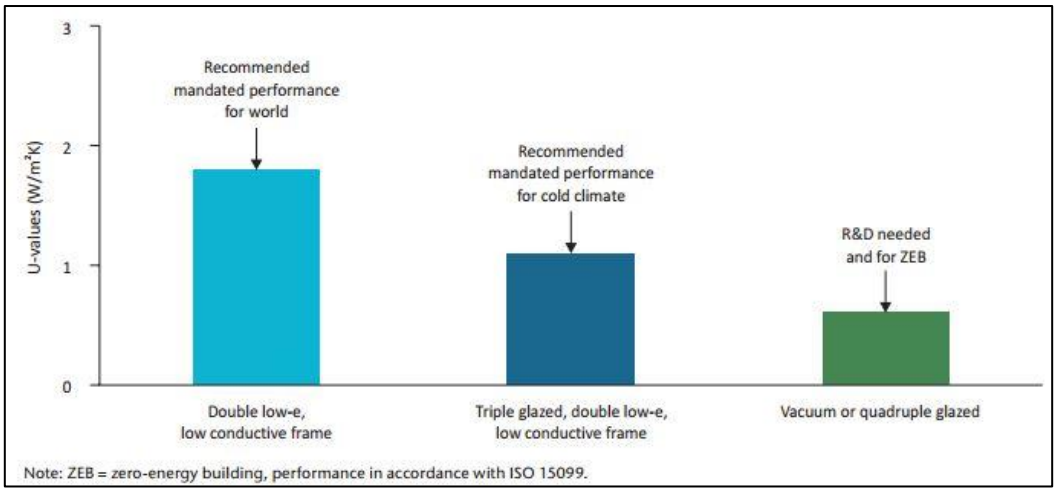

Fig. 2.4: typical windows U-values performance and IEA recommendations [*IEA, 2013*].

IGU technology can be integrated with the application of different types of coatings:

low-e coatings in order to minimize the amount of the transmitted infrared and ultraviolet radiation and reduce the entering heat in the building. This coating is placed in the inner pane, oriented towards the interspace;

sun protective coatings with the aim of reflection of the incident solar energy towards outside. Sun protection coatings are normally applied on the outer pane and oriented towards the interspace. It is useful especially in locations with a warm climate and high levels of direct irradiance;

combined coatings: in this case both the functions of solar-control and of light-redirecting are performed by the glazing.

2.1.3 Future perspectives

The edge seal thermal performance *q* can be improve by working in three ways [*Van Den Bergh at al., 2013*]:

a) reducing the width of the edge of the seal (w), reducing the heat transfer area and thus the size of the thermal bridge at the edge of glass;
b) reducing the thermal conductivity of the edge of the seal (λ), for example omitting high thermal conductivity materials such as aluminium and other metals;
c) increasing the thickness of the edge of the seal (t) to make the insulation effect higher;

$$q = \lambda \frac{w}{t} \qquad (2.1)$$

The best secondary sealant available today on the market has a conductivity of about 0,24 *W/(m² K)*, therefore improvements on that field are possible. However durability and good adhesion are more important properties for the sealant than thermal conductivity.

Another technical opportunity for the future is likely to be vacuum glazing with only two panes. A vacuum glazing combined with highly insulating frames can offer a good solar control and as consequence a significant thermal performance [*IEA, 2013*].

2.2 Dye sensitized solar cells

Another novel and more recent technology, in the field of photovoltaic industry, is the use of the dye sensitized solar cells (DSSC) in the building envelopes, also known as Grätzel cells. In the last years there has been an increasing interest in this type of photovoltaic cell, containing conductive polymer films as an essential part of the device. The

dye sensitized solar cell realizes the optical absorption and the charge separation processes by the association of a sensitizer as light absorbing material with a wide band gap semiconductor of nanocrystalline morphology. This technology have shown conversion efficiency that can almost compete with those of conventional devices (around 12% of efficiency, according to [*Nazeeruddin, 2011*]).

Moreover this type of PV (Photovoltaic) technology can offer the semi transparency of the modules, extending the field of application to glazed façades, thanks to the aesthetical point of view, with an economic advantage respect to the present price of photovoltaic silicon (Si) modules, because of the potential for lower cost of fabrication.

2.2.1 Principle of operation

The basic working principle is the absorption of the solar light that passes firstly through the transparent electrode, and then through a monolayer of a dye coated on a semiconductor surface.

The central part of the system is characterized by a mesoporous oxide layer composed of nanometer-size particles which have been sintered together to allow for electronic conduction to take place; the chosen material is TiO_2. A monolayer of dye is attached to the surface of the nanocrystalline film. The photo-excitation of the latter, due by the solar light, let the injection of an electron into the conduction band of an oxide. The nanometric porosity of the semiconductor's structure increases the active area in which the dye can fix on the TiO_2, improving the performance of the system. The original state of the dye is re-established by electron donation from the electrolyte, that is an organic solvent containing redox system, as the iodide/triiodide couple. The regeneration of the sensitizer by iodide intercepts the recapture of the conduction band electron by the oxidized dye. The iodide is regenerated by the reduction of the triiodide at the counterelctrode. Overall the device is able to generate electric power from solar light without suffering any permanent chemical transformation [*Grätzel M., 2003*].

In Figure 2.5 the mechanism of operation is shown: the sun provides the photo-excitation of the sensitizer S; this phenomenon cause the electron injection into the conduction band of the mesoporous oxide semiconductor. The dye molecule is regenerated by the redox system, which itself is regenerated at the counter electrode by electrode pass through the load. Potentials are referred to the normal hydrogen electrode (NHE). The open circuit of the solar cell corresponds to the difference between the redox potential of the mediator and the Fermi level of the nanocrystalline film indicated in the figure with a dashed line [*Grätzel M., 2003*].

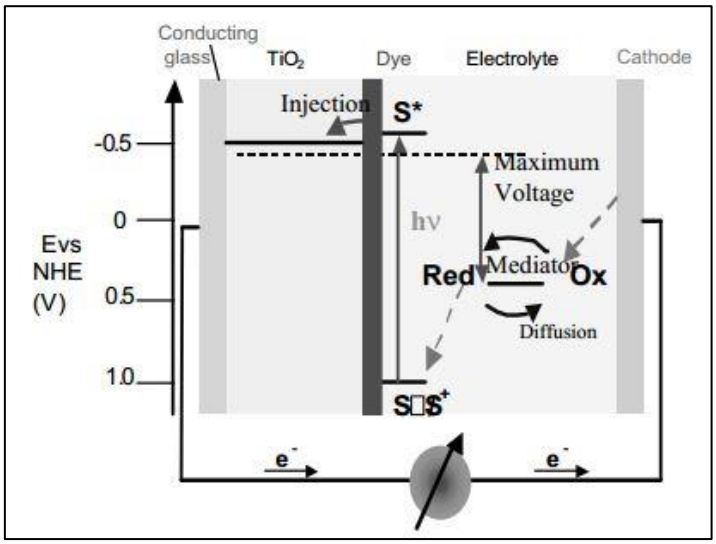

Fig.2.5: principle of operation and energy level scheme of the dye sensitized nano-crystalline solar cell [*Grätzel M., 2003*].

A weak point of this technology might be the durability of the device; a photovoltaic panel must remain serviceable at least for 20 years without significant loss of performance. The guaranteed stability of the system is one of the main questions on which the research in this field is discussing.

So a compromise between stability, efficiency and economic investment has to be reached, in order to make the market entry easier.

2.2.2 Current technology and applications

This technology is still in an early stage of development, but recent progress in device manufacturing indicates that it's approaching maturity for the market integration. In the last decade great strides have been done in this field, both in terms of efficiency and stability.

Concerning the available products market, dye sensitized solar PV modules are not spread, yet. Some companies are starting to introduce this technology on the market in this years, thanks to the improvements that the research has recently reached. The main obstacles are the incertitude on the durability of the product and the lower efficiency, in comparison with the conventional silicon PV modules. Although, with the recent efficiency records reached on the lab scale and the impressive progress reported for test modules, this technology is on the verge of approaching the PV market. The aspect concerning the aesthetic possibilities for architectural elements and building integration, coupled with the feasible use of lightweight modules, is the most important advantage of the DSSCs with respect to the conventional technology. Indeed, there is the possibility to choose to manufacture opaque or semi-transparent multi-coloured cells by tuning the sensitizer adsorbed on the photo-electrode. In this way, the path for many different solutions according to the end use is open. For example, energy producing windows and application on building façades, based on DSSCs, could represent a good way for the integration of photovoltaic, where landscapes restrictions have so far limited their application, or simply for aesthetical reasons [*Parisi M.L., 2014*].

In the field of building envelopes, one of the first architectural integration of DSSCs technology is the EPFL's new Swiss Tech Convention Center, in Lausanne (Switzerland): it has been equipped with an impressive glass façade, composed of dye solar cells. About 1400 solar modules, each one 35 by 50 *cm* in size have been installed on a surface area of 300 m^2. As it can be seen in the Figure 2.6, the five different shades of red, green and orange give the effect of a dynamic and warm aspect in the interior of the building. The aim of this innovative façade is double: it's a generator of renewable energy, slightly contributing to provide a fraction of the energy demand of the building (around 3% of efficiency). Secondly, it has also the function of shading the building from direct sunlight, reducing the need of air conditioning [*paperblog.com, 2013*].

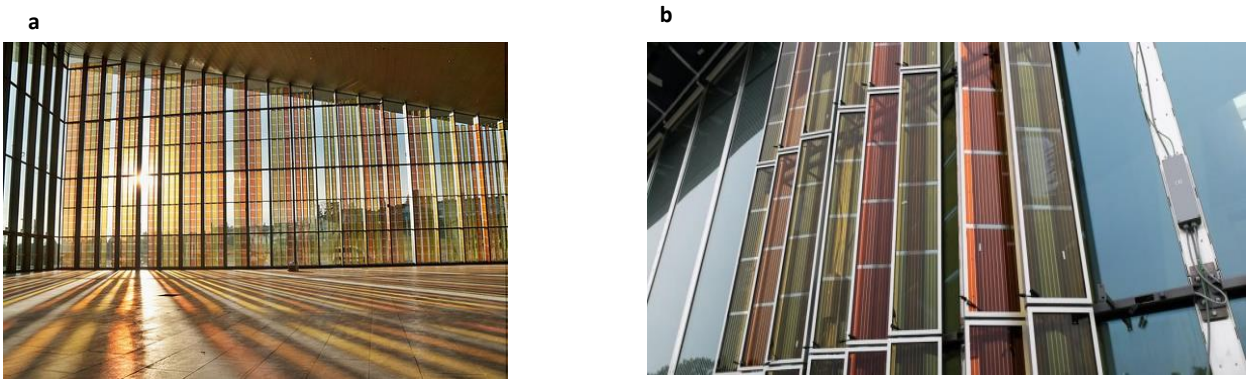

Fig.2.6: Swiss Tech Convention Centre from the indoor(a) and from the outdoor(b).

2.2.3 Future perspectives

Concerning the future development of this type of technology, many fields are actually completely open.

The application field of these cells could fit the standards for integration in the automotive and nautical sectors and additionally give major input to the intelligent sensors industry. This kind of applications would clearly address a high-value market segment in the immediate future. However,, in a realistic perspective of different PV technologies coexistence, these facts corroborate the idea that DSSCs represent the most promising option for a new paradigm of

energy generation systems. Research reports forecast a remarkable growth for DSSC technology in next years. Practical consequences for future PV market are hardly predictable, but it can be said that off-grid applications and the BIPV (Building Integrated Photovoltaic Market) sector, where DSSC already represent a viable solution, are less economically dependent on subsidies and this could be the opportunity to enter the PV market firmly [*Parisi M.L., 2014*].

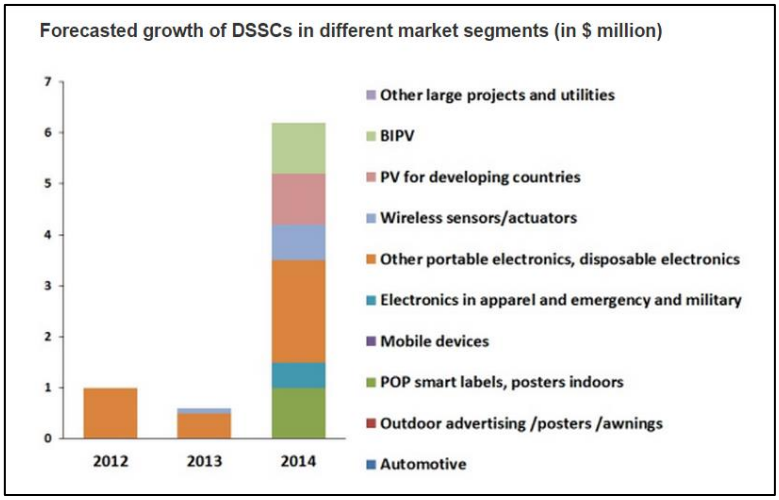

Fig.2.7: future perspective of growth of DSSCs market [*Zervos, 2013*].

As it is shown in Figure 2.7, currently the main field in which DSSCs are used is electronics. However in few years many other possibilities are wide opened: firstly the photovoltaic applications and then also for wireless sensors or mobile devices.

2.3 Complex fenestration systems

The energy balance of the building is strongly influenced by the glazing envelope, as discussed previously. Indeed, windows are the weakest components of the building envelope, in terms of thermal losses. New fenestration technologies have been developed over the last years, aiming at controlling the intensity of the incoming solar radiation, as well as thermal losses and gains. For examples, dynamic fenestration systems have been designed and studied in recent years. The basic principle of dynamic systems, called smart glazing, involves thermochromism (temperature change induces a variation of the optical properties), electrochromism (some materials vary their colours when an electrical voltage is applied and to regain transparency the reverse current has to be applied), gasochromism (a metal oxide interacts with an oxiding like oxygen or hydrogen to produce a reversible colour change), liquid crystals and micro-blinds to provide g-value changes. The main drawbacks of these solutions are the long switching time, the high cost, the extra installation considerations such as wiring and power supply and control system [*Kostro, 2014*].

Among these new technologies, Complex fenestration systems (CFS) are advanced systems that try to take into account the most important variables concerning the building envelopes: energy performance and occupant thermal and visual comfort. CFS are static glazing components, characterized by particular optical and thermal properties (U-value, visible and solar direct transmittance and solar heat gain coefficient), as all the other conventional glazing. This novel glazing technology changes the way in which windows impact the indoor environment. In fact CFS allow exploiting the natural sunlight within the building in the best possible way. Then, depending on the particular device, other advantages can be reached, such as energy savings for the heating and cooling system. CFS address these criteria using a wide variety of novel technologies to exert greater control over the performance of the fenestration system, being able to significantly reduce energy consumption [*Andersen, 2011*].

However, the main aim of CFS is to optimize the availability and the uniformity of daylighting inside buildings, giving at the same time a contribution to the reduction of the energy consumption for heating and cooling and for artificial light. Therefore, the selection of a suitable fenestration system for a building is a crucial decision. It offsets electric lighting use as well as impacts energy performance through heating and cooling systems, influencing occupant comfort.

2.3.1 Current technology and applications

The term CFS refers to all non-specularly transmitting fenestration systems components including layers that provide shading, such as fabric shades louvered blinds, metal mesh systems, and layers that improve interior daylighting, such as prismatic films and mirrored louvered systems. These novel type of glazing will combine the functions of daylighting, glare protection and seasonal thermal control.

CFS can be categorized according to their performance or objectives such as the depth of the daylight penetration in the interior space, the control of the solar gains, the glare control and the shading. Starting from the first criteria, deeper daylight penetration is reached by redirecting incoming light in order to illuminate a greater proportion of the room. Control of solar gains requires less admittance of solar radiation during the hot season, through a lower transmittance or shading, and access of solar gains during winter. Finally glare protection means that shading or redirection of incoming sun rays are implemented so that direct light will not reach the eyes of the occupants or reflective surfaces.

There are many configurations of CFS, some that include shading system to redirect diffuse skylight or sunlight and others that are designed only to redirect the light, without the function of shading [*Ruck, 2000*]. Concerning the *shading* systems, they are divided in systems that reject direct sunlight using only the diffuse and systems that use primarily direct sunlight, sending it onto the ceiling or to locations above the eyes. The *non-shading* CFS are designed primarily to redirect daylight to areas away from a window or skylight opening. The latter are grouped in categories:

a) diffuse light guiding systems: to redirect daylight from specific areas of the sky vault to the interior of the room. They improve daylight utilisation in case of urban environments, where there are a lot of external obstructions;
b) direct light guiding systems: to send direct sunlight in the indoor environment without the secondary effects of glare or overheating;
c) light scattering or diffusing systems: they are used in sky lit or top lit apertures to produce even daylight distribution. They can caused serious glare if installed in vertical windows apertures;
d) light transport systems: to collect and transport sunlight over long distances to the core of the room via optical fibers or light pipes.

Some examples of products and applications of CFSs systems are shown below.

Blinds can be considered the most traditional way to provide modular daylighting and solar protection, because they have been introduced long ago. However, over the years their profile and functionality were fine tuned to prevent glare and protect from overheating while keeping a sufficient daylight level and good energetic performance. At high angles of incidence, most rays are reflected outwards, while the more horizontal rays are partially redirected into towards the ceiling and deep into the room. Automated control for blinds is also possible, in order to optimize the position of shadings adapting to changing conditions all over the day. Recently split blinds with different inclination angles have been introduced: they allow to separately control the upper part to avoid visual discomfort and the lower part of the blinds to provide a dynamic control of light [*Kostro et al., 2011*]. In Figure 2.8 an example of blind shapes optimised can be seen.

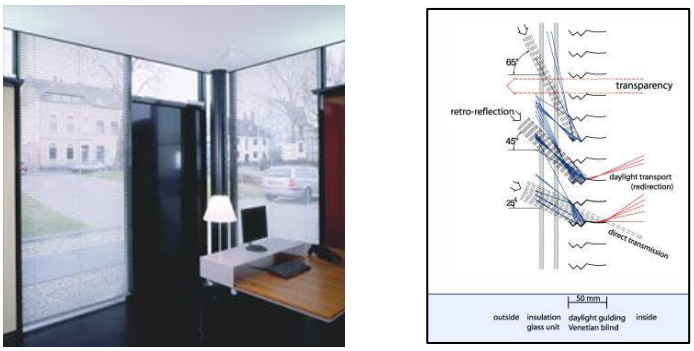

Fig.2.8: Retrolux blinds with a very interesting geometry that permit the daylighting control.

Another interesting kind of CFS are the *anidolic systems*, that are non-imaging optical components like parabolic or elliptical mirrors, used to capture the sun light and redirect it deeply into rooms, while the deviation of the light avoids glare. These architectural solutions usually consist in collectors mounted the exterior wall. One of these integrated anidolic systems with large reflective surfaces has been installed on the LESO solar experimental building's south façade at the Swiss Federal Institute of Technology (EPFL, Lausanne), as it can be seen in Figure 2.9 [*Scartezzini et al., 2002*]. This daylighting system was installed and monitored, giving as result that it can improve the luminous efficiency of the indoor. The overhanging part with the anidolic element, simultaneously offers protection for the window in the lower part that provides mostly the view to the outside. The drawback of this technology is that it often requires complex and non-standard building modifications of the façade concept.

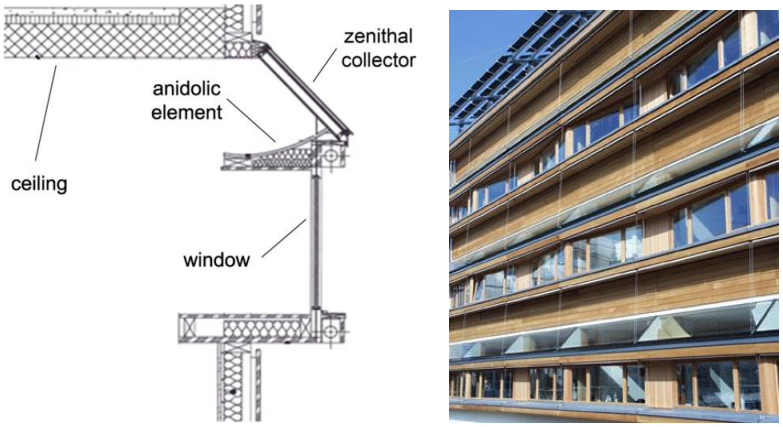

Fig. 2.9: façade integrated anidolic daylighting systems installed in the southern side of the Solar Energy and Building Physics Laboratory (LESO) solar experimental building in Lausanne, Switzerland. Daylight collected from the sky vault is redirected onto the room's diffuse ceiling by a single anidolic element.

Laser cut panels (LCP) are daylight deflection systems produced by making narrow parallel laser cuts spaced by 4 *mm* in a 6 *mm* thick sheet of clear acrylic. Each cut surface deflects the daylight by refraction; the orientation and deflective fraction are determined by the incidence angle and oblique angle of the cuts. Therefore the relevant optical properties of the LCP are the deflection angle, the fraction of light deflected for a given incidence angle and the spread of the light due to the surface roughness of the interfaces produced by the laser used for fabrication. An advantage of the panel is that between the cuts, an outside vision of the window is maintained, but is slightly distorted, offering a good viewing transparency in the near-normal direction; the reduction in viewing transparency respect to a conventional window is however perceptible. The effectiveness of the LCP in improving room illumination strongly depends on the type of fenestration fitting as well as on sky conditions. The main property of the laser cut panel placed in the upper part of a window is the ability to redirect sunlight towards the ceiling; it contributes to the solar protection of the room, admitting low elevation incidence angles and rejecting high elevation light rays [*Edmonds, 1993*]. As it can be noticed in Figure 2.10a and Figure 2.10b, usually laser cut panels are fixed above the eye level to avoid obstruction of external view or glare.

Fig.2.10: (a) Solartran laser cut panels in a classroom installed in the top part of a window (b) Lumitop glass Saint Gobain.

Prismatic panels (Figure 2.11) are another example of one such CFS and can be used to redirect illumination deep into the room, improving the daylighting. They consist in light re-directing devices made of a series of transparent acrylic or polycarbonate prisms on one side, aligned to form a plane. The main advantage is the longitudinal flexibility, low maintenance and very high light transmission, allowing to transport and distribute light in an effective way. Under clear sky, prismatic film refracts sunlight and illuminates the ceiling in the middle of the room. The film performs less well under overcast sky conditions but it mitigates glare risk. The prismatic panels allow the redirection of the daylight to the interior of the room and can act simultaneously as shading devices. The system can be applied in the vertical plane of the façade, sandwiched between the glazing panes to avoid maintenance and dust. They are preferably used at the top of the window, in order to maintain the view to the outside [*Thanachareonkit, 2008*].

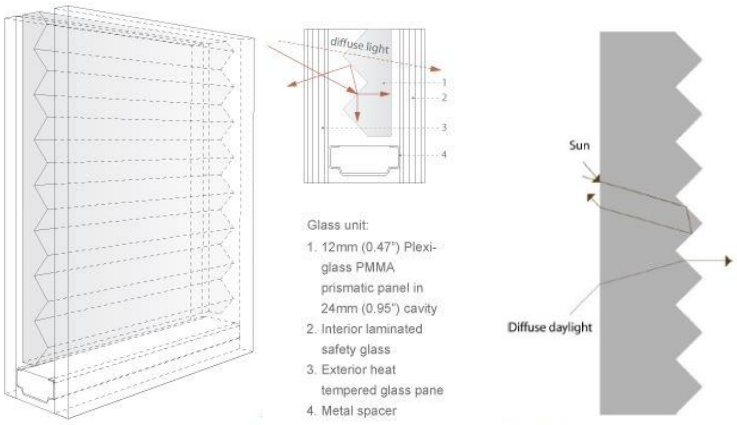

Fig. 2.11: the basic working principle of prismatic panels.

2.3.2 Embedded microstructures technology

Among the different kinds of CFS, previously discussed, one of the most innovative and interesting advanced fenestration systems result the light directing glass with embedded microstructured optical micro-mirrors. There are two different types of this innovative technology: *non-transparent* microstructures, installed in the upper part of the window, and *embedded microstructures*, laminated in the glass pane itself, that try to combine the function of daylighting, glare protection and thermal control.

The first group of optical devices (*non-transparent microstructures*) consists in surface structures with lateral and depth dimensions in the order of 1 μm and 1000 μm. As previously discussed, the majority of the manufacturing techniques to realize microstructures have been developed in the field of micro electronics devices fabrication. However, in the last years the research is focusing in the study of how to apply the microelectronics technologies to the emerging field of microoptics, with rather low cost production. For the fabrication of micro-optical elements special high precision replication processes are required, like precision injection moulding, hot embossing or UV

casting by utilizing suitable transparent polymers. All materials with high optical transparency are principally suited for the realization of such micro structured components, with preference of polymeric materials, due to their easier mass production capabilities. The way in which microstructures provide the redirection of the incident solar radiation when the light is coming from solar altitudes between 15° and 65°, thus reducing glare and exploiting the daylight, is similar to the anidolic mirror-based systems. Concerning the construction, due to the fact that the position above eye level is preferable, in order to avoid glare risk, two solutions are possible, as it can be seen in Figure 2.12. A separating frame with PMMA (polymethylmethacrylate) in the upper side and glass pane below, or a continuous glass pane with micro structured plastic foils laminated at the desired position of the glass sheet [*Klammt et al., 2012*].

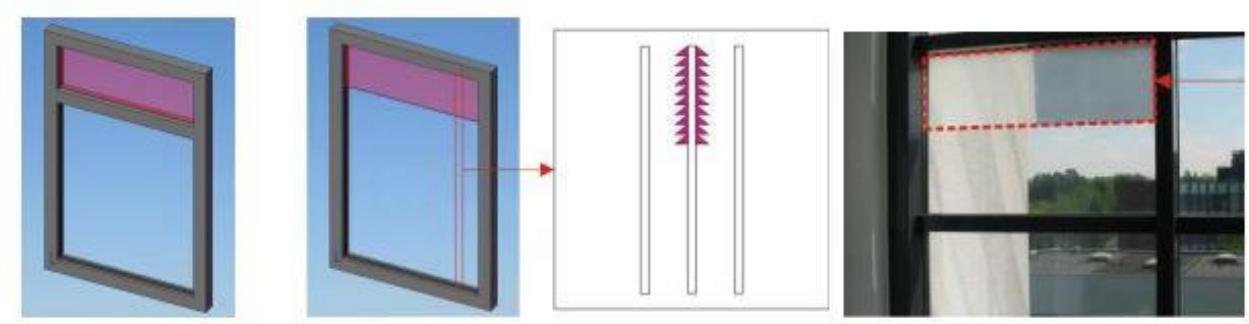

Fig.2.12: possible construction configurations. Left: separating frame between upper and lower window area. Right: lamination of micro-structured foils in the upper part of a continuous glass panel. [*Klammt et al., 2012*].

On the other hand, *embedded transparent microstructures* [*Kostro, 2014*] are static optical devices (CFS), for which the field of application lays in the area of consumer electronics and flat displays where the aim is to enhance the directionality and increase luminosity. Thanks to their properties for light redirection and for the angular transmittance behaviour, a new interesting field of application is the integration and combination with standard doubled glazed windows. One of the purposes is to reach a smart energy management: during the heating season, when temperatures outside are lower than inside, the thermal gains coming from the sun can be exploited to contribute to the reduction of the energy consumption of the room. While, during the cooling season the overheating of the building has to be avoid reducing the gains by the low solar direct transmittance of the glazing. The advantage is the transparency of the micro-mirrors, small enough to allow the human eye the clear view towards outside.

Therefore, the functions for the daylighting and thermal control combined by the microstructures can significantly contribute to reduce the energy consumption in buildings with favourably oriented glass façades. The concept on which is based is shown in the Figure 2.13. During winter, when the angle of incidence of the sun rays is quite low (around 20°-30° for Lausanne), solar gains are used to reduce heating energy demand, while in the hot season, when the angle of incidence can increase until 67°, the proposed devices blocks direct radiation, limiting air conditioning loads as well as overheating risks. Moreover, a judicious use of daylighting lead to reduce energy needs for artificial lighting and improves visual comfort of occupants.

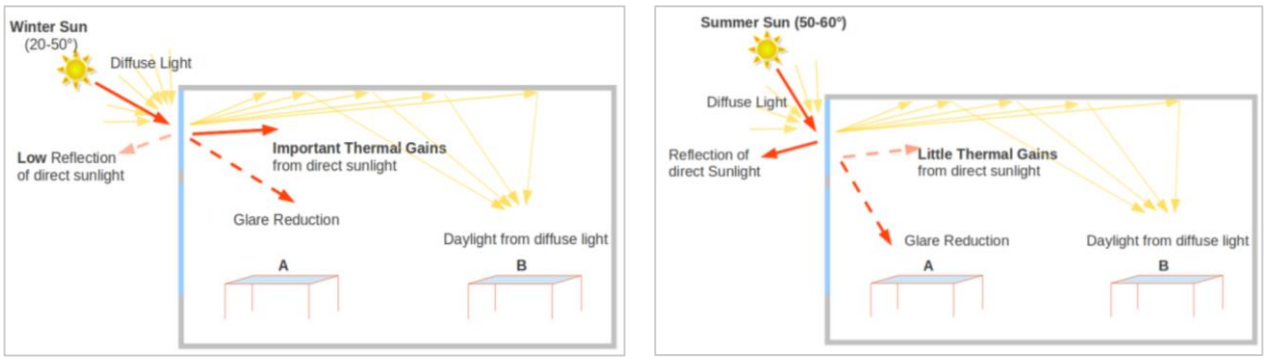

Fig. 2.13: working principle of an ideal embedded microstructure for daylighting, glare protection and seasonal thermal control [*Kostro, 2014*].

As it can be seen in Figure 2.14, the structure includes two optical elements: embedded parabolic micro-mirrors and vertical reflectors, both integrated on the surface of the PMMA polymer. By using the parabolic mirror to focus light from a given angular interval onto the second reflective mirror placed vertically at the rear side of the system, the angular dependent blocking of solar radiation can be reached, increasing daylighting and thermal control performance and reducing glare risks.

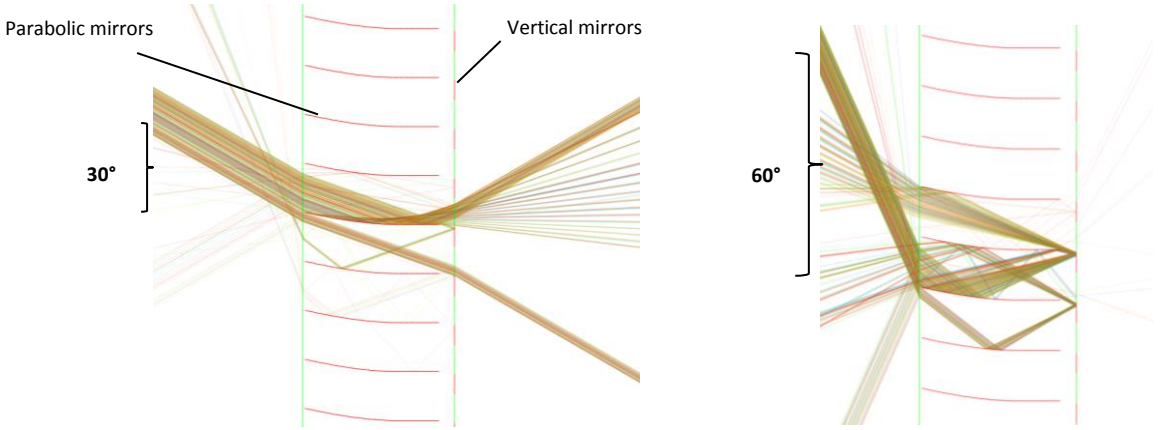

Fig. 2.14: embedded microstructures in the PMMA film with incoming beam at 30° and 60°, respectively sun elevation for winter and summer in Lausanne.

It was shown that this novel device relies on a smart management of the available energy, to reach good lighting levels and the optimal exploitation of the solar radiation. The total thickness of the system is less than a millimetre and it can be laminated to a glass; the micro-mirrors are almost invisible to the human eye (less than one millimetre). A static CFS that perfectly combines the advantages of daylighting, glare protection and seasonal thermal control would require dynamic devices and advanced controls. To get closer to this ideal system, various geometries of embedded mirrors, will be investigated in this work, in order to optimise the performance of the microstructure [*Kostro et al., 2012*].

The fabrication of the embedded microstructures requires multiple steps. Firstly, to produce repeatable results, the substrate needs to *be cleaned in an industrial washing machine using* washing powder for glassware. The next step is to carry out the desired shape for the embedded mirror on a support which is used as a mould for *replication* into a transparent medium. In order to achieve this goal, multiple approaches can be applied, such as electrical discharge machining, laser ablation or grey scale lithography. Therefore, to create curved shapes another method is required: *the grey scale lithography*. The latter uses masks with changing opacity or direct laser writing of the photo resist to realise smooth parabolic surfaces. Then the structure needs to be replicated onto the substrate, by *ultraviolet nano-imprint lithography*. This is a well-established process for the replication of micron and sub-micron scale features into photo-polymerizable. The substrate, resin and mould are placed on a piston that pushes against a quartz window, with strong scratch resistance, above which a UV lamp is switched on to cure the resin. The selected facets of this structure then have to be coated with a reflective material using a deposition technique called *physical vapour deposition (PVD)*; for the reflective material, aluminium can be selected for his high reflectivity and ease deposition. The PVD takes place in a vacuum evaporation chamber, where the material is heated until the melting point. Its vaporised form then condensates on the substrate. Finally the mirrors have to be embedded through the *encapsulation*: the same UV curable polymer for replication is used, in order to have virtually no interface at the structure surface: a change in material would create extra refraction and make to system less transparent and more diffusing. Light passing through the system without interacting with the embedded mirrors need to pass without any other interactions to avoid direction changes and to keep the system imaging and transparent at normal incidence. To create a back side parallel to the front side, the mould has two reference levels next to the structured area; these are used to ensure that during encapsulation, the glass slide placed on the top of the structures is parallel and does not crush the fragile structures. For this step special care is required, to avoid dislocation from the glass slide and creation of air pockets on the microstructured side [*Kostro et al., 2012*].

The decision to focus on this last type of embedded and transparent microstructures comes from the several advantages that this novel technology can have for a building, in terms of energy savings.

2.3.3 Future perspectives

The great potential of these CFS systems is, however, not yet being realised, due to barriers to market entry associated with their complexity, dynamic performance capabilities and lack of understanding of appropriate implementations. CFS aim to achieve improved overall performance in a variety of unique ways but until there is a means to communicate these benefits, their use will be limited [*Andersen, 2011*].

Concerning the embedded microstructures, an interesting study is about the impact of various parameters on the efficiency of the system glazing advanced according to the latitude, trying to find the optimal geometry, depending on the different locations. There are many parameters that have to be considered, such as the climate during all the year, the level of insulation of the building and the dimensions of the glazed façade, as it will be discussed in chapter 5.

For the large scale production a standardized method is needed, to obtain competitive prices. A possible solution could be the roll to roll process: a plastic film through a series of rolls for various stages of manufacturing. This is a suitable process for mass production structure on plastic films.

3 Characterization of glazing samples

In this chapter, the experimental determination of the optical properties of two kind of glazing technologies is performed, in order to completely characterize the materials of the glass, that have a relevant influence on the physical and thermal behaviour of the whole system in which the glass is installed.

Firstly a general overview is presented, concerning the main optical and thermal parameters that have to be measured; then, the description of the experiments performed to obtain measured data follows. Finally, a practical example is showed with results.

3.1 Optical and thermal properties

Optical and thermal measurements are important to quantify properties of the analysed products, in order to evaluate in each case the best solution from the energetic point of view and for the visual comfort of the occupants. This characterization has to be performed in the simplest way possible for every standard commercial glazing. To reach this purpose, the suitable instrumentation is available in the laboratory.

3.1.1 Solar spectrum

The sun can be considered as a black body at 5780 *K* (roughly the sun surface temperature): it means that it can absorb all the incident radiation without any reflective phenomenon. The emission spectrum, that is the distribution of the energy, emitted by a radiant source (the sun itself), is described by the Planck Law, given by (3.1):

$$R(\lambda, T) = \frac{2\pi c^2 h}{\lambda^5 \left(e^{\frac{hc}{k\lambda T}} - 1\right)} \qquad (3.1)$$

The different parameters, describing the behaviour of the radiation in function of the wavelength λ, are showed in Table 3.1 [*Hassel, 2010*]:

c [m/s]	*299792458*
h [J s]	*6,63 10^{-34}*
K [J/K]	*1,38 10^{-23}*
T [K]	*5780*

Table 3.1: physical parameters for the determination of the blackbody spectrum (at 5780 *K*).

Figure 3.1 shows the solar radiation spectra at different values of temperature, obtained applying the Planck Law. It can be noticed that the peak of each curve shifts to shorter wavelengths, with the increase of the temperature. The solar spectrum, considering the sun as a black body, is placed between the green and the yellow line (5780 *K*). Plotting different curves, all the solar spectra of the considered black bodies at different temperatures are normalized.

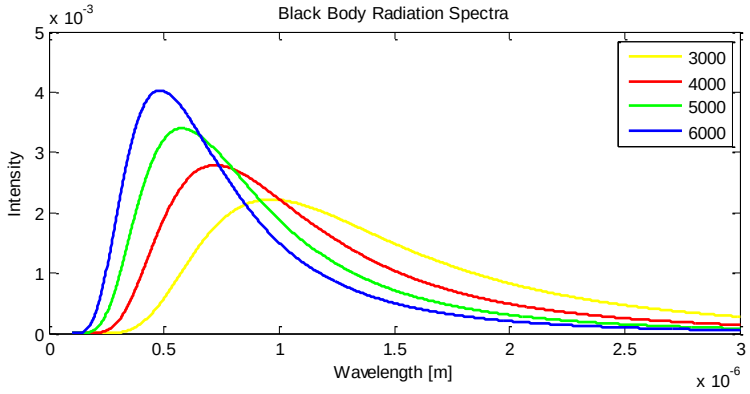

Fig. 3.1: normalized radiation energy of a black body at different temperatures.

The radiation that is emitted from the sun includes a wide range of frequencies of electromagnetic spectrum, as shown in Figure 3.2:

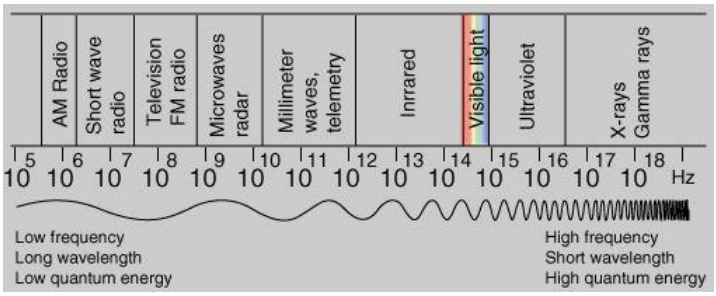

Fig. 3.2: electromagnetic spectrum.

The range of wavelengths that goes from 380 *nm* to 780 *nm* is called the visible light range, because they are perceived by human eyes. All photons with frequency immediately above 380 *nm* are part of the ultraviolet range, while those of the infrared interval start at wavelengths above 780 *nm*.

The average total solar radiation per unit area that would be incident on a plane perpendicular to the rays at a distance of 1 *AU* (that means when the sun and the earth are spaced of 149 597 890 *km*) is called the solar constant. Currently accepted values of this constant are around 1360 W/m^2; the World Metrological Organization (WMO) promotes a value of 1367 W/m^2. The solar constant is the total integrated irradiance over the entire spectrum. The overall solar radiation that is incident on the earth's atmosphere over the course of the year adds up to $1{,}5x10^{18}$ *kWh*.

Once through the earth's atmosphere, some of the photons interact with the gases that are distributed in different layers, such as hydrogen, water vapour, carbon dioxide and ozone, so there is only one portion of the emission solar spectrum that reaches the earth's surface, because of the filtering action of the atmosphere. This emission spectrum is also influenced by meteorological conditions, the altitude, the position of the sun with respect the earth and the pollution. About 30% of this radiation is directly reflected back into the space, 20% is absorbed by gases with specific absorption bands, in the atmosphere and 4% is reflected off the earth's surface. The remaining 46% is absorbed and converted into different form of energy [*Reinhart, 2012*].

Another important factor is the proportion of direct to diffuse light. Solar radiation that reaches a site without being scattered within the earth's atmosphere is called direct sunlight. In contrast, light that is scattered in the atmosphere is referred to as diffuse daylight.

Figure 3.3 shows the solar radiation spectra for direct light at both the top of the earth's atmosphere and the sea level. These curves are based on the "American Society for Testing and Materials (ASTM)" Terrestrial Reference Spectra, which are standards adopted by the photovoltaic industry to ensure consistent test conditions. Regions for ultraviolet, visible and infrared light are indicated *[Gueymar et al., 2002].*

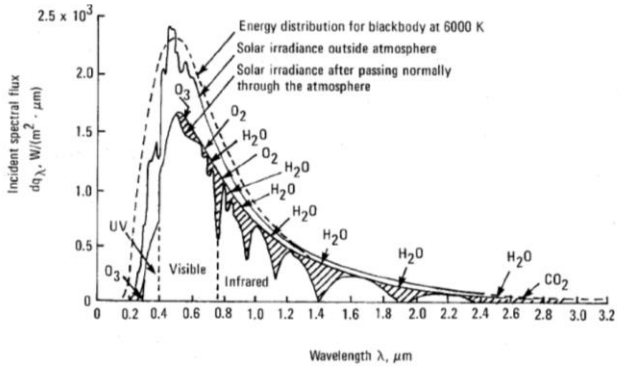

Fig. 3.3: solar radiation spectra at the top of the atmosphere and at sea level, with attenuations due to the molecules in the atmosphere.

The ASTM, in conjunction with the PV industry, developed and defined only these two standard terrestrial solar spectral irradiance distributions. The two spectra define a standard direct normal spectral irradiance (that is the direct component that contributes to the global spectrum) and a standard total spectral irradiance. These current standard references are incorporated in a document: the "*ASTM G-173-03".* In this document data are collected, considering only one set of specified atmospheric conditions, for a receiving surface that corresponds to an inclined plane at 37° tilt toward the equator, facing the a sun elevation of 41,81° above the horizon. The specified atmospheric conditions are [*NREL, 2014*]:

a) the *1976 U.S. Standard Atmosphere* in which atmospheric temperature, density and pressure are defined over a wide range of altitudes;

b) the absolute air mass of 1.5 (corresponding to a solar zenith angle θ of 48,19°), where the air mass coefficient is defined as:

$$AM = \frac{L}{L_o} \qquad (3.2)$$

L is the path length through the atmosphere for solar radiation incident at angle θ, relative to the Earth's surface and L_0 is the zenith path length (normal to the earth's surface) at sea level;

c) total column water vapour equivalent of 1,42 *cm* and total column ozone equivalent of 0,34 *cm*;

The table included in the "*ASTM G-173-03"* (global and direct) shows the following data in columns:

- wavelengths range that goes from 280 *nm* to 4000 *nm*;
- extra-terrestrial radiation at mean earth-sun distance;
- spectral radiation from solar disk plus sky diffuse and diffuse reflected from ground on south facing surface tilted 37° from the horizontal plane.

It has to be considered that the ASTM G-173-03 is used as reference spectrum to elaborate data from the measurements in the laboratory.

3.1.2 Definition of optical and thermal properties

There are two kind of parameters that have to be considered to completely analyse the performance of a glazing envelope: the optical parameters and the thermal ones. The European Standard for the determination of luminous and solar characteristics of glazing in buildings is EN 410 (March 2011). In the Standard, applicable to all transparent materials except those which show significant transmission in the wavelength interval between 5[μm] and 50[μm] of ambient temperature radiation, the appropriate formula for single, double and triple glazing are provided, in order to evaluate the influence of the glass on the daylighting and thermal control.

Considering that D_λ is the spectral distribution related to the visible spectrum (normalised illuminant D_{65} defined by the International Commission on Illumination), V(λ) is the luminosity function describing the average spectral sensitivity of human visual perception of brightness, and S_λ is the spectral distribution related to the solar radiation, all these are variables referred to the European Standard that offers an overview on the needed parameters to fully characterise a glazing sample.

First, the optical parameters related to the visible spectrum are defined:

a) visible light transmittance τ_v: it is the directly transmitted visible radiation, therefore in the wavelength range of 380 *nm* and 780 *nm*, weighted by the spectral response of the human eye (dimensionless measure);

$$\tau_v = \frac{\sum_{380\ nm}^{780\ nm} \tau(\lambda) D_\lambda V(\lambda) \Delta\lambda}{\sum_{380\ nm}^{780\ nm} D_\lambda V(\lambda) \Delta\lambda} \qquad (3.3)$$

b) visible light reflectance ρ_v: it is the directly reflected visible radiation, therefore in the wavelength range of 380 *nm* and 780 *nm*, weighted by the spectral response of the human eye (dimensionless measure);

$$\rho_v = \frac{\sum_{380\,nm}^{780\,nm} \rho(\lambda) D_\lambda V(\lambda) \Delta\lambda}{\sum_{380\,nm}^{780\,nm} D_\lambda V(\lambda) \Delta\lambda} \quad (3.4)$$

c) visible light absorptance : it corresponds to the complementary of the sum of the visible light transmittance and the visible light reflectance (dimensionless measure).

$$\alpha_v = 1 - \tau_v - \rho_v \quad (3.5)$$

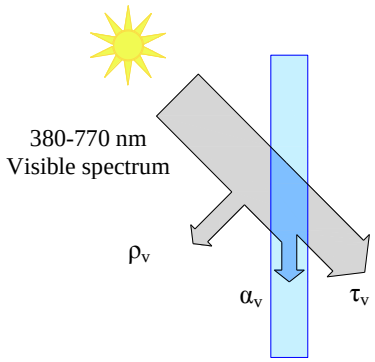

Fig. 3.4: visible light transmittance, reflectance and absorbance, according to EN 410 energy distribution.

Then the thermal parameters, referring to the whole solar spectrum, are defined:

a) Solar direct reflectance ρ_e : it is the ratio of the reflected flux of solar radiation on a glass surface to the incident radiant flux (dimensionless measure);

$$\rho_e = \frac{\sum_{300\,nm}^{2500\,nm} \rho(\lambda)\, S_\lambda\, \Delta\lambda}{\sum_{300\,nm}^{2500\,nm} S_\lambda\, \Delta\lambda} \quad (3.6)$$

b) Solar direct transmittance τ_e : it is the ratio of the transmitted flux of solar radiation on a glass surface to the incident radiant flux (dimensionless measure);

$$\tau_e = \frac{\sum_{300\,nm}^{2500\,nm} \tau(\lambda) S_\lambda\, \Delta\lambda}{\sum_{300\,nm}^{2500\,nm} S_\lambda\, \Delta\lambda} \quad (3.7)$$

c) Solar direct absorptance α_e : it is the amount of solar energy absorbed by the glass that can in part be emitted to the external environment(dimensionless measure). It can be obtained from the equation 3.8:

$$\alpha_e = 1 - \tau_e - \rho_e \quad (3.8)$$

The absorbed part α_e is split into two parts which are the energy transferred to the inside and outside, respectively shown in equation, valid in steady state conditions:

$$\alpha_e = q_i + q_e \quad (3.9)$$

Where q_i is the secondary heat transfer factor of the glazing towards inside and q_e is the secondary heat transfer factor of the glazing towards outside.

d) g-value (solar heat gain coefficient): it's the total solar energy transmittance of glazing for solar radiation in the wavelength range between 300 *nm* and 2500 *nm*. The value is significant for HVAC calculations (heating, ventilation and air conditioning systems) and it is expressed in percentage (dimensionless).
It can be calculated as the sum of the solar direct transmittance τ_e and the secondary heat transfer factor q_i of the glazing towards inside:

$$g = \tau_e + q_i \quad (3.10)$$

Where q_i is resulting from the heat transfer by convection and long wave IR-radiation of the part of the incident solar radiation which has been absorbed from the glazing.

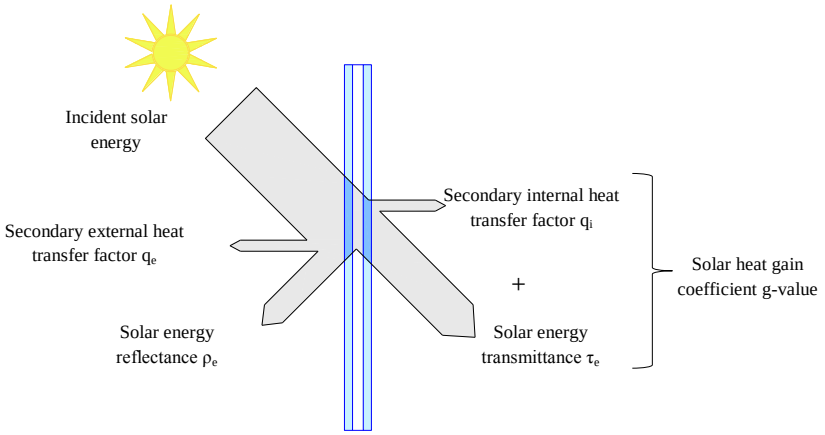

Fig. 3.5 : total solar energy transmittance and g-value, according to EN 410 energy distribution.

e) U-value in W/m^2K (thermal transmittance): it's the measure of the heat transmission through the glazing thickness and it specifies in steady state conditions the heat flow per unit time through 1 m^2 of the glass surface for a temperature difference between the outdoor and indoor ambient of 1 K. The higher the U-value, the worse the thermal performance of the window in terms of insulation. It is a function of the type of gas filling of the intermediate space between the glass sheets, the distance between the sheets and the number of sheets (double or triple glazing with low-e coating).

Concerning the thermal properties of the glass, the most important parameters are the g-value, that characterizes the solar gain of a glazing, and the U-value that allows to evaluate the thermal losses of a glazing.

The last parameter that has to be consider to completely characterize an insulating glass unit is the energy load coefficient, defined by the ratio of the solar direct transmittance to the visible light transmittance:

$$ELC = \frac{\tau_e}{\tau_v} \quad (3.11)$$

There are databases that show all these optical and thermal values for a certain number of products, in order to compare the performance of different glazing and install the best configuration for a particular location; the table below (Table 3.2) compares the parameters catalogued in the database "Glass dBase", concerning a Pilkington Suncool, that combines high visible light transmittance with low-emissivity performance, and a Econtrol Glas Dunkel, that is based on the electro-chromic effect (the variation of the difference of voltage can regulate the light transparency of the glass pane):

	Pilkington Suncool Brilliant 66/33	**Econtrol Glas Dunkel-4**
τ_e (φ=0°)	0,359	0,096
τ_v (φ=0°)	0,679	0,180
ρ_e (φ=0°)	0,330	0,105
g-value (φ=0°)	0,409	0,127
ELC	0,529	0,533

Table 3.2: comparison of the optical and thermal characteristics between two commercial glasses [Glass dBase].

It can be noticed that the first glass has an higher value of transmittance. Therefore, for a cold climate the first glass could be the better because let a larger amount of solar energy enter in the building. This point is underlined also by the g-values. The absorptance is relevant in the case of the electro-chromic glass (around 80%), so most of the energy is spread being absorbed by the glass itself. In both cases the visible light transmittance is higher than the solar direct transmittance and this influences the visual comfort of the indoor environment.

3.2 Examples for optical characterisation

The determination of the angle-dependent optical properties of glazing products is necessary for more accurate estimation of the total solar gains in buildings. Indeed, manufactures of commercial glasses usually provide the optical properties such as transmittance and reflectance only for normal light incidence, a situation that rarely is applicable to reality. In fact, at European latitudes, a significant portion of the annual solar irradiance on a vertical surface, is incident at angles in the range of 30°-70° from the surface normal. Consequently, calculations based on transmittance and reflectance values at the normal incident angle, overestimate the total solar gain. The need to know the angular dependent optical properties of windows has increased with the use of advanced glazing materials such as those for solar gain control or with low emissivity coatings.

The experimental set up for the determination of the spectral and angular dependent optical properties of the glazing samples is described by transmittance and reflectance measurements. This experiment is very useful to completely characterise the glass, measuring both the direct transmittance and reflectance at different incident angles φ, starting respectively from 0° and 15°. Therefore, the aim is to add optical data about products available on the market, in order to have a clear idea of the behaviour of the optical properties, varying the angle of incidence of the light, in order to evaluate the energetic and daylighting performances in buildings.

3.2.1 Experimental set up

The window test bench capable of measuring transmittance and reflectance at different incidence angles was developed originally at University of Basel [*Steiner et al., 2005*] and now installed at EPFL/LESO-PB in Lausanne. The experimental set up can be seen in Figure 3.6. It consists in a special light source to simulate the solar spectrum, a revolving support carrying the glass samples, and a receiver collimator positioned in the main axes of the light source to measure transmittance or at various angles φ for measuring the reflectance (respectively T collimator and R collimator in Figure 3.6). Moreover, two diode array spectrometers are installed for the acquisition of the experimental data through the program AspectPlus; one spectrum is typically measured in a few seconds.

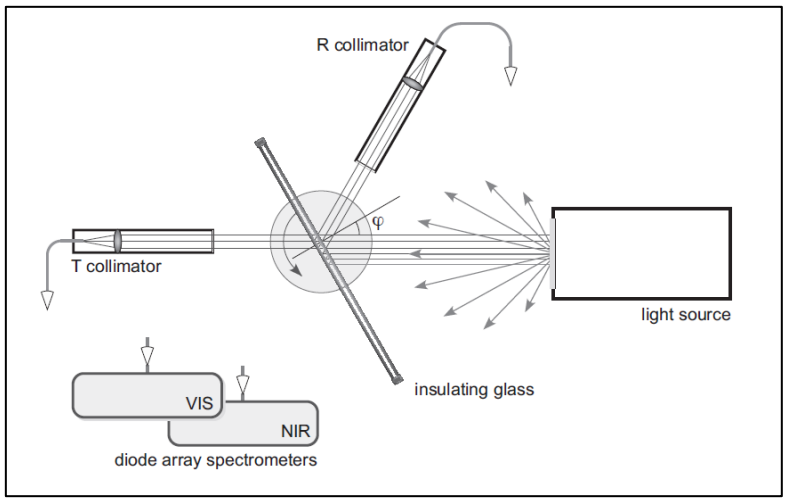

Fig.3.6 : experimental set up for spectral optical, angular dependent measurements of both the direct transmittance and reflectance in the UV, visible and near infrared wavelength range [*Steiner et al., 2005*].

The detailed description of all these instruments follows [*Steiner et al., 2005*]:

a) light source: the rectangular area of the front diffusor plate of the light source measured 25x38 cm^2 and it provides homogenous diffuse radiation in the near UV, visible and near infrared wavelength range. Two types of lamps are used: a matrix of 25 quartz tungsten halogen lamps (35 *W*) with integral aluminium coated reflectors and three UV fluorescence lamps (20 *W*);

b) receiver collimator: it defines the direction of the transmitted or reflected bundle of parallel radiation, which contributes to the transmittance and reflectance measurements. This instrument consists in a

quartz lens with an aperture of 28 *mm* and a focal length of 76 *mm*. The incoming radiation is focused to the entrance area of a y-shaped quartz fiber bundle, which enables a permanent connection to the two diode array spectrometers;

c) diode array spectrometers: the acquisition of data is realised thanks to these instruments and it is efficient in terms of timing (few seconds for one spectrum). The measured spectrum includes the wavelengths that goes from 340 *nm* until around 2100 *nm*.

Before performing the experiment, some hypothesis have to be considered. Firstly the diffuse light coming from the luminous source must be homogenous. This can be checked measuring at different distances along the light source: if for a fixed value of wavelength the measured energy is always the same, the light source is assumed homogenous. Then, the temporal stability of radiation intensity during the time period of the measurements has to be satisfied: all variations in time of the radiation intensity are not allowed and this is obtained by making use of three stabilised DC power supplies (84,6 *V*, 88,6 *V* and 120,9 *V* of voltage, respectively). One for the UV light and the others for the standard lamps. Another important point is to assure the stability of the measurements; for this reason the spectrometer should not to reach saturation. Finally, in order to avoid errors in the measurements, the glazing sample has to be cleaned. The light transmittance of the glazing is calculated from the spectral transmittance of the glazing for the visible range and considering to the sensitivity of the human eye for a white illuminant.

The experiment is performed to find the variation of the direct transmittance and reflectance with respectively 12 and 11 incident angles. A reference measure that corresponds to the dark condition is needed before starting with the measurements for the following φ angles: 0° (only for transmittance), 15°, 30°, 45°, 50°, 55°, 60°, 65°, 67.5°, 70°, 72.5°, 75°. These values are used to determine the coefficient of solar direct energy transmission τ_e, the light transmissionτ_v, the solar direct reflectance ρ_e and the absorbance, according to the EN 410.

3.2.2 Experimental results

Once all the measurements were performed, optical data (including spectral transmittance and reflectance) coming from AspectPlus need to be elaborated using another program, such as Labview (Laboratory Virtual Instrumentation Engineering Workbench) or Matlab. The first one is an established program, primarily used for data acquisition and analysis. In order to obtain results more quickly, a Matlab program has been used to plot all the main figures. The validation of the implemented program was necessary and it has been performed comparing the results with those coming from Labview. In Figure 3.7, the two different curves are shown: the direct solar transmittance implemented in Matlab (blue line) and the obtained direct solar transmittance values with Labview. The relative error between the results is acceptable, around 0,9% .

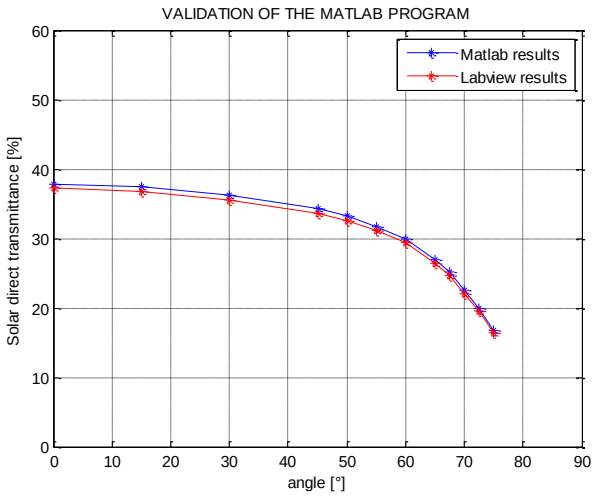

Fig. 3.7 : validation of the Matlab program; comparison between Labview and Matlab results concerning a measured IGU.

Therefore, the Matlab program can be used, in order to obtain the optical properties of measured glazing samples.

As first example, an IGU is analysed: a double glazing *Pilkington Insulight TM Sun Neutral 68/34* for building envelopes. The transmittance and reflectance in the solar spectrum were measured for the glass, from 350 *nm* to 2100 *nm*, corresponding to the wavelength limit of the solar simulator. Spectral data were obtained at angles of incidence φ between 0° and 75°. In Figure 3.8, the measured transmittance is shown as a function of the wavelengths.

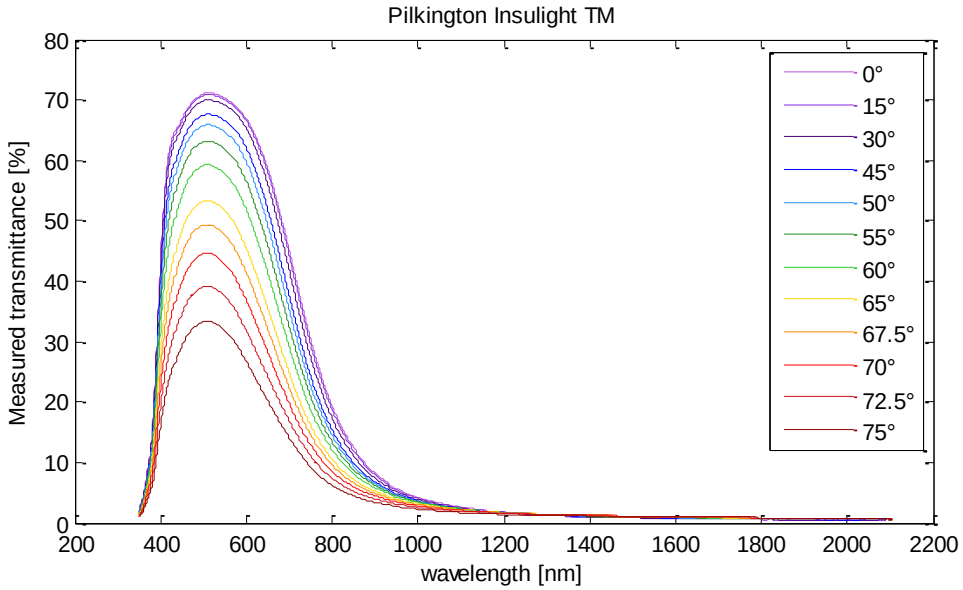

Fig. 3.8 : spectral transmittance of the Pilkington IGU; the spectra have been obtained at 12 different angles of incidence.

The transmittance is high only in the visible range of wavelength, where it has a peak at 70% at normal incidence angle, around 500 *nm*. In the infrared interval of the spectrum, the transmittance reaches very low values, closed to zero. This behaviour is typical for the IGU with selective coatings, because the aim is to avoid the overheating of the indoor ambient.

In Figure 3.9 the angular behaviour of the visible and solar direct transmittance is shown. The amount of visible transmittance is almost doubled, compared to the solar transmittance. Consequently the energy load coefficient is equal to 0,5 and it is quite constant for all the angles of incidence, except for the highest angles, where it slightly decreases. This is an indication of a good daylight exploitation.

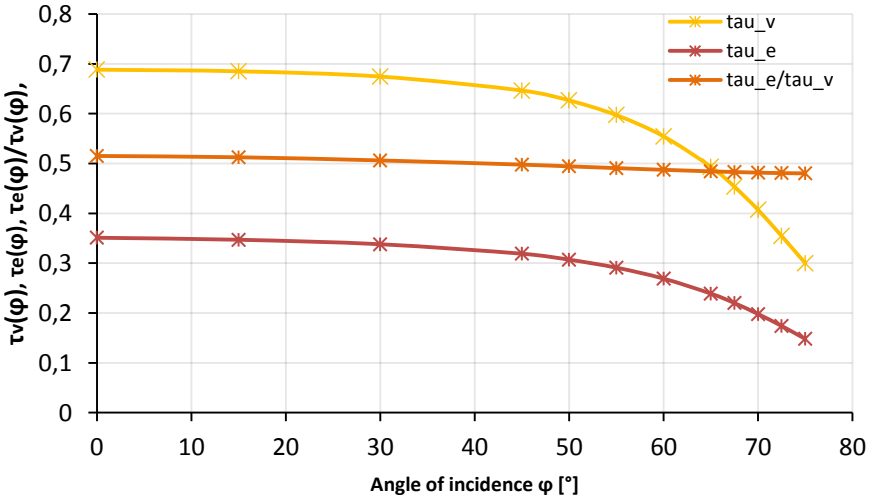

Fig. 3.9: visible and solar direct transmittance angular dependence for the Pilkington IGU. Crosses represent experimental data points.

Also reflectance measurements have been performed for both light propagation directions, corresponding to both mounting possibilities: normal mount when the radiation firstly reaches the exterior of the IG and reverse mount when it goes from the interior of the building to the outside. Figure 3.10 displays absorbance, reflectance and transmittance concerning the normal mount configuration, varying the incidence angle of the light.

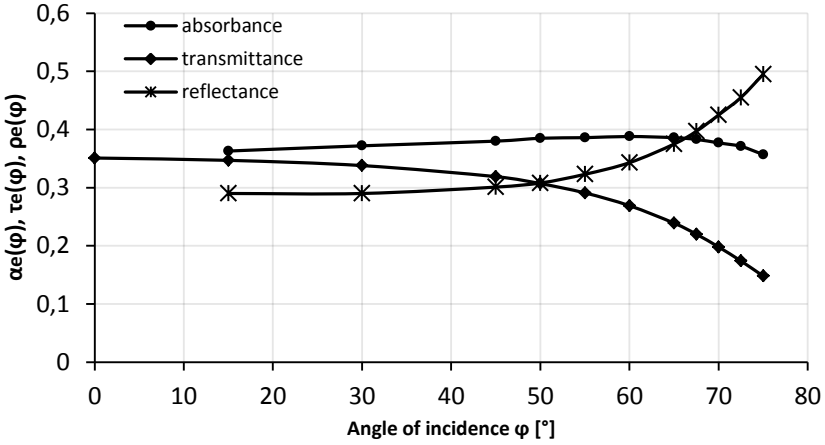

Fig. 3.10: optical properties of the Panorama IGU varying the angle of incidence φ.

It can be noticed that, as the angle of incidence of the sun light increases from 0° to 90°, the reflectance will rise more and more, especially for high angles φ (from 60°), approaching 100% for the highest angle. For angles of incidence up to approximately 40°, the reflectance remains nearly unchanged. On the other hand, the transmittance will decrease, increasing the incidence angles. The initial values of reflectance and transmittance are not so far, because there is a difference of only 6% until 30°. Then, at higher incidence angles (above 60°),the transmittance significantly diminishes and the reflectance increases amounting to 50% at 75°. The absorbance vary in a low range: it starts to be around 35% for the normal incidence, with a maximum for φ=60°, amounting to 39%. Finally it slightly decreases reaching the same value of the normal incidence. This glazing sample is intended to be installed in classical residential buildings. The transmitted energy in the infrared range of wavelength is very low, as well as in the near UV range(below 5% of transmittance when the wavelength is larger than 1000 *nm*) in order to avoid the overheating risk.

The following experiment concerns, as second example, an insulating glass unit (IGU), intended for the public transport sector. In particular this glazing (classified as *Panorama IGU*) is an application for railroad cars and it consists in a double glass fill with air. The transmittance and reflectance in the solar spectrum were measured for the glazing (between 350 *nm* and 2100 *nm*). The measured spectral data at angle of incidence φ between 0° and 75° can are displayed in Figure 3.11 and 3.12, as a function of the wavelengths.

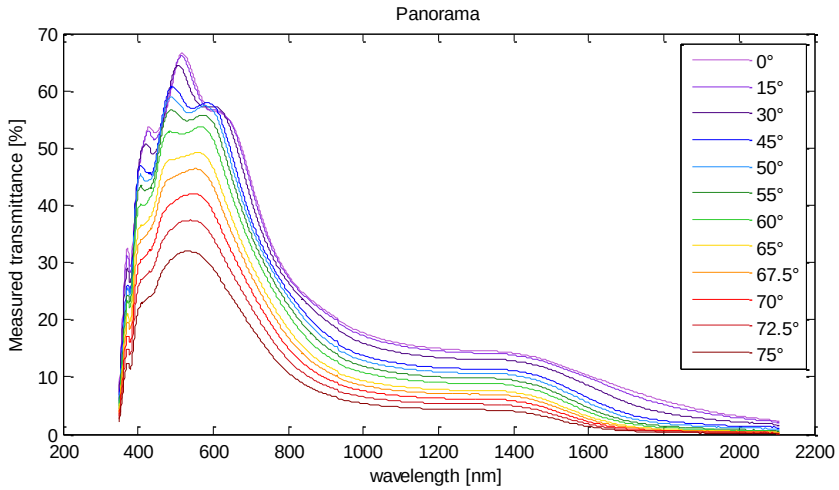

Fig. 3.11: spectral transmittance of the Panorama IGU; the spectra have been obtained at 12 different angles of incidence.

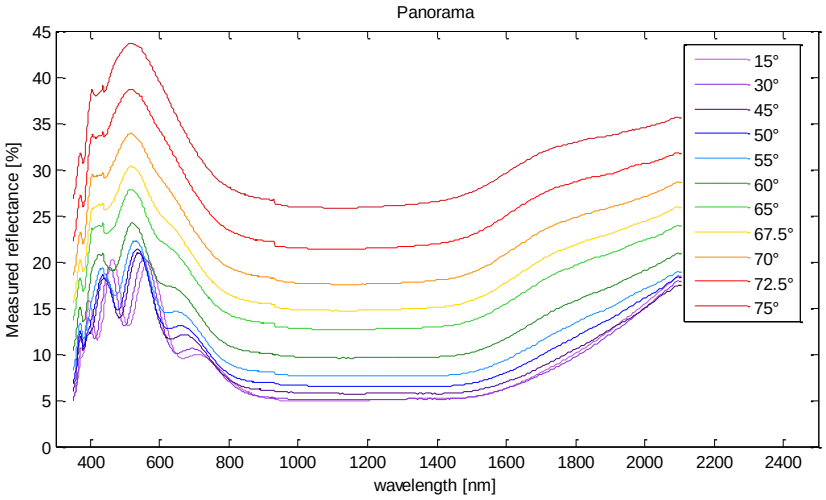

Fig. 3.12: spectral reflectance (only shown for the normal mounting) of the Panorama IGU; the spectra have been obtained at 11 different angles of incidence.

Concerning the transmittance, increasing angle of incidence, as it can be expected, it progressively diminishes. In the near UV range and in the beginning of the visible range the transmitted energy is characterized by oscillations. The main characteristic of the glass is the selective behaviour. Therefore, the maximum of the curve is in the range of the visible light while in the infrared interval of wavelength the values of the solar direct transmittance are lower: at φ=0°, for wavelengths from 780 *nm* to 2100 *nm* the transmittance is lower than 30% and it continues to decrease reaching very low values under 5%.

The reflectance has a peak in the visible range but for the infrared interval is more or less constant (around 5% for φ=0° and 25% for φ=75°). As consequence, the assumed values by the absorbance in the ultraviolet and infrared intervals are relevant, in order to prevent the indoor environment from the overheating. Moreover, the high absorbance values (around 50%) in the infrared wavelength range gives a contribution to the g-value of the glazing.

Measured transmittance and reflectance spectra are used, in order to determine the following parameters as a function of φ, according to the European Standard: solar direct transmittance τ_e, visible transmittance τ_v, solar direct reflectance ρ_e and solar direct absorptance α_e. In Figure 3.13 both the solar direct and the visible transmittance are shown. The visible part of the transmittance remains above 50% until an incidence angle of 60°. The total transmittance is between 30% and 38% when the incidence angle is below 60°. Consequently, the direct to visible transmittance ratio is 63% at normal incidence angle and becomes 55% at 75°.

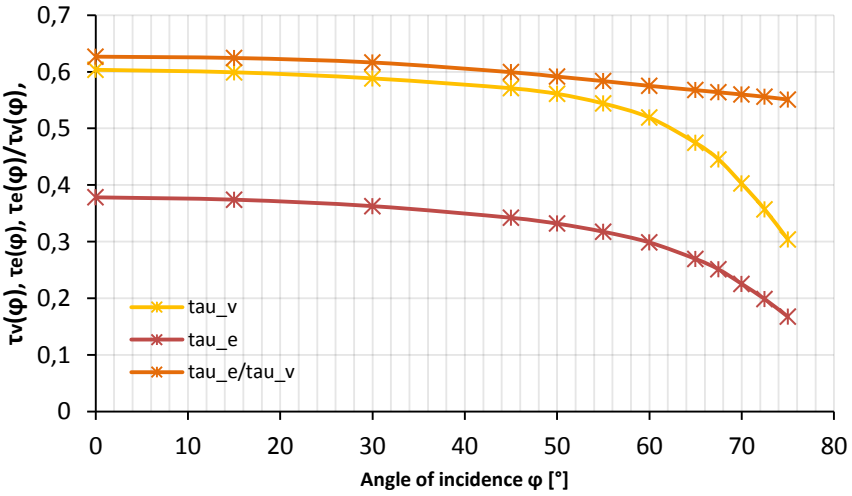

Fig. 3.13: visible and solar direct transmittance angular dependence for the Panorama IGU. Crosses represent experimental data points.

Figure 3.14 the absorbance, the reflectance and the transmittance at different incidence angles are displayed.

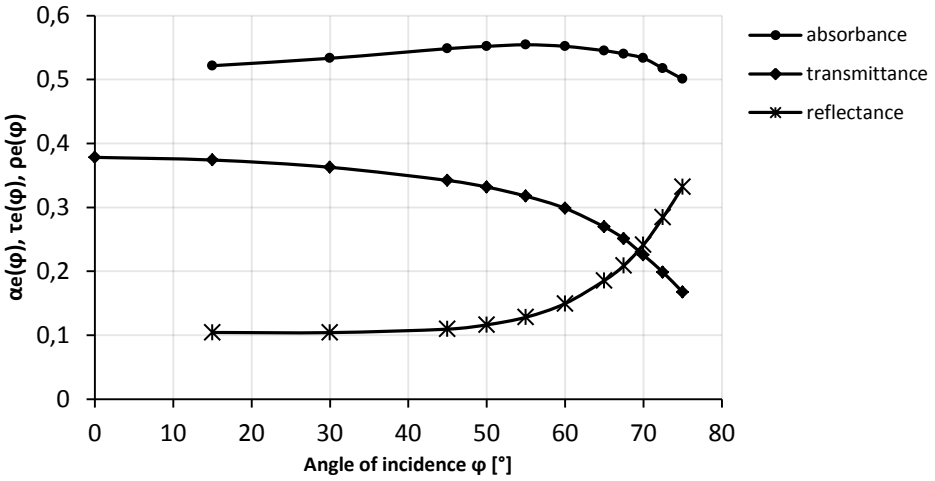

Fig. 3.14: optical properties of the Panorama IGU varying the angle of incidence φ.

The transmittance is slightly decreasing from a value of 38% at normal incidence to 17% when the angle is 75°. The reflectance is almost constant until 40° (around 10%). Then it starts to increase, reaching more than three times the initial value at φ=75°. The measurements of the transmittance and the reflectance lead to the calculation of the absorbance. The latter remains above 50% at all incidence angles, varying in a range between 50% and 55%. This second glazing sample finds his application in the transportation field. In particular, it is intended to be installed on the train carriages. Due to the fact that the glazing envelope covers a high percentage of the train carriage, the function of sun protection is crucial, in order to assure the thermal comfort of the passengers. As previously discussed, this function is guaranteed: the measured glazing has a lower transmittance in the infrared range of wavelength. Concerning wavelengths above 1000 *nm*, at normal incidence angle the transmittance is 17%, while when the incidence angle is above 50° the transmittance is below 10%. Overpassing 1800 *nm*, the transmitted energy becomes less than 5% at all the incidence angles. The sun protective property of the glazing is not best performing but it is sufficient to avoid the overheating of the train carriage.

Finally, optical properties of four semi-transparent photovoltaic modules based on dye-sensitized solar cells were obtained, according to [*Bouvard, 2015*]. All the four panels were fabricated using the same light sensitive dye and they were provided by the same manufacturer: Glass2Energie, a Swiss company which is developing semi-transparent PV modules, in order to facilitate architectural integration of renewable energy in buildings. However, they differ in terms of colours, shades and nuances. These products can potentially be promising, because they can be laminated to the glass pane of a classical glazing and installed as a classical window. As it is shown in Table 3.3, the dye coats the nanoparticles of titanium dioxide (TiO_2).

Glass2Energie

Product	Denomination	Carrier layer	Frame
14170107	Green opaque	TiO_2	Single glazing
14011717	Green transparent	TiO_2	Single glazing
14170106	Red opaque	TiO_2	Single glazing
14011722	Red transparent	TiO_2	Single glazing

Table 3.3: the four DSSCs panels optically characterized.

Figures 3.15a and 3.15b show on the left the green and red modules provide clear but yet coloured view to the surroundings; on the right only some contours can be seen through the modules.

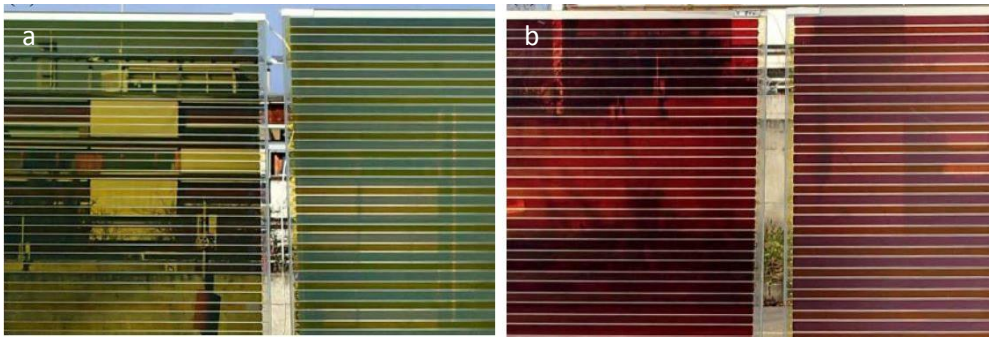

Fig. 3.15: photographs of (a) transparent (left) and opaque (right) green samples; (b) transparent (left) and opaque (right) red samples.

The set-up of the performed experiment in the LESO laboratory is illustrated in figure 3.16:

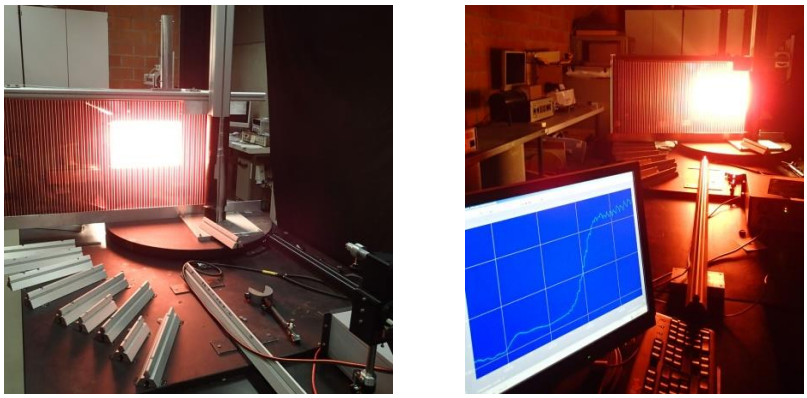

Fig. 3.16: experimental set-up for the measurements of the optical properties of the four PV modules.

The graphs below (Figure 3.17) illustrate the measured spectral transmittance and reflectance measurements, at angles of incidence φ between 0° and 75°, as a function of the wavelength. Reflectance measurements have been performed for both the exterior of the glass (normal mount) and the interior one, denoted as reverse mount.

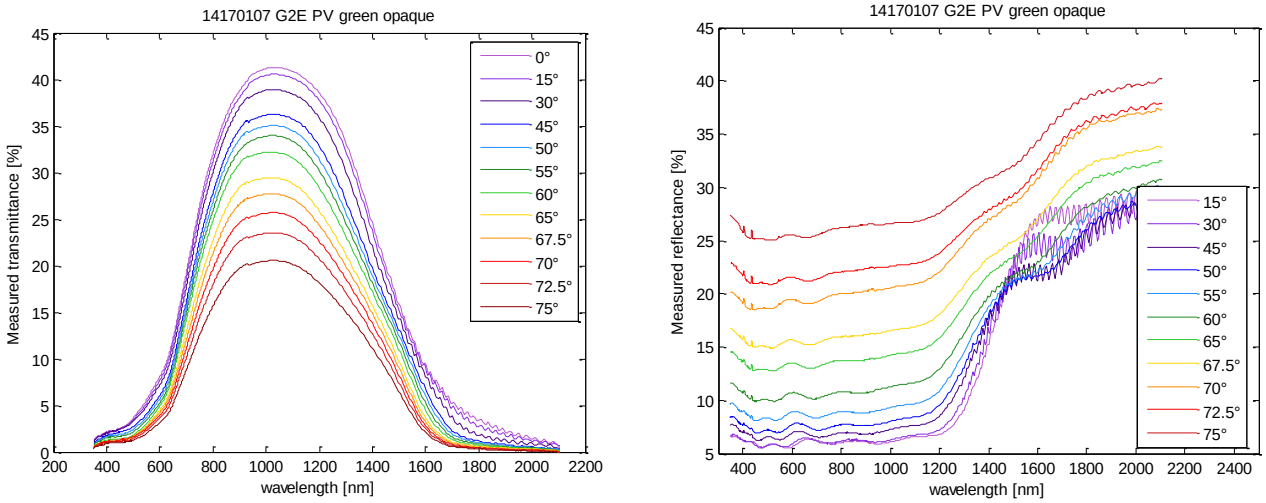

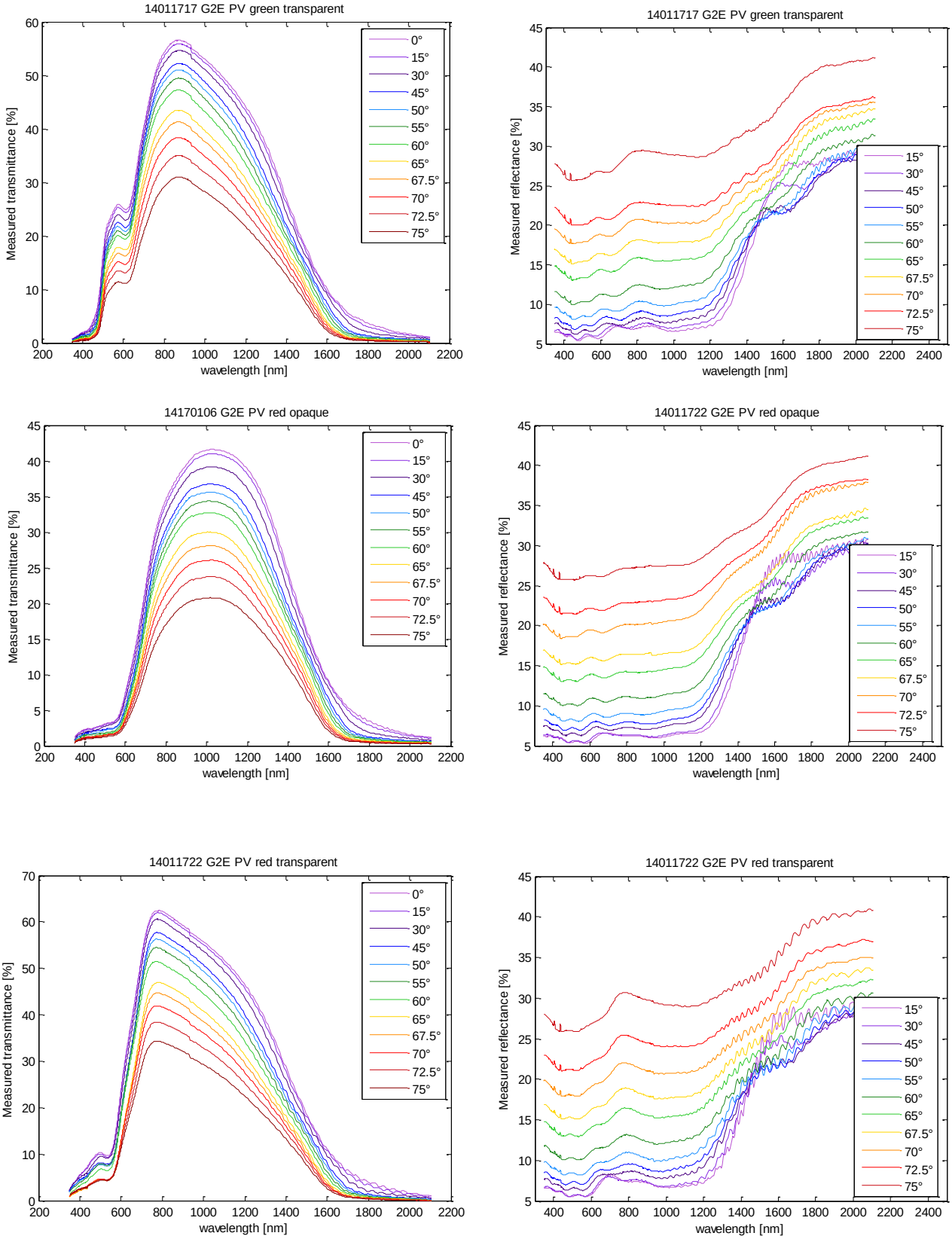

Fig. 3.17: spectral transmittance (on the left) and reflectance (on the right) for the normal mounting of four Glass2Energie PV modules; the spectra have been obtained respectively at 12 and 11 different angles of incidence.

Generally, in all the four cases, increasing the angle of incidence, the transmittance decreases. The behaviour of the four curves is similar, with a maximum placed in the infrared interval. Compared to the conventional IGU glazing, in the visible range, the transmittance of each sample is very low, due to the dye absorption. Especially concerning the

red and green opaque modules, the optical response in the 600-2100 *nm* range is very similar. For the opaque samples, the maximum transmittance is slightly above 40% at normal incidence, around 1000 *nm*. Then, it decreases in the near infrared, reaching almost zero transmittance after 2100 *nm*. In the case of the transparent modules the peak is more shifted near to the visible range. Furthermore, as it can be expected, the transmittance of the transparent modules is higher than in the opaque cases. The green module has a maximum transmittance of 56,6% at 873 *nm* and the red module reaches a peak of 62,5% at 786 *nm* (considering φ=0°).

From the measurements, it can be observed that for the opaque modules, in the visible interval of wavelength there is a particular behaviour, with one small oscillation: this is due to the fluorescence phenomenon. In fact this process could occur in certain types of dyes, when the source of UV light causes the photo-excitation of the electrons, that will emit light in a lower wavelength interval (usually in the visible range, as in this case). In order to check that the peak is due to this phenomenon, the experiment has been performed by switching off the UV lights: it can be noticed that the oscillation in the visible range is no longer present. Concerning the two green modules, they are characterized by a small peak around 500-600 *nm*; the higher transmittance in this range of wavelength gives the green colour to the modules. Concerning the red panels, below 600 *nm* the transmittance is very low (below 3%) because the dye absorbs. Then it significantly increase.

Next to the transmittance figures, the reflectance is shown: going to larger wavelengths, the reflectance increases until 40% and it presents an oscillating trend. Concerning this optical measurement, there is no a significant difference between the opaque and the transparent modules. Consequently the absorbance will present two different behaviours, for opaque modules and for the transparent one, because of the trend of the solar direct transmittance. The oscillations that can be observed in the infrared range of wavelength are probably due to the dye and to the TCO filament interference.

The spectral transmittance, the visible transmittance, the ELC, the spectral reflectance and absorbance are illustrated in Figure 3.18, as a function of the angle of incidence, for all the four modules.

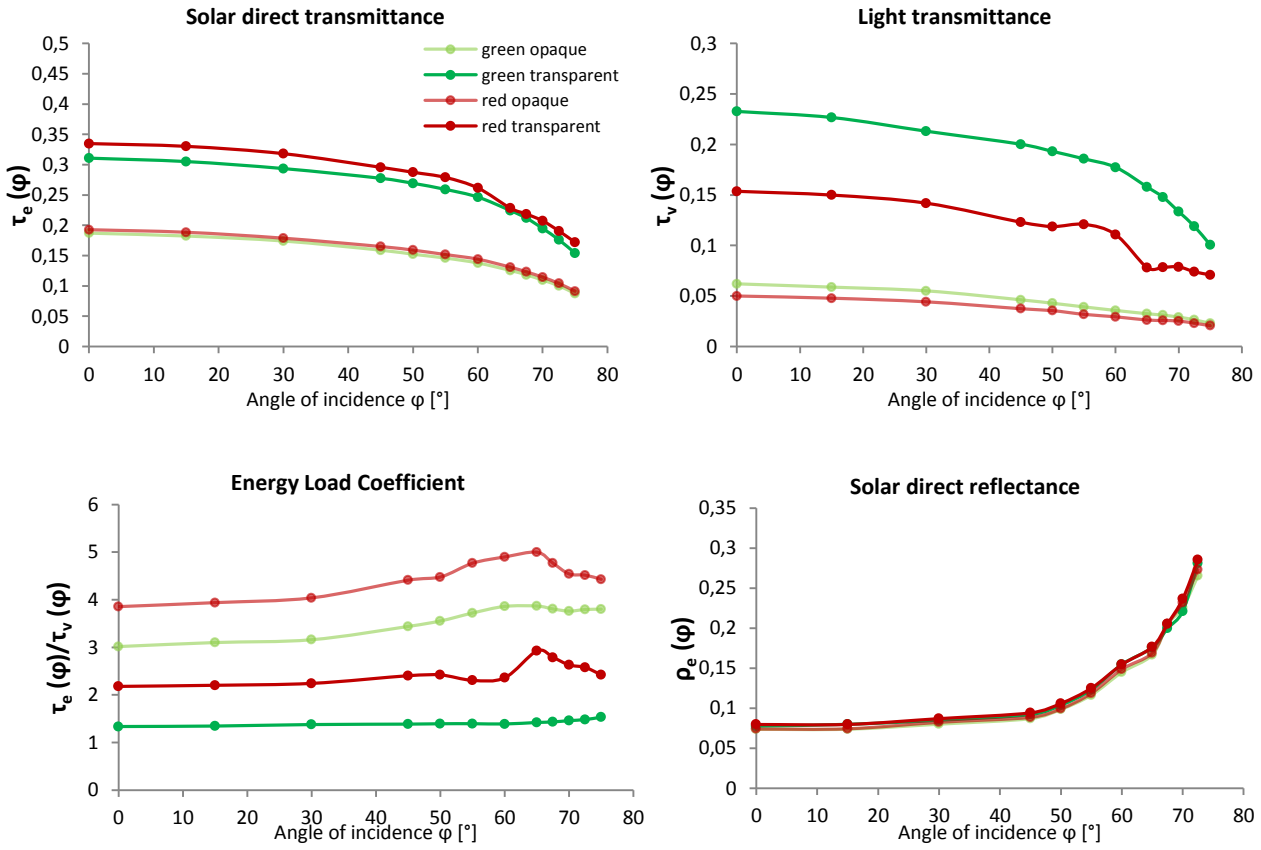

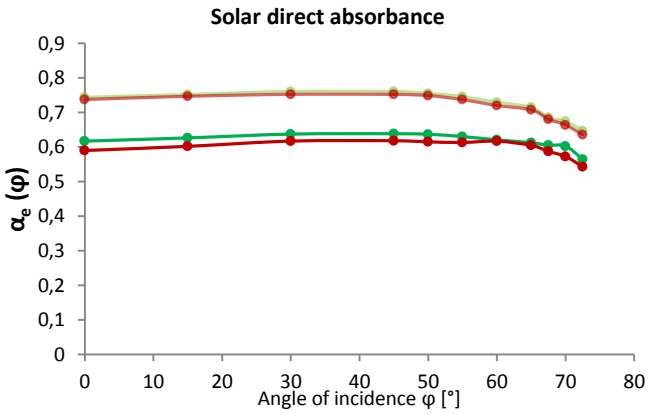

Fig. 3.18: angular dependence of solar direct transmittance, light transmittance, ELC, solar direct reflectance and absorbance for the four Glass2Energie PV modules. Dots represent experimental data points.

Concerning the solar direct transmittance, it becomes lower and lower, as the incidence angle increases. It can be noticed that the transparent modules as an higher transmittance at all the incidence angles. For the transparent is above 30% at normal incidence and remains above 15% at 75°. On the other hand, for the opaque modules, it starts to be 19% at normal incidence and it decrease until 10% at the highest incidence angle. In comparison with conventional glazing envelopes, the visible transmittance is low, reaching the maximum for the transparent modules (23% and 15% at normal incidence for the green and the red panels, respectively). The opaque modules have a light tranmittance below 5%. Consequently, the energy load coefficient is very high for the red and green opaque, remaining above 4 and 3, respectively. In general, when the energy load coefficient (ELC) is higher than 1, the glazing is not selective; the property of selectivity is relevant if the ELC has values below 0,5. Therefore, the four PV panels are not selective. The solar direct reflectance remains almost constant around 9% until an angle of 50°. Then it increases until 30% at the highest angles. It can be noticed that the four modules present almost the same values of reflectance. As result, the absorbance has similar trend to that of the transmittance. The most relevant difference, that influences the optical properties, is not the color but it's still between the opaque and the transparent modules. For example, comparing the green opaque and the green transparent PV panels, the reflectance has similar values. However, the transmittance of the transparent is higher than the transmittance of the opaque of about 10%; these values lead to an higher absorbance for the opaque PV panel, that touches the 80%. The same situation can be noticed for the red opaque and the red trabsparent modules.

In conclusion, having the function of photovoltaic modules, from the energetic point of view the performance of the opaque modules are better. However, installing these panels on a building façade, also the exploitation of the daylight has to be considered and in this case the transparent modules allow an higher intake of natural light within the indoor ambient. The final choice of the type of module is closely linked to the specific features of the building, because a compromise between the energetic and the daylighting efficiencies has to be found.

Moreover, for all four modules, the visible transmittance τ_e is lower than the solar direct one τ_v. Generally for an IGU (for example the Panorama glass previpusly analysed), the visible transmittance is higher, because of the need to have a good visual and thermal comfort. In the case of DSSCs panels the visible transmittance has very low values and this is due to the coloured dyes used for the photovoltaic effect. For an opaque module the visible transmittance is in the order of 6%, for a transparent one around 23%. The energy load coefficient has quite high values and it is lower for the transparent modules. Therefore, in order to not have a disadvantage on daylighting, it is advisable to install them on no more than one façade.

In Table 3.4 ,the measured values for the reflectance in the reverse mount side are shown.

Reverse mount REFLECTANCE				
φ [°]	**Green opaque**	**Green transparent**	**Red opaque**	**Red transparent**
15	0,0737	0,0778	0,0743	0,0796
30	0,0733	0,0783	0,0744	0,0794
45	0,0798	0,0853	0,0803	0,0870
50	0,0863	0,0922	0,0874	0,0941
55	0,0958	0,1045	0,0982	0,1061
60	0,1159	0,1227	0,1177	0,1251
65	0,1467	0,1550	0,1471	0,1554
67,5	0,1678	0,1747	0,1629	0,1773
70	0,1992	0,2046	0,1965	0,2044
72,5	0,2293	0,2391	0,2286	0,2390
75	0,2711	0,2823	0,2741	0,2861

Table 3.4 : reverse mount reflectance values for all the four PV modules.

Moreover, the evaluation of the Colour Rendering Index (CRI) has been performed. This index allows to quantitatively evaluate the ability of the sample to reveal the colours of the various objects in the environment. The highest possible value for the CRI is 100 (black body as source). The calculations have been performed according to the EN 410, by assessing the colour rendering of eight different colour standard illuminated with a standard light source through the glazing sample. A CRI above 90 indicates high colour neutrality. Results are shown in Table 3.5:

Denomination	**CRI**
Green opaque	54,5
Green transparent	70,8
Red opaque	29,4
Red transparent	35,1

Table 3.5: CRI of the four PV modules.

As it can be noticed, the green modules result to reveal better than the red modules: their CRI overpass 50. The reason is linked to the green colour, that allows to give the object around a more natural colour. The red opaque module has the lowest CRI, equal to 29,4%.

In conclusion, all these analysed optical properties may readily be compared for different glass fabrications, in order to select the most appropriate glass material for the specific building application. The final purpose of these experimental studies is to select glazing basing on their optical properties, for a high efficiency of the glazed façades. The choice has to be made regarding the energetic point of view (cooling and heating), the visual comfort issue (glare risk and daylighting) and the aesthetic one. Due to their very limited visible light transmittance, these modules cannot be used as a proper window. However they can be used in combination with windows having high visible transmittance. Furthermore the view through the PV modules is clear but coloured. Therefore, where decorative colour is desired, light effects similar to stained glass can be obtained, such as in the Swiss Tech Conference Center in Lausanne. In highly glazed buildings, the part of the façade that includes photovoltaic dye-sensitized modules, can provide a fraction of the energy demand of the building.

3.3 Example for thermal characterisation

The experimental set up with a corresponding example for the thermal characterisation of the samples is described. The aim is the determination of the angular dependent solar gain factor (g-value(φ)) of an insulating glass unit. The method is based on the optically measured angular dependent solar transmittance $\tau_e(\varphi)$, coming from the experiment described previously, and on the determination of the heat transfer factors q_e and q_i from the outer and the inner surfaces of the insulating glass to the ambient under simulated solar radiation.

3.3.1 Method

The solar gain factor for a IGU is an important parameter for calculating the internal heat load or making dynamical simulations for buildings and for realistic simulations g-value must be known as a function of the light incidence angle φ.

Factor g is given by the equation 3.10:

$$g = \tau_e + q_i \quad (3.10)$$

Where the solar direct transmittance τ_e is obtained by the experiment for the optical characterisation of the samples. While q_i is the secondary internal heat transfer factor, that can be calculated for normal light incidence through a complex procedure, that requires the knowledge of the spectral transmittance, reflectance and absorptance of all the individual components (glass panes and if present polymeric membranes and low-e coatings) and of the thermal conductance coefficients between adjacent pairs of components. Therefore, an alternative approach is needed in order to predict angular dependency of g-value without having to perform a large amount of measurements or detailed calculations. This direct and efficient experimental method is explained below, according to [*Steiner et al., 2005*].

Since the solar direct transmittance τ_e (φ) and the solar direct absorptance α_e (φ) are known from the optical characterisation of glazing samples previously explained, the only missing information is how the solar absorptance is split into the heat flows q_e and q_i from the outer and the inner glass panes' surfaces to the ambient, being valid the following equation (3.9):

$$\alpha_e = q_i + q_e \quad (3.9)$$

The two heat transfer coefficients are determined experimentally thanks to a solar simulator that irradiates the glass sample with radiation closed to the solar spectrum by measuring the outer and the inner surface temperatures of the IGU. The temperature increments are related to the heat flows from the surfaces towards the ambient in the quiescent air, according to heat transport theory for free convection flows at vertical plates.

The secondary internal heat transfer factor q_i depends on the external and internal heat transfer coefficients h_e and h_i, that are fixed in the European Standard EN 410 to h_e = 23 W/m^2K and h_i =8 W/m^2K. Since the experiment is not performed in these conditions, because it will required a forced convection of the order of 4 *m/s* at the outer surface and an internal surface temperature of 12 *K* with respect to the ambient, q_i for standard conditions has to be computed. An advantage of this procedure is the ability to compute q_i for any conditions of interest, which may considerably deviate from the standard conditions, such as for insulating glass units installed in vehicles (like railroad cars or busses).

In Figure 3.19, the scheme used for the transformation of heat flows determined in the experiment (q_i^1 and q_e^1) to the corresponding values for standard conditions (q_i^N and q_e^N).

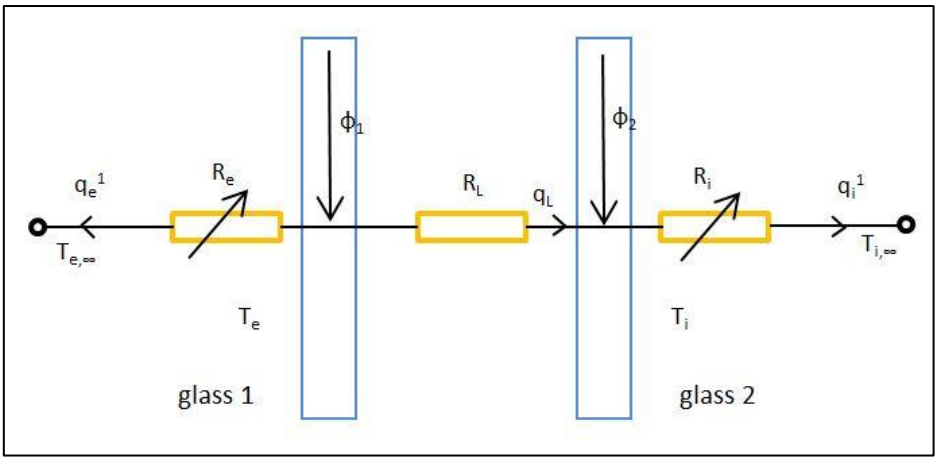

Fig.3.19: schematic illustration of heat flows and temperatures in the double glass IGU [*Steiner et al., 2005*].

The ambient temperatures have been set to $T_{e,\infty}$ = 0°*C* and $T_{i,\infty}$ =0°*C*. R_e and R_i represent respectively the external and internal reciprocal surface heat transfer coefficients, and R_L is the reciprocal heat conductance coefficient of the IGU, excluding the outer and inner surface heat transition. ϕ_1 and ϕ_2 represent heat flows in W/m^2, originated from the absorption of the solar radiation in the two glass panes. The sum is known in the experiment:

$$S\,\alpha_e = \phi_1 + \phi_2 \quad (3.12)$$

Where S represents the intensity of the incident radiation in W/m^2.

ϕ_1 and ϕ_2 can be calculated as follows:

$$\phi_1 = q_e^1 + \frac{T_e - T_i}{R_L} \quad (3.13\text{ a})$$

$$\phi_2 = q_i^1 - \frac{T_e - T_i}{R_L} \quad (3.13\text{ b})$$

From ϕ_1 and ϕ_2 the corresponding parameters for the standard conditions are obtained:

$$q_e^N = \frac{\phi_1 R_L + \phi_1 R_{i,N} + \phi_2 R_{i,N}}{R_L + R_{i,N} + R_{e,N}} \quad (3.14\text{ a})$$

$$q_i^N = \frac{\phi_2 R_L + \phi_1 R_{e,N} + \phi_1 R_{e,N}}{R_L + R_{i,N} + R_{e,N}} \quad (3.14\text{ b})$$

Finally the angular dependant $q_i(\varphi)$ is obtained through the knowledge of the angular dependant solar direct absorptance $\alpha_e(\varphi)$ [*Steiner et al., 2005*]:

$$q_i(\varphi) = \frac{q_i^N\,\alpha(\varphi)}{q_i^N + q_e^N} \quad (3.15\text{ a})$$

$$g(\varphi) = \tau_e(\varphi) + \frac{q_i^N\,\alpha(\varphi)}{q_i^N + q_e^N} \quad (3.15\text{ b})$$

3.3.2 Experimental set up

In Figure 3.20, the experimental set up is shown: the light source consists of a water-cooled xenon high-pressure arc lamp (1000 [W]) with an elliptical aluminium reflector. The use of specific filters improve the spectral distribution of the radiation in order to achieve a close match to solar radiation. The distance between the light source and the glazing sample is of order of 5 to 7 *m*. The central light intensity close to the sample is around 200 W/m^2 and a circular light spot with a diameter of about 60 *cm* is obtained; this light spot is positioned with its centre corresponding to the

thermocouples installed on the sample. These thermocouples, glued to the glass surface, are used to measure internal and external temperatures as a function of time along with two ambient temperatures, T_1 positioned centrally underneath of the glass and , T_2 representing the room temperature more remote from the glass.

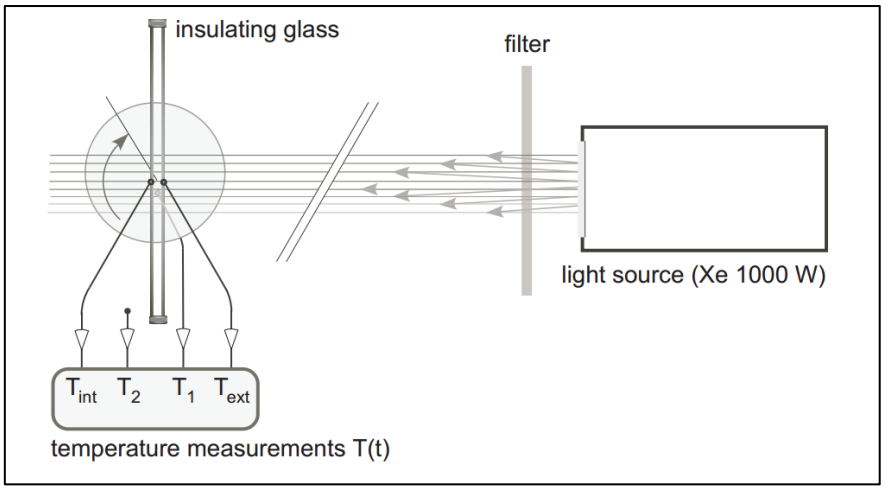

Fig. 3.20: experimental set-up for the determination of total solar energy transmittance g(φ) consisting of solar simulator light source, matching filter and temperature measurement [*Steiner et al., 2005*].

The experiment is located in a large room, without heat load by direct solar light that could minimise the long term drifts of ambient temperature during the experiment. After the experiment data are elaborated in order to obtain the angular behaviour of the solar heat gain coefficient.

3.3.3 Experimental results

For the determination of the solar heat gain coefficient, results are shown only for the sun protection glass Pilkington Insulight TM Sun Neutral 68/34, that has the U-value equal to 1,1 W/m^2K. Figure 3.21 shows the obtained temperature measurements $T_e(t)$ for the external, $T_i(t)$ for the internal and $T_a(t)$ for the air temperature underneath the IGU. Ambient temperature is recorded to identify possible general rise of temperatures. The measurements have been performed for around 8 hours.

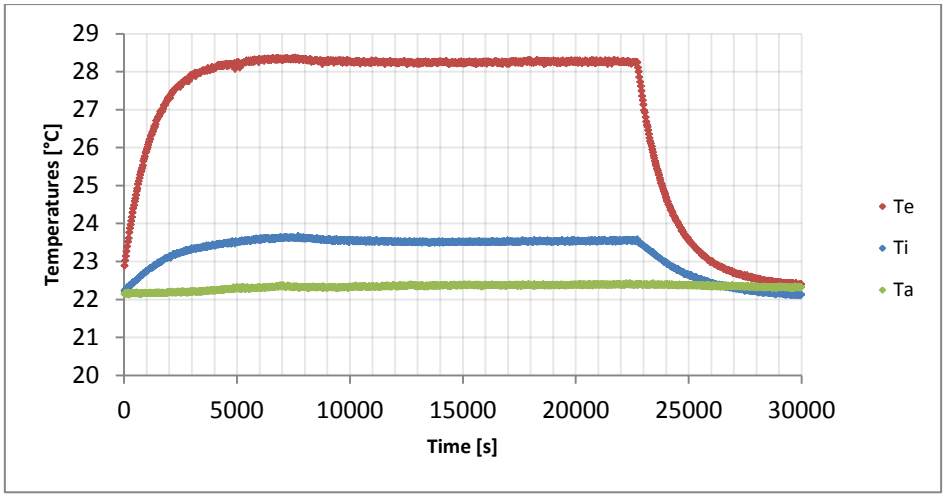

Fig. 3.21: surface temperature measurements at the sun protection glass Pilkington.

At the beginning, every element has the same temperature, and then the light source is turned on facing the exterior glass pane. After approximately one hour and half, a stabilization of the temperatures is observed. The temperatures of the exterior glass pane and the interior glass pane at stabilization are used to determine the internal coefficient of

heat transfer q_i. Once q_i is known, it is possible to calculate g(φ) as a function of the angle of incidence by using the solar direct transmittance previously found. Calculations are listed below.

From the above values for $T_e(t)$ and $T_i(t)$, the increments amounts of temperatures (compared to the air temperature) and the heat transfer coefficients obtained are:

$$\Delta T_e = 5{,}8\ °C \qquad h_e = 7{,}08\ \left[\frac{W}{m^2 K}\right]$$

$$\Delta T_i = 1{,}25\ °C \qquad h_i = 6{,}34\ \left[\frac{W}{m^2 K}\right]$$

From these values the heat flows under experimental conditions are:

$$q_e^{\,1} = \Delta T_e\, h_e = 41{,}04\ \left[\frac{W}{m^2}\right]$$

$$q_i^{\,1} = \Delta T_i\, h_i = 7{,}92\ \left[\frac{W}{m^2}\right]$$

Finally for the heat flows under standard conditions from equation 3.14(a) and 3.14(b):

$$q_e^{\,N} = 46{,}94\ \left[\frac{W}{m^2}\right]$$

$$q_i^{\,N} = 2{,}02\ \left[\frac{W}{m^2}\right]$$

Now the angular dependant $q_i(\varphi)$ is obtained through the knowledge of the angular dependant solar direct absorptance $\alpha_e(\varphi)$. Knowing also the angular dependence of the transmittance, the solar heat gain coefficient as a function of the angle of incidence can be obtained (Figure 3.22):

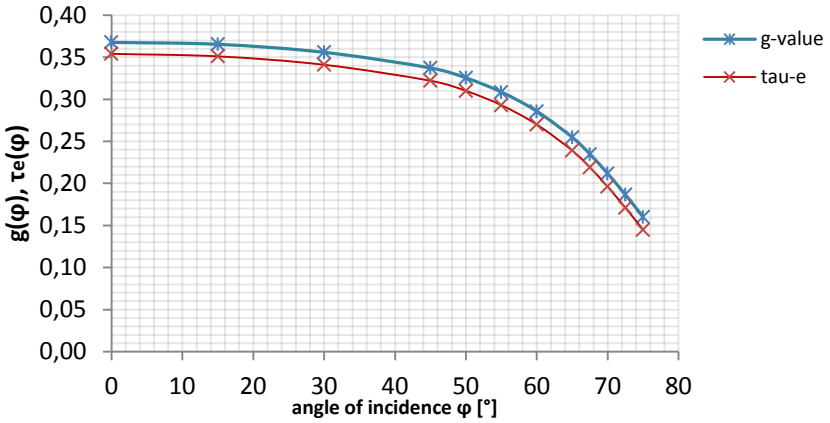

Fig. 3.22: solar gain factor g(φ) and solar direct transmittance τe(φ) of the sun protection glass Pilkington. Crosses represent experimental data points.

At normal incidence the total energy transmittance is g(0°)=38,8%, while the direct energy transmission is 35,4%. An amount of energy equal to 3,4% is re-emitted inside the building. Comparing the transmittance and the solar heat gain coefficient, clearly it's revealed that the solar direct transmittance represents the dominant contribution; this it is due to the fact that most of the absorbance is lost outside and it is not converted in heat flow. However the solar heat gain coefficient is not too high; in fact for a sun protection glass the g value usually assumes values from 0,3 and 0,7, depending on the climate and on the type building. For example, if the aim is to avoid the overheating, the lower is the g-value, the better is the performance of the system.

4 Embedded microstructures for glazing envelopes: parametric study

The following chapter contains a general overview on the subject about the second part of this thesis. The analysis is now focused on a novel complex fenestration system for glazing envelopes. Firstly the description of the glazing device is performed; therefore the explanation of the ray tracing program used for the simulations of the building follows. The set-up of the parametric case study is necessary, in order to properly consider all the variables that play a relevant role in influencing the thermal control of the building. Finally the considered assumptions are mentioned and the input data of the problem and the adopted method are explained in the last paragraph.

4.1 Embedded microstructures technology

Today the glazing is a widely used structural façade component, that has the function to create comfortable working or living spaces. Conventional fenestration systems are not the best solution if the growing importance of smart energy management and low carbon emissions has to be taken into account. Single glazed windows have been the weak part of the building's shell for centuries. Meanwhile double glazing with low emissivity coatings and noble gases have become the standard for a low overall heat transfer coefficient (U-value), good insulation and reduced energy losses. This property applies mainly during the heating season when temperatures outside are lower than inside; in the cooling season however, large surfaces of transparent material create high thermal gains due to transmitted radiation. These gains can be reduced with the sun protection glazing by lowering transmittance. The important thing is that, in the in the visible range of the spectrum, the transmittance is maximized and in the infrared and the ultraviolet range it's minimized, in order to maintain a good level of light for the visual comfort issue. This kind of double glazing therefore has a high value of visible transmittance and a low total energetic transmittance and can have a positive impact on the reduction of visual discomfort and cooling loads. Furthermore, too high values of visible transmittance can lead to a problem, such as glare. On the other hand, a low value of total energy transmittance could cause the increase of the heating energy consumption during the cold season.

Therefore, fenestration systems play a very important role in the energetic balance of the building, having impact both on the thermal and visual comfort. Windows can lead to high solar gains and glare problems. Both can strongly influence the energy consumption and the indoor comfort.

Due to the fact that building envelopes are subjected to important energetic constraints, a compromise has to be found in order to identify a good solution both for thermal control and for daylighting performances. A novel CFS, using embedded microstructured in the glazing, was proposed. It can ideally achieve good lighting levels and a smart management of the seasonal thermal control. This novel technology is a static device and it potentially presents an economic advantage. In the future development, microstructured glazing can be characterized by a rather easier integration, combined with the low cost of the product (roll to roll fabrication) [*Kostro et al., 2012*].

The present study is focused on this embedded microstructured glazing, trying to analyse their influence on seasonal thermal loads. The control of solar gains through this novel CFS technology requires less admittance of direct light into the space during cooling seasons, and a higher total energy transmittance during the heating season. At the same time, this glazing envelope provides a good lighting level to guarantee the visual comfort. It is interesting to compare this novel angle dependent system, that accepts heat gains in cold months and rejects them in the hot season, with the conventional glazing envelopes, from the energetic point of view.

4.2 Simulation framework and tools

In order to perform the parametric studies, the ray tracing program developed by Kostro André was used to carry out all the simulations and calculate hourly heating and cooling requirements in the building. This software can take into

account complex geometrical characteristics for the modelling of glazing envelopes and material features, such as refractive indices or absorption coefficient. It can be used for the statistical evaluation of the bidirectional transmission distribution function of CFSs. In particular, it is adapted to compare CFS performance with conventional fenestration systems.

This simulation program is based on Monte Carlo algorithms, that randomly describe the distribution of physical phenomena (reflection, refraction, absorption), according to their physical law. The accuracy of the result depends on the number of the random paths. Ray tracing is the most suitable technique to model the path taken by the light, passing through the optical device, in order to reach the indoor environment. [*Kostro, 2014*].

The following parametric analysis is focused on the energetic performance of the novel CFS, according to the angular dependence of the transmittance. With such an angular dependent transmittance, the solar gains vary greatly over time. A nodal thermal model is used to derive the hourly thermal loads for a certain space. The thermal gains depend on the CFS geometry but also on the location and time dependent variations of the irradiance distribution of the sky [*Kostro, 2014*]. For accuracy, direct and diffuse irradiance are computed separately. The location dependence on the hourly solar path is considered for the direct radiation. A realistic sky luminance distribution is considered for diffuse irradiance, according to the Perez model [*Perez et al., 1993*]. There are three main variables that strongly influence the climate: the temperature, the irradiance and the sky luminance distribution over the year. Temperature and irradiance data are provided for each location by direct measurements during the year, thanks to meteorological stations. The Perez Model consists in a parameterisation of the insolation conditions. It's a widely used model for the determination of the sky luminance and is also used by Meteonorm. To define the distribution of the sky, five coefficients, function of insolation conditions, are included in a mathematical expression; these coefficients can be adjusted to account for luminance distributions ranges from totally overcast to very clear. Therefore the level of clearness of the sky is evaluated through a scale of values that go from 1 to 8, where 1 corresponds to the most overcast sky and 8 to the clearest condition.

Many parameters characterize the microstructured glass geometry. This novel CFS comprises parabolic micro-mirrors, combined with a series of vertical reflectors, as it can be seen in Figure 4.1 [*Kostro et al., 2012*].

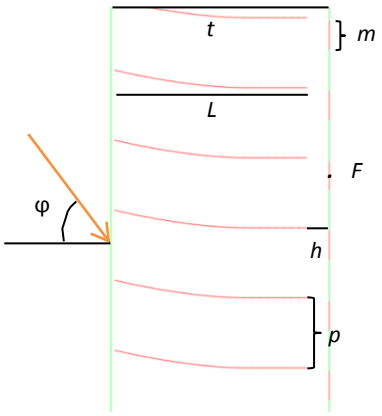

Fig. 4.1: geometric characterization of the embedded microstructures.

The ray tracing program allows to define the following parameters:

a) PMMA thickness *t*, that corresponds to the thickness of the PMMA polymer film;
b) concentrator length *L*: the length of the parabolic embedded mirrors in the PMMA polymer film;
c) sub segments: are the number of segments forming the parabolic mirrors;
d) count *n*: it is the number of vertical reflectors (in Figure 4.1 *n*=6);
e) mirror at focus *m*, corresponding to the length of the vertical reflectors;
f) period height *p*, that is the period between two parabolic mirrors;

g) focus offset *F*: it is the point in which the focus of the parabola converges (the focal point is on the back side of the CFS);
h) horizontal offset *h*: it is the offset between the parabola ending point and the focal point;
i) incoming focus angle φ, corresponding to the incident angle of the sun light through the glass.

It is possible to set all these parameters, in order to define a suitable geometry of the embedded micro-mirrors. In this thesis the aim is to evaluate the thermal performance of this glazing envelope. Therefore all the geometric parameters are set in order to minimize the annual thermal loads.

4.3 Parametric study definition

A parametric study consists in an analysis taken to describe and examine the different relations amongst various variables. These variables are called parameters and they describe sets of input values; each input value specifies one application execution, which is referred to a particular aim. In order to perform this analysis, different sets of input parameters are carried out, through simulations.

The general objective of this parametric study has the purpose of investigating the influence that the installation of the embedded microstructures for glazed façades has on the thermal loads of the building, in terms of energy consumption. The final aim is to identify the best performing solution in terms of glazing envelopes, trying to achieve the minimization of heating and cooling demand for an office room. All the simulations are performed based on the program described in the previous chapter. The adopted iterative approach foresees the analysis of a sequence of parametric studies, to reach the best possible configuration for each considered range of latitude and for different building's typologies. Numerous parameters influence the performance of such embedded microstructures for glazing envelopes: microstructure geometry, latitude, orientation, climate conditions as well as geometry and thermal properties of the considered room. Two parametric analysis have been performed in this project work. The first one is focused on the study of the thermal performance of the microstructured glass at different latitudes. The second study concerns the evaluation of the microstructured glazing performance for different building configurations, in the same location.

As starting point, in the first study, the influence of the latitude is considered; defining the room configuration in terms of geometry and thermal properties and optimizing the microstructured glass in terms of blocking angle and blocking width for a particular location, the parametric analysis is performed in order to evaluate the thermal loads as a function of the latitude, that is related to the climate, the irradiance and the temperature. The final aim is to find the best performing microstructures for different ranges of latitude and then to evaluate the amount of energy savings that can be reached during the year.

The second parametric study involves other kind of variables; it concerns the evaluation of the influence of the type of building on the thermal loads. The purpose is to determine the impact of various geometric and thermal characteristics of the reference room on the energy consumption of the building, comparing the embedded microstructure solution with more conventional glazing envelopes. For each range of latitude identified in the first analysis, for which the optimisation of the microstructured glass was performed, three building configurations have been defined. Energetic performances of the glazing envelopes are analysed for each type of building, as a function of the transmittance of the window and of the window to wall ratio. This approach is needed because of the complex relationship between all the variables that play a key role regarding the influence on the thermal control of the building.

4.4 Hypothesis

The following assumptions have been made, in order to perform the simulations.

Firstly, the parametric study has been performed supposing that the considered glazing envelope, that can be a microstructured window, a solar glass or a standard double glass, is always installed in the south orientation of the

room; in other words the azimuthal angle for the glazed façade is equal to 0°. This corresponds to the optimal orientation, that brings to the maximum value of solar gains during the cold season.

A realistic sky luminance distribution is considered in each location for diffuse irradiance, according to the Perez model [*Perez et al., 1993*]. The location dependence on the hourly solar path is taken into account for the direct irradiance.

The chosen locations are at many different longitudes but as first approach, the longitude is not considered as a parametric variable because the hypothesis is that the type of microstructure is influenced by the latitude; different longitudes can slightly influence the microclimate of the zone but this point will be considered for the climatic classification in different regions.

The strong angular dependence of the transmittance of light rays creates an intrinsic seasonal control. Ray tracing simulation can be used to design and optimise a novel static optical system that takes into consideration both the daylighting aspect to reach the visual comfort and the thermal aspect to reach energy savings [*Kostro, 2014*].

The optimization of the embedded micro-mirrors geometry has been performed mainly focusing on the minimization of the cumulated annual thermal loads that the heating-cooling system has to provide.

4.5 Input data and methodology

Considering the big amount of variables that have to be considered , influencing the annual thermal loads, in the Table 4.1 the system of matrices and parameters is shown.

<table>
<tr><th></th><th>CLIMATE</th><th colspan="2">MICROSTRUCTURED WINDOW</th><th>ROOM</th></tr>
<tr><td rowspan="2">MATRICES</td><td>Direct and diffuse irradiance</td><td rowspan="2">Geometry of micro-mirrors</td><td rowspan="3">Bidirectional Transmission Distribution Function (BTDF)</td><td>Thermal model</td></tr>
<tr><td>Distribution of the sky</td><td>Daylight model</td></tr>
<tr><td rowspan="3">PARAMETERS</td><td>Location</td><td>Blocking angle and width</td><td>Geometry</td></tr>
<tr><td>Micro-climate</td><td rowspan="2">U-value</td><td rowspan="2"></td><td>Thermal properties</td></tr>
<tr><td>Temperature and irradiance</td><td>HVAC system</td></tr>
</table>

Table 4.1: overview on the set up of the performed parametric study.

There are three main key elements having an impact on the energy balance of the building. Firstly the climate variable, including the site (longitude and latitude), the temperature and the irradiance data. Then the glazing envelope (microstructured window), for which the geometry have to be properly defined. The blocking angle and width correspond to the range of solar elevation angle for which the micro-mirrors avoid the entrance of the light inside. Consequently, for these incoming angles the transmittance is low. The value of the thermal transmittance of the window is another input. The third important element that has to be defined is the test room. Input data such as the geometry and the stratigraphy of the walls with related thermal properties have to be described. The efficiency of the HVAC system providing energy to the building has to be defined.

All these parameters concerning the meteorological data, the glazing envelope characteristics and the reference room properties have to be set. Moreover, the program is based on a set of matrices, allowing to carry out simulations. Regarding the climate, hourly data for the direct radiation and the luminance distribution of the sky are considered. Concerning the CFS system, the matrix is based on the BTDF (Bidirectional Transmission Distribution Function), in order to characterized the angularly transmission of light [*Kostro et al., 2014*]. Finally, for the room two models are used by the program: the daylight model and the thermal model. The analysis of this study is focused on the thermal performance. Therefore, simulations are performed using only the thermal model in the ray tracing program. This is based on the discretization of the building system in nodes, in order to evaluate the heat flux [*Kostro, 2014*].

5 Case study locations

In this chapter the first parametric study has been performed to study the thermal performance of CFS in a set of locations. For all the simulations, the geometric and thermal properties of the reference office room were considered fixed. A glazed microstructured envelope is installed on the building façade of the office room. The final aim is to optimize the geometry of the embedded microstructure, mainly regarding the blocking angle range, for a particular range of latitude. The thermal loads overall the year can be quantified, as a function of the latitude. Results are obtained also for a standard glazing envelope and a solar glass, to perform a comparative analysis on the annual energy savings.

5.1 Choice of the locations and climatic analysis

Complex fenestration systems, in particular embedded microstructures on which this analysis is focused, unlike standard fenestration systems, have a very angular dependent transmittance. Consequently, the incident solar elevation angle on the façade surface is a critical variable in assessing their performance and this parameter is strictly linked to the latitude. Moreover, when aiming to describe annual performance, it is necessary to comply to realistic climate conditions. The definition of the locations for assessment of CFS performance has two implications. First, solar position depends on both latitude and longitude. However, it is more dependent on latitude because for longitude, there are the conventional time zones, that take into account the variation in sunrise and sunset time associated with different longitudes coordinates. Second, locations are associated with particular climate conditions; these conditions are evaluated on the basis of meteorological variables, such as the incident solar radiation and the outdoor temperatures. Therefore, both latitude and climatic conditions contribute to the variability in performance of the embedded microstructures across different locations.

In order to perform an accurate analysis of the influence of latitude on the type of microstructure installed, it is sufficient to focus the study on the European continent, because it offers the proper variety of microclimatic zones. Twenty-two locations were selected, evenly distributed over Europe, in order to study the behaviour of different types of embedded microstructures over the diversity of European climates. The locations were properly chosen in a range of latitude between 38°N and 60°N, in order to illustrate the diversity of European climates (Figure 5.1). In Table 5.1 the list of case study locations with the relative latitude, longitude and altitude above sea level is shown.

	Athens	*Madrid*	*Rome*	*Marseille*	*Turin*	*Lausanne*	*Zurich*	*Wien*	*Munich*
Latitude [°]	38,0	40,5	41,8	43,4	45,2	46,5	47,4	48,3	48,4
Longitude [°]	23,7	- 3,7	12,6	5,2	7,7	6,7	8,6	16,4	11,8
Altitude [m]	107,0	669,0	131,0	6,0	282,0	461,0	556,0	209,0	447,0

	Strasbourg	*Paris*	*Prague*	*Frankfurt*	*Gent*	*London*	*Berlin*	*Hamburg*
Latitude [°]	48,6	48,8	50,0	50,1	51,0	51,5	52,5	53,7
Longitude [°]	7,6	2,3	14,5	8,6	3,8	- 0,1	13,4	10,1
Altitude [m]	150,0	75,0	304,0	111,0	15,0	77,0	50,0	49,0

	Copenhagen	*Glasgow*	*Goteborg*	*Stockholm*	*Bergen*
Latitude [°]	55,7	55,9	57,7	59,3	60,4
Longitude [°]	12,3	- 4,5	12	18,1	5,3
Altitude [m]	28,0	59,0	4,0	52,0	12,0

Table 5.1 : considered European locations for the evaluation of the influence of latitude on the thermal performance of the glazing envelopes.

Fig. 5.1: map of the twenty-two chosen locations in Europe at different latitudes.

Geographical and meteorological data for all case study locations are taken from the meteorological database Meteonorm [*Meteonorm, 2014*]. This software provides hourly and monthly diffuse horizontal irradiance, direct horizontal irradiance, direct beam irradiance, mean temperature of the air, sun azimuth and the sun elevation for each location. The albedo is assumed equal to 0,2.

The first approach for the analysis of the climate, is grouping locations into climate zones, trying to identify where there are areas with similar meteorological conditions. The definition of the climate zones is important to maintain integrity of the performance characteristics; available hourly and monthly data are useful to statistically represent climate condition in each location.

The climate over Europe can be briefly summarized as follows. There are mainly three macroclimatic zones, in which all the locations can be roughly classified:

a) Mediterranean region: it consist in mild winters, warm and dry summers and quite high solar irradiation over the whole year (at least in winter months the value of global horizontal irradiance is around 65 W/m^2).
b) Continental region: winters are cold and they last a long time, while the hot season is short and humid.

c) Atlantic region: it has mild temperatures in summer and quite cold winters (temperatures just a little above 0°C), with quite rare snowfalls. During the year the rainfalls are abundant.

Basing on the data from Meteonorm, it is possible to obtain the behaviour of the mean temperature in a particular month, varying the latitude. In Figure 5.2 this trend is shown for the two extreme cases (the warmest month that is July and the coldest that is January). As it was expected, increasing the latitude coordinate, temperatures tends to drop down. Each dot in the graph corresponds to each considered location and the oscillations are due to the microclimatic zones that are present over the Europe, to which each city belongs.

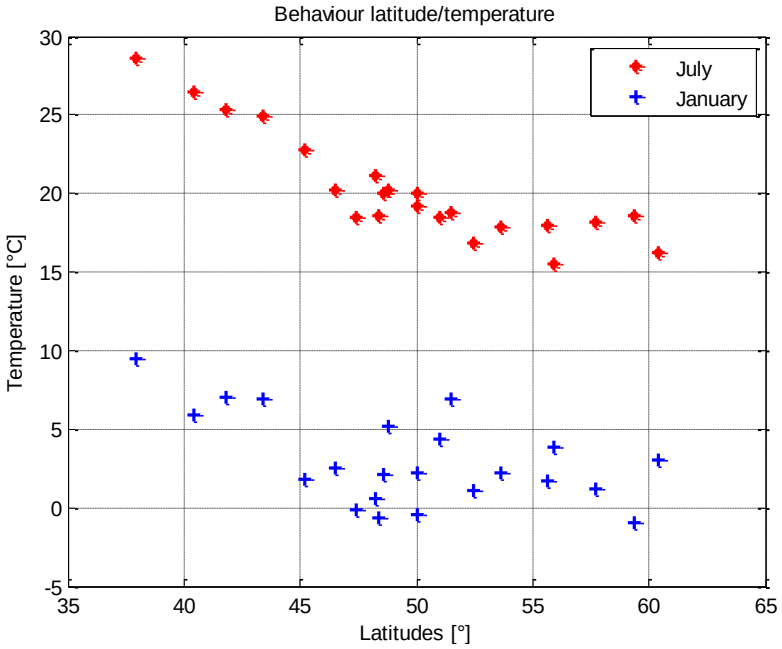

Fig. 5.2: mean monthly temperature for different latitudes all over Europe. The analysis was performed for twenty-two locations.

Moreover, it can be noticed that the most relevant variation of the temperatures takes place during the winter, especially for latitudes around 50°, where the temperatures go from under -0,7°C (Munich) to 6,9°C (London). This variation is mainly due to the influence that the microclimate in that particular zone can have on the temperatures. In fact, all the locations are at different latitudes, but the longitude and the morphology vary from one region to another. For example, being at a similar latitudes, London is near the seaside, while Munich sees a continental climate, not mitigated by the ocean; this causes a substantial temperature difference in the same winter period. Furthermore, the relatively high values of the temperature experienced by a big city like London or Paris could be influenced by the Urban Heat Island effect (UHI). This is a phenomenon that consists in the different type of climate that large city centres have with respect to the surrounding.

The second obtained graph (Figure 5.3) shows for the same two months considered previously (January and July), the temperatures changes, varying the mean irradiance of global horizontal radiation. Even in this case the oscillation of the dots, representing each location, is major in the cold season. Imagining to show all the months of the year, the behaviour of the temperatures with irradiance is approximately linear. In both July and January, the locations situated in the Mediterranean zone are the most detached from the others, because the level of irradiance are significantly higher in that region.

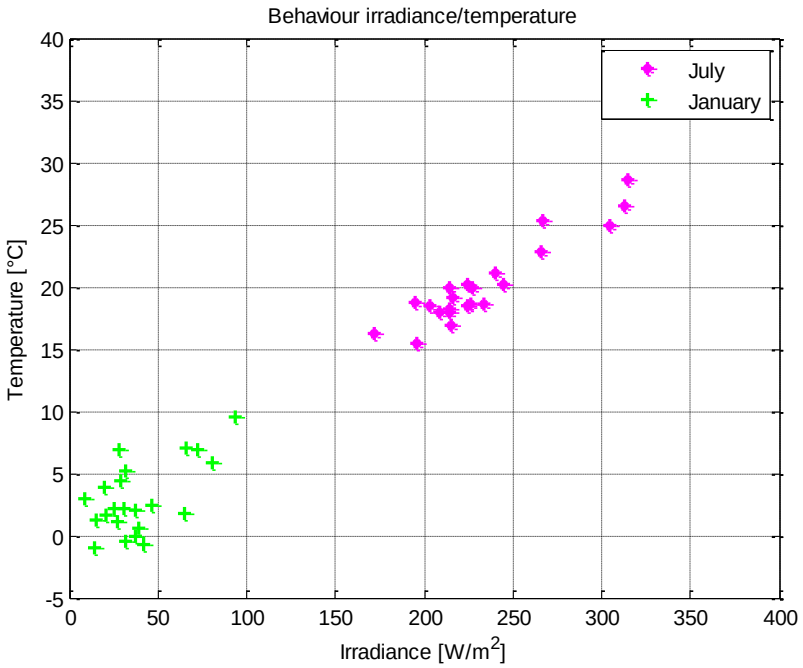

Fig. 5.3: mean monthly temperature trend varying the global irradiance all over Europe. The analysis was performed for twenty-two locations at different latitude coordinates.

Therefore, on the basis of this two graphs, it's possible to roughly classify all the locations in three main groups, depending on the general trend of the climate during the whole year (Table 5.2).

Mediterran	Athens	Madrid	Rome	Marseille						
Continental	Turin	Lausanne	Zurich	Wien	Munich	Strasbourg	Paris	Prague	Frankfurt	Berlin
Atlantic	Gent	London	Hamburg	Copenhagen	Glasgow	Goteborg	Stockholm	Bergen		

Table 5.2: classification of the twenty-two locations in three main climatic regions.

In each group there are some exceptions, such as Lisbon that in summer has a similar climate to the other Atlantic locations but during the cold months presents a quite high mean temperature, closer to the Mediterranean climate; however the classification has been performed mainly basing on the European geographic zone.

In the following graph (Figure 5.4) the mean monthly temperature is plotted against the global irradiance monthly provided by Meteonorm). One location per climatic group is illustrated. The three chosen reference geographical locations in Figure 5.4 are Rome, Lausanne and Stockholm. They can be taken as reference because these cities don't present any exceptional behaviour such as for example London; the latter in fact, in winter presents a temperature behaviour that is completely different from the other locations, belonging to the Atlantic region. London has a relatively high mean temperature in the winter (in January 6,9°) and it presents a mild summer with the mean temperature in July that is around 18°*C*.

Each dot in the graph corresponds to a month; all the locations have the same circular behaviour that links the temperature with the irradiance: increasing the latitude, the circle is shifting to higher temperatures and irradiances but the trend is always the same. Starting from January, the coldest period of the year, all the other months follow counter clockwise.

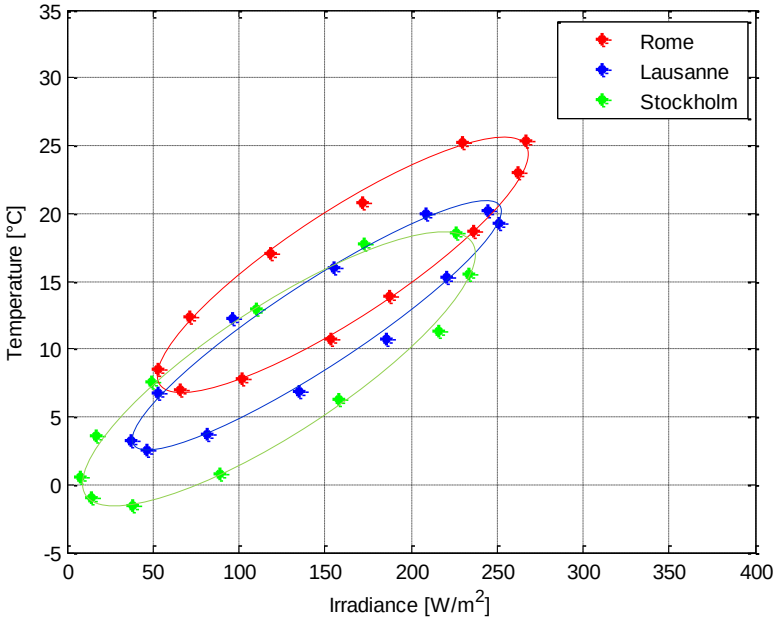

Fig. 5.4: mean monthly temperature against global horizontal irradiance for all twelve months in Rome, Lausanne and Stockholm.

5.2 Office room reference

Concerning the first parametric study, the final aim is the determination of the variation of thermal loads, changing the latitude, supposing the most suitable microstructured glass for a particular location and evaluating for which range of latitude coordinates it let obtain reasonable energy savings. Results were compared with conventional glazing, such as a double standard glass and a sun protective glass.

All the simulations are performed taking in consideration a reference office room, in order to analyse only the influence of the geographic parameters on the performance of the novel glazing envelope. The detailed description of the office room follows.

5.2.1 Geometric characteristics

The geometric characteristics of the reference office room have been fixed and maintained for all the geographical locations. They are shown in Table 5.3.

	Office room
Façade wall area	10,06 m^2
Floor area	29,5 m^2
Window area	4,024 m^2

Table 5.3: geometric characteristic of the office room.

The office has only the south oriented façade that is exposed to the external ambient. All other three vertical walls are partition walls that separate the room from other office rooms or from the corridor of the building. Both the floor and the ceiling are separate other office rooms.

The floor area is equal to 29,5 m^2 and the façade wall area corresponds to 34% of the floor area. The height of the room is about 2,8 m^2.

In the Figure 5.5 the plan view and the frontal view of the considered office is shown:

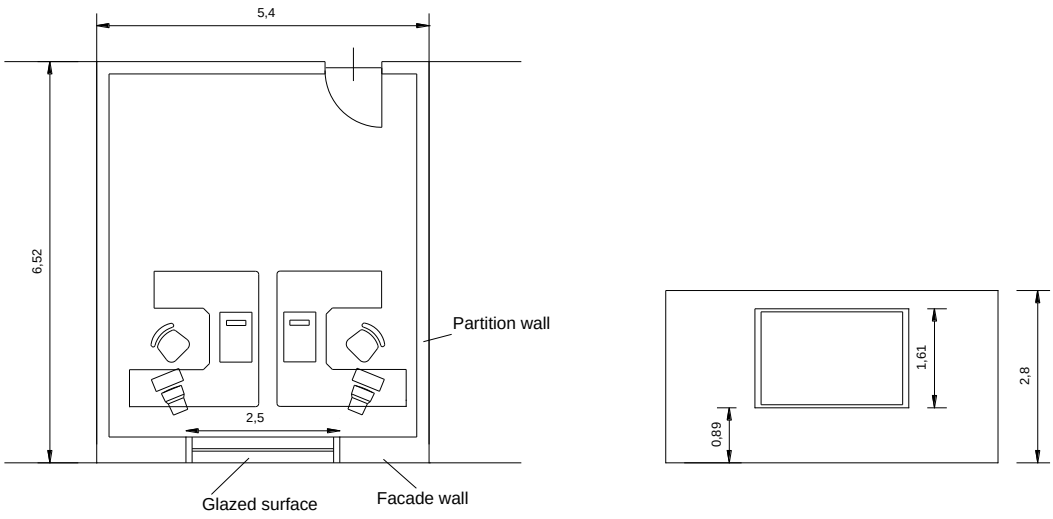

Fig. 5.5 : plan view showing the window location of the reference office room.

Another important geometric parameter is the window to wall ratio (WWR), that corresponds to the surface area of the fenestration system divided by the surface of the façade wall on which the window is installed. It is very useful to compare window surface area across different buildings. Providing a reference parameter to define how much of a façade is dedicating to a glazing, is a useful approach for the energy performance assessment of a building. A high window to wall ratio value (up to 60% or 70%) usually significantly contribute to increase the annual thermal loads of the building and the risk of overheating, due to the increasing need of cooling.

The façade area dedicated to fenestration systems is a crucial design decision that affects not only the visual perception of the building and the structural considerations, but also the energetic balance of the whole system.

Therefore the window to wall ratio is an excellent metric to compare the window's surface area across different buildings; for this first study a WWR fixed value is supposed, in order to suitably compare the obtained results varying only the latitude. However, a second parameter study has been performed in which the influence that this parameter has on the building performance is analysed for different types of buildings.

The considered glazed area to wall area ratio is equal to 0,4, therefore the total window area is 4,024 m^2; the resulting percentage of glazing respect to the floor area is about 14%.

5.2.2 Thermal properties

In order to set up all the thermal properties of the reference office room, the stratigraphic layout of the walls and of the horizontal surfaces (ceiling and floor) have been defined.

Only the south oriented façade is exposed to the external environment. Therefore the most relevant thermal transmittance is this one. The façade wall consists in an external layer made of plaster, with a low thickness of 2 *cm*, the layer of 20 *cm* of rock wool to suitably insulate the office room and the last internal layer of wood (about 20 *cm* of thickness). The ceiling and the floor are supposed with the same stratigraphy, consisting of 24 *cm* of concrete. The three partition walls are made of brick with 20 *cm* of thickness.

The determination of the thermal transmittance for the walls is important, in order to define the thermal performance of the building. The office room that is considered in this first parametric study can be described as well insulated.

In Figure 5.6 the stratigraphy of each surface can be seen.

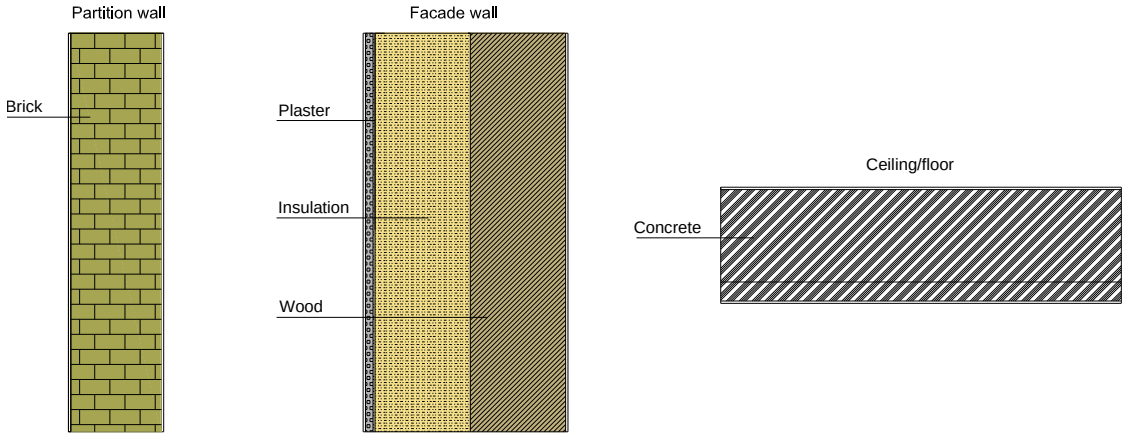

Fig. 5.6: stratigraphic layout of the partition wall, the façade wall, the floor and the ceiling of the reference office room.

The heat transfer coefficients for the free convection heat exchanges, due to the air from the internal (h_i) and the external (h_e) side of the walls is assumed equal to h_i = 8 *W/m²K* and h_e = 25 *W/m²K* (vertical surfaces), with an air density of 1,22 *kg/m³*. For horizontal surfaces with down flow, the internal heat transfer coefficient is assumed h_i = 6 *W/m²K* [*EN ISO 6946, 2008*].

For the calculation of the thermal transmittance the following expression is used:

$$U - value\ [\frac{W}{m^2 K}] = \frac{1}{\frac{1}{h_i} + \sum_{j=1}^{n} \frac{s_j}{\lambda_j} + \frac{1}{h_e}}$$

Where:

- h_i is the internal heat transfer coefficient;
- h_e is the external heat transfer coefficient;
- s is the thickness of the considered layer;
- λ is the conductivity of the material of the layer.

In Table 5.4 below the properties of construction materials of the walls, of the floor and of the ceiling, such as conductivity, density and specific heat, are shown with the corresponding thickness:

	Façade wall			**Ceiling/floor**		**Partiton wall**
	plaster	insulation	wood	concrete	concrete	brick
Thickness [m]	0,02	0,2	0,2	0,04	0,2	0,2
Conductivity $[\frac{W}{m\,K}]$	0,4	0,04	0,13	1,35	1,35	0,7
Density $[\frac{kg}{m^3}]$	1000	40	500	2000	2000	1200
Specific heat $[\frac{J}{kg\,K}]$	1000	840	1600	1000	1000	1000

Table 5.4: stratigraphy of the walls, the ceiling and the floor of the office room [*ISO 10456, 2007*].

The resulting U-value for the wall façade is 0,15 *W/m²K*. As previously mentioned, this value underlines that the office is well insulated from the outside. The other resulting U value are 1,96 *W/m²K* for both the ceiling and the floor, and 1,87 *W/m²K* for the partition wall. The thermal capacity is equal to 1880 *kJ/K* for the façade wall and to 4380 *kJ/K* for the partition walls.

Moreover, for the window, a reasonable U-value has to be defined. The transmittance for the glazed surface is a measure of the window's heat transfer resistance across the indoor/outdoor temperature difference. A full fenestration system is made of different components, including the frame, edges, dividers and the glass itself. The U-

value for the installed window, including all its components, is assumed equal to 1,3 W/m^2K, that is the minimum required U-value for glazing, referring to the Italian DL 311/06, for the F climate zone.

Air change rates for natural ventilation in buildings is another important parameter and it depends on building layout, occupancy, location and weather conditions. In the office room natural ventilation is assumed, due to the air infiltration, with an air change rate of 0,5 h^{-1}, that is an acceptable value, referring to UNI EN 15242 [*UNI EN 15242, 2006*].

5.2.3 HVAC system

The Heat Ventilation and Air Conditioning system (HVAC), that provides heating and cooling in the reference office room, is a reversible heat pump. Indeed, in many non-residential buildings, this system represents an attractive energy saving opportunity, using the refrigeration machine for heat production. This can be done by condenser heat recovery whenever there is simultaneity between heating and cooling demand. When there is no simultaneity, full reversibility has to be looked for. A heat pump is reversible in this last case, therefore the advantage can be taken of the heat given off by the condenser, or the heat absorbed by the evaporator, depending on the HVAC system thermal demand.

In order to perform this parametric study, the non-simultaneity of the heating and cooling demand of the system is assumed. Therefore the operational mode of the HVAC system is always based on the full reversibility. In principle, heat pumps are suitable for demand response because of several reasons. Firstly, they allow to have an integral heating and cooling system. Then, the demand response of the system to peaks fits well either for cooling and heating. Finally the efficiency of the heat pump can be quite high and maintenance costs low.

It has to be considered that the parametric analysis should be focused on the window performance. Consequently, the fixed COPs are theoretically assumed fixed equal to 1 in order to study effective annual thermal loads for heating and cooling. However, the COP value equal to 1 is not index of good performance of the heating and cooling system. Furthermore, a variation of the reversible heat pump efficiency strongly influence the annual thermal loads of the building. Therefore, a study of the obtained energy savings at different COP values has been performed in paragraph 5.5.

According to the technical standards, the maximum acceptable temperature for the cooling has been set up to 26°*C* and the minimum acceptable temperature for the heating has been set up to 20°*C*, in order to assure the thermal comfort in the indoor environment.

5.3 Glazing envelopes

The energetic performance of the office room has been evaluated comparing three different typologies of glazing envelopes, in order to determine the best solution for a particular range of latitude and quantify the energy savings. The novel microstructured glass comprised of micro-mirrors was compared with two conventional reference glazing: a sun protective glass and a standard double glass.

Therefore, this first parametric study is focused on the evaluation of the advantages that the installation of a glazing envelope with embedded microstructures can bring to the building from the energetic point of view. The typology of glazed surface is a parameter that varies in the reference office room. All the other variables, such as the geometric characteristics and thermal properties of the office room have been maintained.

5.3.1 Standard double glass

Firstly, a standard double glazing (with low-e coating) was considered in order to perform the simulations. Refraction is a significant phenomenon for glazing envelopes, that consists in the change of direction of light rays at the interface between two different mediums. This is due to the variation of the speed of light in the medium. The refraction index

quantifies the decrease of speed of propagation of the radiation when it passes through a material. The angle of refraction is defined by the Snell law [*Born et al., 1999*]:

$$n_i \sin(\theta_i) = n_t \sin(\theta_t) \quad (5.1)$$

where n_i and n_t are the refractive indices of the materials on the incoming and transmitted side of the interface respectively; θ_i and θ_t are the incoming and transmitted angles respectively. This phenomenon can be observed in Figure 5.7, where the incoming light from the sun undergoes a change of direction passing through the first pane, the inner space and the second pane. A very small variation of the refractive index can change the light path by some degrees. As it can be seen in the Table 5.5, the standard double glass thickness is equal to 2,5 *cm* and the refraction index 1,5.

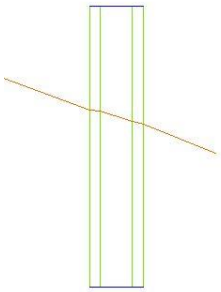

Fig. 5.7: ray tracing of the standard double glazing for an incidence angle of 30°.

STANDARD DOUBLE GLASS	
Number of panes	2
Glass thickness [m]	0,025
Refraction index	1,5

Table 5.5: properties of the standard double glazing.

The total energy transmittance of the standard glass, varying the incidence angle of the light, is shown in Figure 5.8. Negative angle of incidence (from -90° to 0°) are not considered because they correspond to the incoming rays reflected from the ground. Increasing the incidence angle, the transmittance decreases. It starts to be around 70% at normal incidence angle and then it decreases when the angle becomes to be around 40°. If the incidence angle is 90°, the transmitted energy is null. Depending on the location and on the period of the year, the sun elevation angle is different (higher at lower latitudes). However, among all the chosen locations the maximum value of elevation of the sun is in the summer solstice in Athens (75,4°) and the lower is in the winter solstice in Bergen (5,7°). Consequently the value of transmittance to be considered are between this range of incidence angle. Especially in southern locations, there is the risk of overheating in buildings, because of the high transmittance during the hot season. For example in Athens, in the summer solstice, the transmitted energy through the double glass is above 20% and in general during summertime it can reach values around 50% (in August).

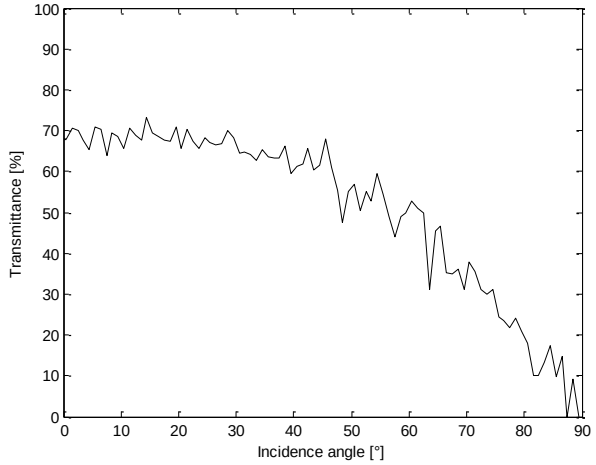

Fig. 5.8: total energy transmittance of the standard double glass at different sun elevation angles.

5.3.2 Sun protective glass

Secondly, a sun protective glass was considered to be installed on the façade of the office room. In this case the most relevant parameter is the absorption of light in the medium. When a material is absorbing, the intensity of a light beam diminishes exponentially with the distance in the material, according to the Lambert law, as it is shown in equation 5.2 [*Born et al., 1999*].

$$I(x) = I_o e^{-\alpha x}, \qquad \alpha = \frac{4 \pi k}{\lambda} \qquad (5.2)$$

Where I is the transmitted light, I_o is the incidence light, x is the thickness of the glass and α is the attenuation coefficient, that depends on the extinction coefficient k of the material (a measurement of the absorption) and on the wavelength λ of the light. In Figure 5.9 the sun protective glass is illustrated, with the related characteristics in Table 5.6.

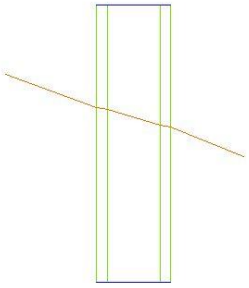

Fig. 5.9: ray tracing of the sun protective glazing for an incidence angle of 30°.

SOLAR GLASS	
Number of panes	2
Glass thickness [m]	0,02
Refraction index	1,5
Extinction coefficient	$2{,}1\ 10^{-7}$
Spacing [m]	0,02

Table 5.6: properties of the sun protective glazing (optimization in Lausanne).

In Figure 5.10 the total energy transmittance is displayed, at positive incidence angles. The shape of the curve is similar to that of the standard double glass. However the curve is shifted down and the transmitted energy through the glass is lower, in comparison with the standard glazing. It can be noticed that the maximum value of transmittance is around 50%. At higher incidence angles the transmitted energy is lower; it is around 20% in Athens, during summertime. In general, this kind of glazing envelope is useful in warm climatic regions, where it is crucial to minimize the solar transmittance, in order to achieve lower heat gains through the window and avoid the overheating of the building. On the other hand, at higher latitudes, 50% of transmittance through the glass during the cold season is not sufficient to allow the proper exploitation of the solar gains and minimize the heating loads.

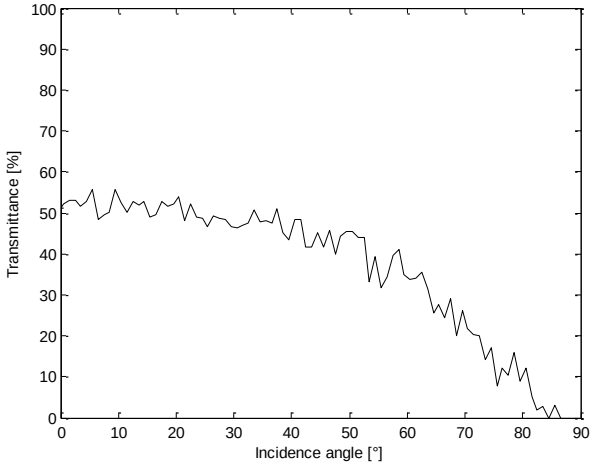

Fig. 5.10: total energy transmittance of the sun protective glass at different sun elevation angles.

5.3.3 Glazing with embedded microstructures

Embedded microstructures in a double glazing consist in the third novel glazing technology of analysed glazing envelope. In order to define the geometry of the CFS, an iterative method has been followed. The aim is to minimize the annual thermal loads required by the HVAC system. Many parameters have been varied, in order to optimize the micro-mirrors. Firstly, a reasonable seasonal variation of the total energy transmittance has to be reached. Secondly, a suitable configuration of the microstructures has to be designed, with a proper blocking angle and width, depending on the location. Therefore, varying the concentrator length, the mirror at focus, the incoming focus angle and other parameters, the best solution that allows to minimize the thermal loads, can be found.

As an example, in Figure 5.11 the embedded microstructured PMMA film optimized in Lausanne is shown. The related geometric characteristics are listed in Table 5.7. The PMMA combined with the micro-mirrors has a thickness equal to 620 μm. This PMMA film is then laminated with a double glass; the two panes have a thickness of 4 mm, while the inner space is 8 mm.

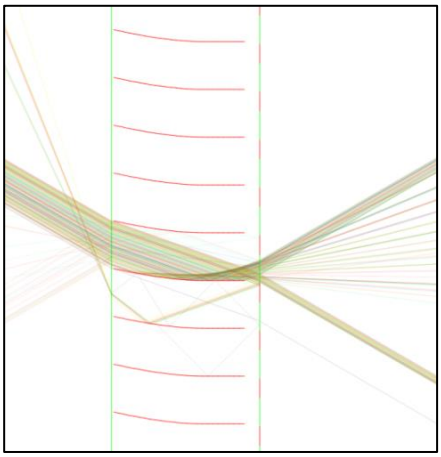

Fig. 5.11: ray tracing of the microstructured glazing for an incidence angle of 30°.

MICROSTRUCTURED GLASS	
Number of panes	2
PMMA thickness [µm]	620
Concentrator length [µm]	550
Sub segments	25
Mirror at focus	0,4
Period height [µm]	200
Incoming focus angle [°]	67
Focus offset [%]	30
Horizontal offset [µm]	10

Table 5.7: properties of the microstructured glazing (optimization in Lausanne).

In Figure 5.12 the total energy transmittance of the microstructured glass optimized in Lausanne is displayed. It can be noticed that a seasonal dynamic effect can be achieved by the embedded micro-mirrors. This angle dependent system can accept heat gains in cold months and reject them in the warm season.

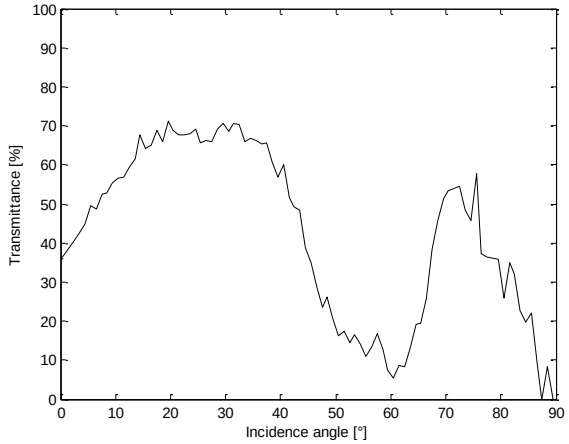

Fig. 5.12: total energy transmittance of the sun protective glass at different incidence angles (elevation).

In Lausanne, the solar altitude all over the year is in a range between 20° (winter solstice) and 67° (summer solstice). During the cold months, such as November, December, January and February, the incidence angle to the glass is around 20°-30°. In this period is important to maintain the transmitted energy through the glass quite high (around

70%), in order to better exploit the solar gains and minimize the heating requirements. On the contrary, in summer (June, July, August), a problem of overheating can occur if the glazed surface has an high transmittance. In these months, when the solar altitude is between 52° and 67°, the aim is to minimize the transmitted energy. In this case the total transmittance varies from 5% to 20%.

5.4 Simulation results

In this chapter, all the results obtained by the simulations are presented. Considering as a reference site the Swiss city of Lausanne, due to its middle latitude in Europe (46,5°N), both the geometry of the microstructured glass and of the sun protective glass were optimized. Thermal loads and energy savings, in comparison with the two conventional glazing were obtained in the first paragraph. Then the optimization, pursuing the same iterative approach, were performed for other locations. However, it emerged that, from the energetic point of view, only the optimization in southern European locations it is reasonable. For this second optimization, Athens has been chosen as the reference location. In the following paragraph, focusing on the HVAC system, energy savings varying the COP of the reversible heat pump have been evaluated. Finally, the future climatic scenario, considering the global warming effect has been analysed, in order to foresee the impact on thermal loads and the advantage of the microstructured glass in a future climate change perspective.

5.4.1 Optimization criteria

Both summertime and the cold season affect the energy balance of the building: during the warm months the solar gains should be minimized, in order to avoid the overheating of the building. While in winter the transmitted energy coming from the sunlight should be well-exploited, reducing the heating requirement. Unlike conventional glazing envelopes, the proposed CFS solution is characterized by an angular dependent transmittance, that induces a seasonal thermal control. Therefore, designing the suitable geometry of the embedded micro-mirrors, the solar elevation pathway between summer and winter has to be considered, in order to maximize the solar energy transmittance in winter and minimize solar gains in summer, reducing the air conditioning loads. The geographic position strongly influence the geometric configuration of the microstructured glass: in southern locations the blocking angle should be larger because of the higher amount of direct irradiance, lasting more months. Depending on the latitude, the shape of the parabolic mirrors and the length of the vertical reflectors can be optimized to block or transmit sun radiation.

The optimization of the sun protective glazing was also performed, in order to compare the microstructured glass with the best-performing glazing envelope.

Firstly, choosing Lausanne as reference location, the optimization of the microstructured glass and of the sun protective glass were performed, in order to minimize the annual thermal loads. The geometrical parameters, such as the polymer film thickness and the length of the micro-mirrors and of the vertical reflectors, have been modified, obtaining a suitable design. Energy savings were calculated on the basis of the obtained thermal loads through simulations, as described by equation:

$$E_S = \frac{Q_{SP} - Q_M}{Q_{SP}} \, 100 \quad (1)$$

Where E_S (%) are the relative percentage energy savings, Q_{SP} (kWh/m^2) the annual thermal loads using the sun protective glass and Q_{SP} (kWh/m^2) the annual thermal loads using the microstructured glass. Energy savings comparing the microstructured glass with the standard double glass were calculated using the same approach. Moreover, the same iterative method of optimization has been followed for locations in which the energy savings compared to the sun protective glass could potentially be improved.

5.4.2 Optimization for the location of Lausanne

This paragraph is partially based on the publication for the 6th International Building Physics Conference in Turin (14-17 June 2015). In order to evaluate the achievable thermal performance of the building system using different glazing envelopes, both the optimization of the sun protective glass and of the microstructured glass was carried out. The glazing were adapted to Lausanne, as reference location.

Concerning the optimization of the sun protective glazing, the solar energy transmittance of the glass was considered, by neglecting the contribution of the secondary heat transfer factor to the g-value, for simplicity. Simulations were performed varying the solar energy transmittance of the glazing at normal incidence angle, in order to obtain the corresponding annual thermal loads. In this way, only the gains resulting from the transmitted radiation were considered. Therefore, the best performing sun protective glazing is characterized by the energetic transmittance for which annual loads are the lowest. In Lausanne, the solar direct transmittance at normal incidence angle that minimizes the energy consumption turns out to be equal to 52% (Figure 5.13a). The minimum reachable annual loads, with the sun protective glass, amount to 23,5 kWh/m^2, including 31% of cooling loads. In general, as the transmitted energy through the glazing rises, the cooling requirement increases: when the transmittance is equal to 70%, cooling loads cover about 16,5 kWh/m^2 on the total 27,3 kWh/m^2 of energy consumption (corresponding to 40%).

On the other hand, the optimization of the microstructured glass was performed. A suitable geometric configuration for Lausanne was found, through an iterative method. The proper blocking angle and width were determined varying the concentrator length of the parabolic micro-mirrors, the width of the vertical reflectors and the focus angle of the parabola. The solar course in Lausanne was considered: from 20° of sun elevation angle in the summer solstice to 67° in the winter solstice. The seasonal dependence of the transmittance induced by the embedded microstructures geometry allows to reach lower annual thermal loads, compared with the sun protective glass. In Lausanne, the novel CFS technology enables a reduction of annual loads in comparison with the optimized sun protective glass, from 23,5 kWh/m^2 to 19,4 kWh/m^2, as shown by the dots in Figure 5.13a. Therefore, the potential saved energy is equal to 17% in Lausanne. Cooling loads are significantly reduced, of about 35%.

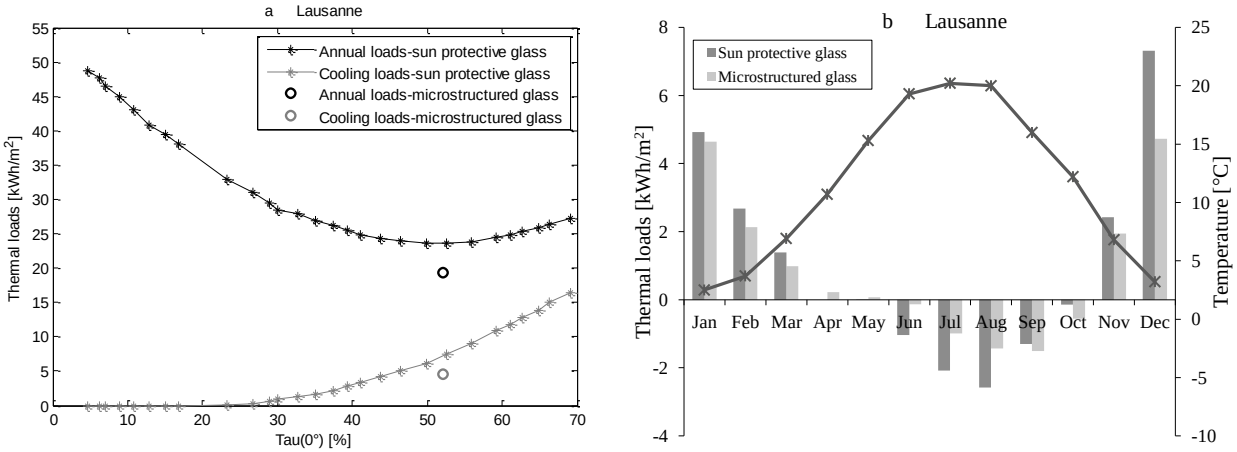

Figure 5.13: (a) annual thermal loads and cooling loads varying the solar energy transmittance of the sun protective glass in Lausanne; the dots represent the annual thermal loads and the cooling loads of the microstructured glass. (b) mean monthly temperature and cooling and heating loads during the year in Lausanne using the sun protective glass and the microstructured glass.

In Figure 5.13b the monthly heating and cooling loads in Lausanne are shown, comparing the microstructured glass and the sun protective glazing. The microstructured glass allows reducing both the heating and cooling consumption, compared with the sun protective glazing. In spring and autumn (April, May, September and October), the amount of loads using the novel CFS envelope is slightly higher than in the case of the conventional glazing. However, during the coldest months the relative energy savings are significantly reduced. For example in December, heating loads amount to 4,7 kWh/m^2 with the microstructured glass and 7,3 kWh/m^2 with the sun protective glass. During summertime the same situation is reproduced: in July and August the reduction of the cooling loads is 53% and 44%, respectively.

Figure 5.14 shows the total energy transmittance of the microstructured glass optimized in Lausanne. The highest value of transmittance (around 70%) is between 20° and 40°, corresponding to the winter time. Then the total energy transmittance drops down until to reach a value of 5%, when the incidence angle of the light is 60°. Therefore, the blocking angle is between 50° and 67°, when the solar gains are mainly rejected. In this range of incidence angles, the transmitted energy is low (around 5%-20% of transmittance); the sun elevation corresponds to the months of May, June, July and August. Consequently, the blocking range is able to minimize the need for cooling in summer, avoiding the risk of overheating in the building.

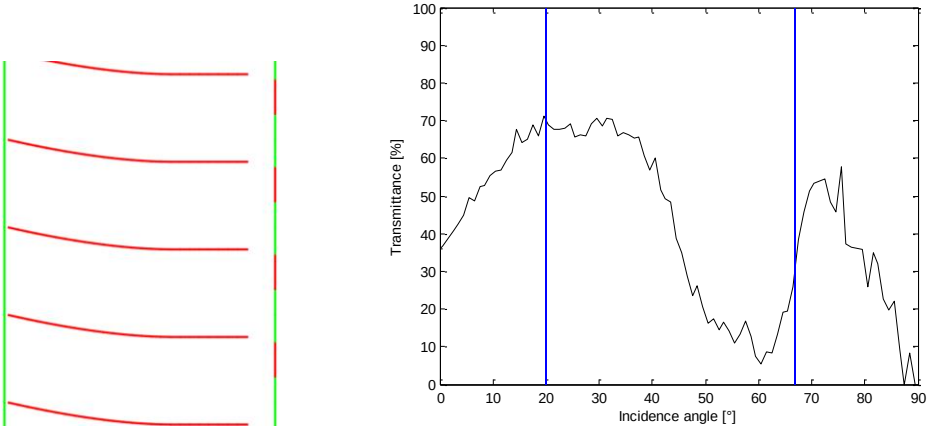

Fig. 5.14: (a) geometric configuration of the embedded micro-mirrors optimized in Lausanne. (b) solar energy transmittance of the optimized microstructured glass in Lausanne at different sun elevation angles. Blue lines indicate the solar altitude at noon on solstices for Lausanne.

The aim is to evaluate the thermal performance of the microstructured glass, at different latitudes. All the simulations have been performed, using the optimized microstructures in Lausanne. In the table below (Table 5.8), the geometric characteristics of the PMMA film with the embedded micro-mirrors is shown. At certain angles of incidence can happen that in the microstructures there is a phenomenon of multiple reflections. This effect should be avoided, slightly decreasing the concentrator length for example. The latter is about 550 μm, or rather 11% less than the PMMA thickness. The mirror at focus is equal to 40% and the incoming focus angle is 67°. Fixing these parameters, the microstructured glass is adapted for the latitude of Lausanne, from the energetic point of view.

EMBEDDED MICROSTRUCTURE	
Number of panes	2
PMMA thickness [µm]	620
Concentrator length [µm]	550
Sub segments	25
Mirror at focus	0,4
Period height [µm]	200
Incoming focus angle [°]	67
Focus offset [%]	30
Horizontal offset [µm]	10

Table 5.8: properties of the microstructured glazing (optimization in Lausanne).

Therefore, the energetic performance of the office room has been evaluated comparing three different glazing in order to determine the best solution in each case: firstly the novel microstructured glass, then the sun protective glass and the standard double glass.

There are different types of transmittance that can be evaluated. The hemispherical transmittance is the ratio of the total energy transmitted into the subtending hemisphere to the energy incident on the surface. The semi-hemispherical is defined in the same way but in this case the upper semi-hemispheric surface is considered (sky outside and ceiling inside). The semi-hemispherical transmittance is important because, concerning the impact on thermal loads, most of the radiation comes from the sky (the upper part of the external environment) and not from

the ground or the surrounding environment. The total transmittance for hemispherical and semi-hemispherical (upper half, sky) of the sun protective glazing is comparable with the microstructured glass (Table 5.9). For the standard double glass they are higher: the hemispherical and semi-hemispherical are equal to 61%, while the transmittance at normal incidence angle is about 69%. It can be noticed that only for the microstructured glass the hemispherical and semi-hemispherical transmittance are different (37% for the hemispherical and 49% for the semi-hemispherical). The reason is that, if the glass is microstructured, the parabolic micro-mirrors and the vertical reflectors cause a redirection of the light inside the room. They can reflect sun rays at high incidence angles and transmit them inside for lower incidence angles. The semi-hemispherical is higher because in the upper part the total transmitted energy is higher than in the lower part of the room. For the reference glazing, the hemispherical and semi-hemispherical transmittance are the same, because there is no redirection of the light.

	Microstructured glass	Sun protective glass	Standard double glass
Hemispherical	37	44	61
Semi-hemispherical	49	44	61

Table 5.9: total hemispherical transmittance and total semi-hemispherical transmittance (upper half, sky) for the three glazing envelopes.

Once the microstructured glass has been optimized, simulations results can be obtained.

In Figure 5.15 the annual thermal loads with the corresponding temperatures are illustrated with the standard double glass in Lausanne. The reference office room requires an amount of annual loads equal to 27,2 kWh/m^2. When there is no need of heating or cooling, the cumulated curve is flat because the temperature in the room is between 20°*C* and 26°*C*. When the indoor temperature decreases (during the winter period), becoming under 20°*C*, the HVAC system has to provide heating. On the other hand, in the hot season, when the indoor temperature is higher than the set up temperature (26°*C*), the HVAC system has to provide cooling. In this case, the heating loads are 10,8 kWh/m^2 and the cooling loads 16,4 kWh/m^2. The standard glass causes an overheating of the building in summer, so that the cooling loads are higher than the heating loads, despite the latitude (46,5°N).

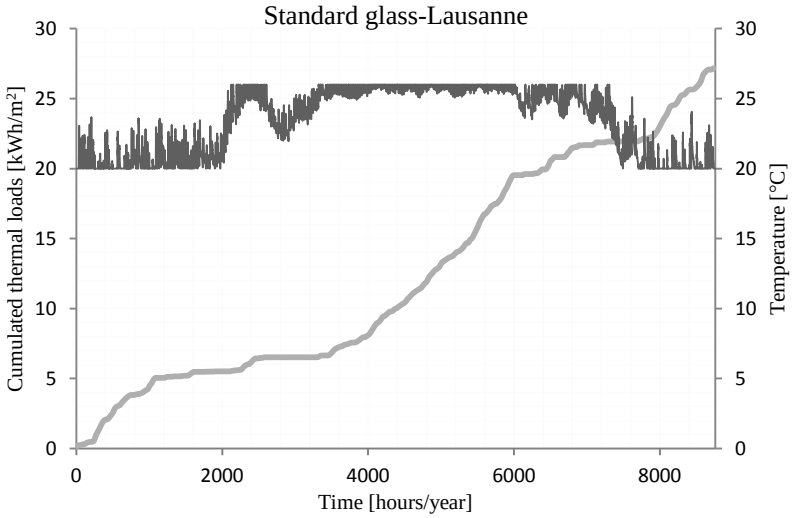

Fig. 5.15: cumulated thermal loads and temperature in Lausanne with the standard double glazing.

Until the end of February the office room requires 5,5 kWh/m^2 of heating loads. During the month of March there is the risk of overheating of the building. In this early period 1 kWh/m^2 of cooling loads is needed. Then, in April no thermal loads are needed because the climatic conditions guarantee the suitable indoor temperature. From May to the beginning of October, if the glazed surface is a standard double glass, 15,4 kWh/m^2 of cooling loads are required. Finally, during the end of the year, the HVAC system has to provide 5,4 kWh/m^2.

Figure 5.16 shows the annual thermal loads in Lausanne, for the three different glazing envelopes: the two reference conventional cases and the microstructured glass (green line).

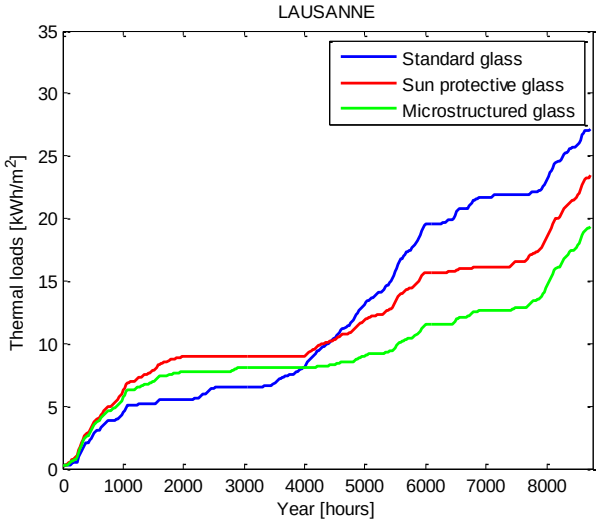

Fig. 5.16: cumulated thermal loads in Lausanne for the three glazing envelopes.

The optimization of the embedded microstructures has been carried out for Lausanne, bringing the thermal loads down to 19,4 kWh/m^2. In comparison, the sun protective glass leads to annual thermal loads equal to 23,5 kWh/m^2 and the standard glass around 27,2 kWh/m^2. It can be noticed that the standard double glass brings to the highest amount of cooling loads, because the slope of the curve in the summer months is the highest. Moreover, the microstructured glass causes a significant reduction of the cooling loads in comparison with the reference cases. The reduction of the heating loads is from 16 kWh/m^2 to 14,4 kWh/m^2 when compared with the sun protective glass.

At different latitudes, depending on the meteorological conditions, the heating and cooling requirements vary all over the year. Figure 5.17 illustrates the cumulated annual thermal loads for the considered glazing envelopes in three locations at very different latitudes: Athens (38°N), Lausanne (46,5°N) and Stockholm (59,3°N). The standard glass is expected to cause the highest amount of thermal loads in extreme climatic conditions (cold or hot climate). The sun protective glass should perform better in southern locations than in the north of Europe. However it has to be considered that the characteristics of the sun protective glass are adapted to Lausanne. For this reason, as it can be seen in the figure, it brings to a smaller amount annual thermal loads in Lausanne, than in Athens. Due to the fact that the embedded microstructures have been optimized for Lausanne, both in southern and northern locations the annual thermal loads are higher. In the south of Europe much more cooling loads are required, while at high range of latitudes (around 55°N-60°N), the need for heating is more important than in Lausanne.

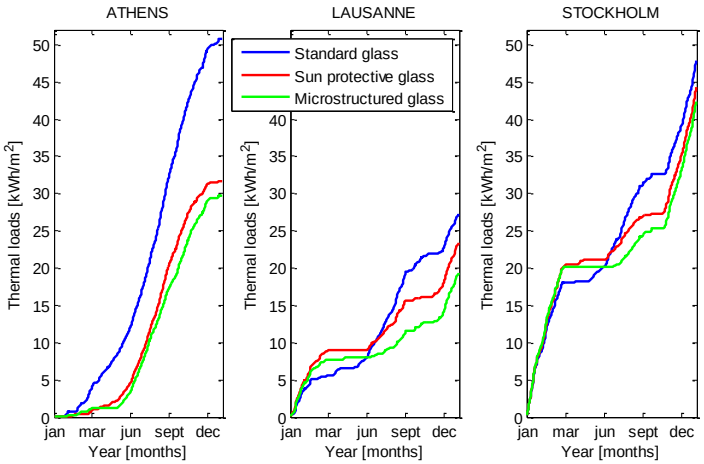

Fig. 5.17: cumulated annual thermal loads for Athens, Lausanne and Stockholm, for the three glazing envelopes.

It can be noticed that, as it was expected, for the other two locations the total annual thermal loads with the double glazing are larger than in Lausanne. The reason is that for locations in the south of Europe more cooling is required to compensate for higher solar gains. The use of a sun protective glass (31,7 kWh/m^2) reduces by about 37% the thermal loads in southern locations, compared to the standard double glass (50,8 kWh/m^2). On the other hand, at latitudes around and above 50°N, in the winter season, a higher amount of heating loads is needed. Moreover, for Stockholm the microstructured glass and the solar glass roughly bring to the same energy consumption during the year, equal to 42,4 kWh/m^2 and 44,2 kWh/m^2, respectively. This is due to the lower amount of cooling loads, making the sun protective glass less useful. The standard glass remains the worse performing glazing envelope, bringing in Stockholm to 47,9 kWh/m^2 of thermal loads.

The difference in climate can be noticed not only looking at the difference of temperatures (lower at higher latitudes) but also looking at the irradiance. In Figure 5.18 the direct (a) and diffuse (b) irradiance are displayed for the three considered locations. The amount of direct irradiance is very high in Athens, overcoming 200 W/m^2 in June, July and August. The direct irradiance is higher in Lausanne than in Stockholm all over the year, except in May, where is about 113 W/m^2 and 124 W/m^2, respectively. During winter, in Stockholm the direct irradiance is low, amounting to 7 W/m^2 in December and 9 W/m^2 in January. A big amount of direct irradiance can be the cause of the high building overheating risk in the south of Europe. Therefore, the microstructured glass can be properly optimized for these locations, in order to avoid this big amount of solar gains. Concerning the diffuse irradiance, in Athens, especially in summer it is low. The diffuse irradiance in summer is higher in Lausanne and Stockholm than in the Greek capital (below 100 W/m^2). Moreover, in Stockholm the amount of direct and diffuse irradiance is almost the same all over the year. This can be the reason of a mainly overcast sky, for which the microstructured glass is not efficient and the difference between annual loads with the reference glazing is not marked. Global and diffuse horizontal irradiance are provided by the software Meteonorm and data are an average on the overall daily values.

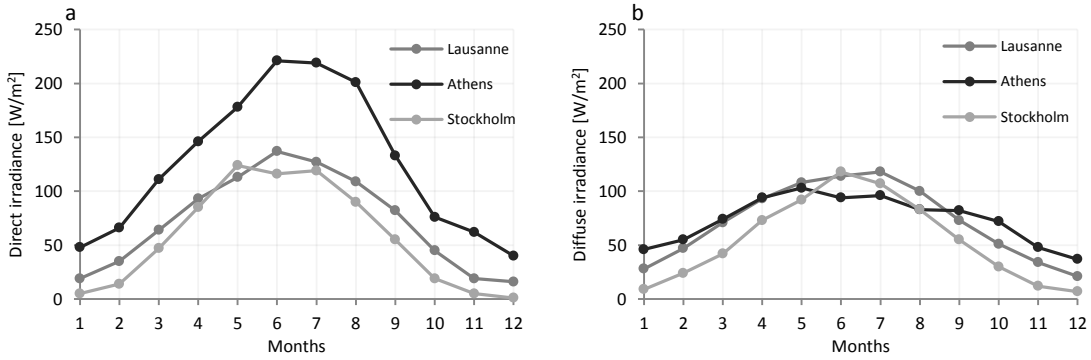

Fig. 5.18: direct irradiance (a) and diffuse irradiance (b) during the year in Athens, Lausanne and Stockholm.

The total annual thermal loads for the chosen twenty-two European latitudes are shown in Figure 5.19. The energy consumption is highest in locations requiring more cooling or heating. The fluctuation of the three curves is due to the changing temperature and irradiance all over the year, that is not only dependent on the latitude, but also on the particular micro-climate of the region (alpine, oceanic, continental).

It can be noticed that the lowest reachable thermal loads with the microstructured glazing are in Turin (16,7 kWh/m^2), and the highest in Stockholm. London and Glasgow present quite low thermal loads, in comparison to cities with the same latitudes. This is because they belong to the Atlantic region, with milder climatic conditions. Concerning especially London and Paris, another reason explaining the lower amount of thermal loads can be the Urban Heat Island (UHI) effect that causes a relevant increase of temperature in large urban areas. In general, the standard double glass is the type of envelope that causes the greatest amount of loads, reaching the highest values for a low range of latitudes (from Athens to Marseille), where the use of a sun protective glass significantly decreases the annual energy consumption. The cities located in the continental area of Europe such as Zurich and Prague, correspond to the two maximum in a middle range of latitude (from 47°N and 51°N): they involve a higher energy consumption to cover the heating demand.

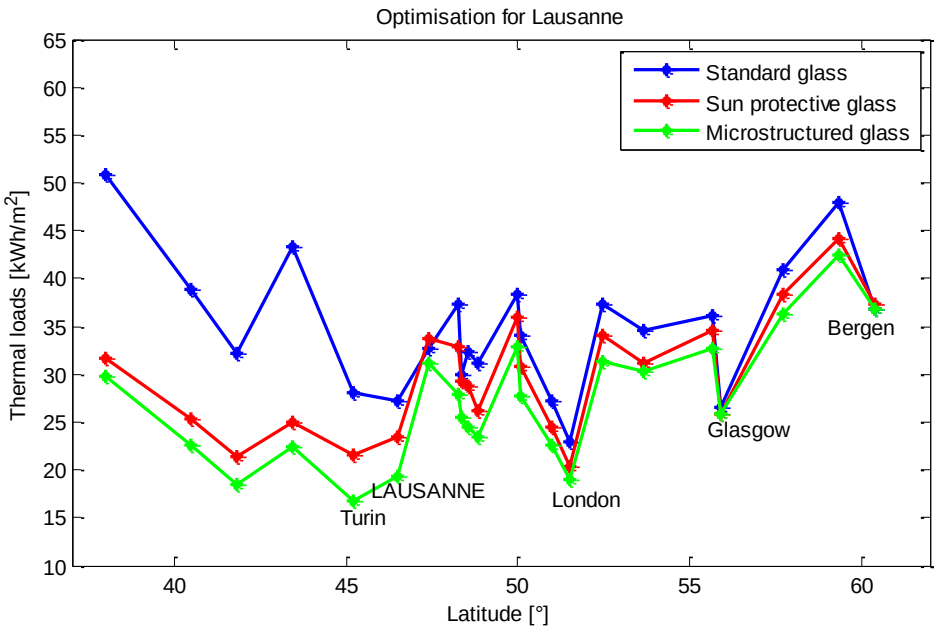

Fig. 5.19: annual thermal loads at different latitude and for the three glazing types.

However the installation of the embedded microstructured glass is an advantage for all the locations, except Glasgow and Bergen, where all the glazing envelopes have the same effect on thermal loads, due to the overcast sky that governs in these regions roughly all over the year.

Figure 5.20 illustrates the relative energy savings of the microstructured glass when compared to a standard glass and a sun protective glazing. In the studied locations, the installation of the novel static device as glazing envelope is convenient from the energetic point of view (energy savings are always positive).

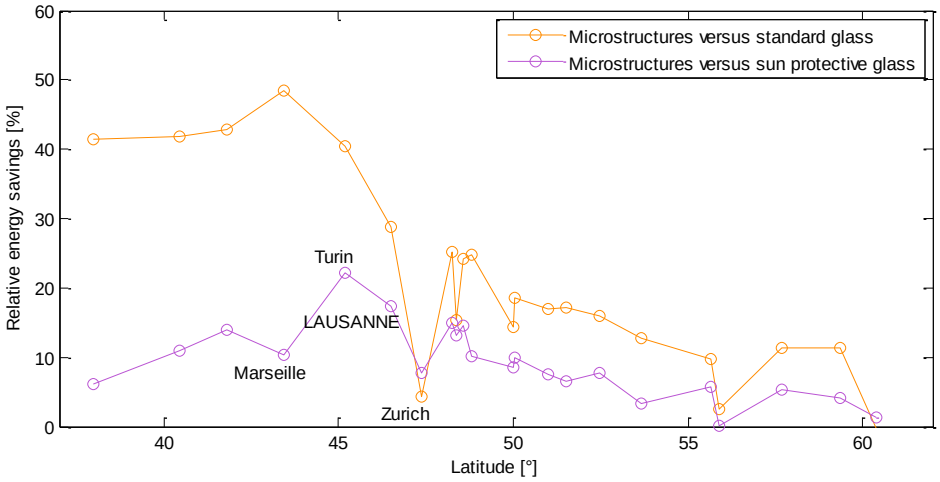

Fig. 5.20: relative energy savings at different latitudes, in comparison with the standard double glass and the sun protective glass.

The only two exceptions are Glasgow and Bergen, where the relative energy savings are null. However in the majority of cities the microstructured glass brings relevant savings in comparison to the sun protective glazing. Only in Zurich and Bergen the saved energy in comparison with the standard glass is lower than the saved energy in comparison with the sun protective glass. This is due to the inefficiency of the sun protective glass in these regions. The savings are highest in Turin with 22%, while in Lausanne they amount to 17%. In general energy savings in comparison with the standard double glass are higher, especially for latitudes lower than 46°N. In this case, from Athens to Rome the savings reach 40% and in Marseille there is the maximum value, almost 50%.

Zurich presents lower savings than in Lausanne (8% if compared with the sun protective glass), despite similar latitudes. This is explained by the difference in climate. Zurich has lower monthly mean temperatures (2°C less) and energy loads are dominated by heating. Because of the high portion of diffuse light in winter the solar gains are reduced for this location. To maximize solar gains in winter the direct part of the irradiance should be high. For a microstructured glazing, the transmittance is especially high for direct radiation with an incidence angle between 10° and 40°. However the overall transmittance is relatively low.

The difference between energy savings in Turin and in Marseille is also explained by differences in the climate. First of all, the blocking range of the micro-mirrors is more adapted to the solar path in Turin. Moreover in Marseille the irradiance levels are higher; in particular the part of direct irradiance is higher than diffuse irradiance all year around. This induces an overheating problem starting in spring, before the sun elevation angle reaches the blocking range. This effect can be observed in Figure 5.21. Annual thermal loads in Turin are reduced by 25,3% in comparison with Marseille. This is because of the amount of cooling loads that in Marseille results to be very high (21,5 kWh/m^2). In Turin they are equal to 8,5 kWh/m^2. The early overheating in spring can be noticed in the graph and it starts from the mid of February, lasting up to the end of April. In Turin in this period there is not the need for cooling, because temperatures remain between 20°*C* and 26°*C*.

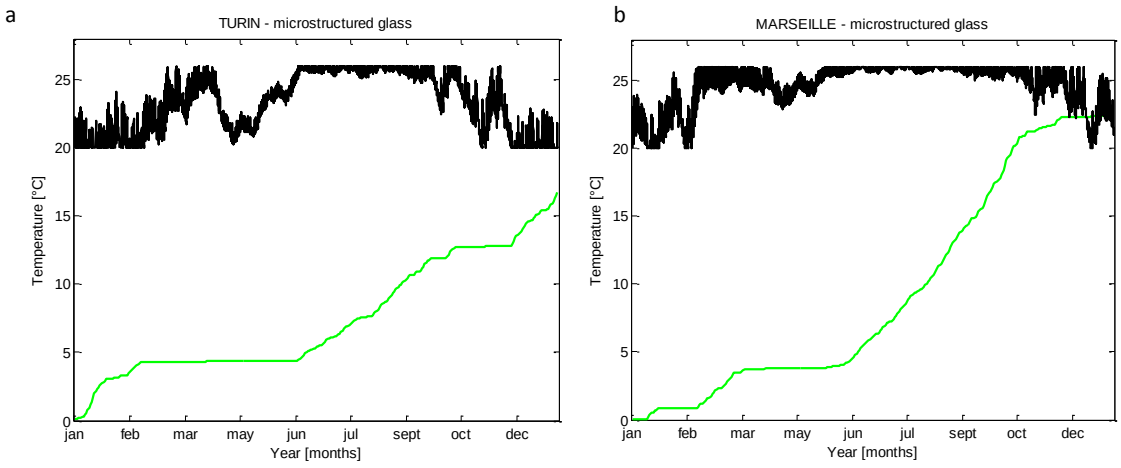

Fig. 5.21: cumulated thermal loads with the microstructured glass in Turin (a) and in Marseille (b).

This first result demonstrates that a static system with an angular dependent transmittance can create high seasonal thermal dynamics, bringing important energy savings. In Lausanne for example, in a well-insulated building with 40% window area on the facade, an optimized microstructured glass reduces thermal loads by 29% if compared to a standard double glazing and by 17% in comparison with the sun protective glass (U value of the window equal to 1.3 W/m^2K).

The thermal performance of the novel microstructured glazing optimized for Lausanne was analysed in several climates all over Europe and compared with a standard double glass and a sun protective glass. A parametric study for quantifying the needed thermal loads during the year was presented, based on simulations with a ray tracing program. Focusing on a south-oriented well-insulated room, the impact of the embedded microstructures on the yearly energy consumption was shown for different climates. The study demonstrates the impact that a suitable design of the glazing envelope can have on the energy balance of the building. For southern located cities, embedded microstructures are competitive, in comparison with the use of a sun protective glass. The geometry of the CFS could be improved to obtain higher energy savings, for southern locations. In the north of Europe, energy savings are slightly lower but still around 5%, except for Glasgow and Bergen.

5.4.3 Optimization for the location of Athens

The improvement of the performance of the microstructured glass is analysed in this paragraph. The aim is to optimize the geometry of the microstructured glass, in order to find a suitable solution for southern locations. Varying the geometric parameters of the embedded micro-mirrors at higher latitudes than Lausanne, an important

improvement is not reachable. At this range of latitudes the sky is mainly overcast and the microstructures cannot significantly bring to lower thermal loads. On the contrary, as the latitude decreases, the direct irradiance rises and another optimization of the embedded microstructures can be obtained. Indeed, especially concerning locations in southern regions of Europe, windows can lead to high solar gains and glare problems, that can strongly influence the energy consumption and the indoor comfort. A proper design of the glazing envelope is necessary, to prevent overheating in the building and at the same time to provide a good level of daylighting.

The microstructured glazing was optimized in Athens, as reference city and it is suitable for the lowest range of latitudes (from 37°N to 43°N). This glazing can be properly designed in order to block the high amount of solar gains, reducing the cooling loads much more than with the microstructured glass optimized in Lausanne. In general, the transmittance in southern climatic conditions should be very low in spring and summer and quite high for a smaller interval of incidence angles, due to the short cold season. The standard double glazing is considered with the same properties that in the case of the optimization in Lausanne; the sun protective glass has to be optimized (Table 5.10 and 5.11). The minimized thermal loads with the optimized sun protective glass are reached with an absorption coefficient of 0,85.

STANDARD DOUBLE GLASS	
Number of panes	2
Glass thickness [m]	0,025
Refraction index	1,5

Table 5.10: properties of the standard double glazing.

SOLAR GLASS	
Number of panes	2
Glass thickness [m]	0,02
Refraction index	1,5
Absorption coefficient	0,85
Spacing [m]	0,02

Table 5.11: properties of the sun protective glazing (optimization in Athens).

The same iterative approach used for the optimization of the embedded microstructures in Lausanne was followed, considering Athens as reference location. The first step is to minimize the thermal loads. Varying the mirror at focus (from 40% to 60%) and the incoming focus angle (from 67% to 10%), thermal loads become equal to 18,2 kWh/m^2. The reduction is significant (39%) because with the optimization in Lausanne annual loads amount to 29,7 kWh/m^2. Moreover, the Canyon effect can be avoided with the up-redirection of the light in the exterior environment. However, Figure 5.22 shows that this geometry can cause excessive inter-reflections in the PMMA film.

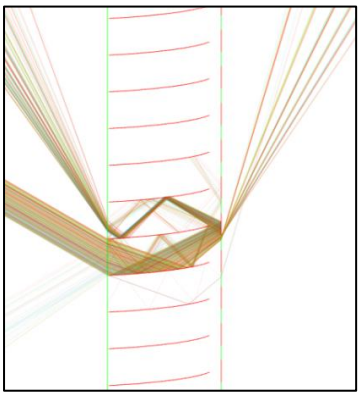

Fig. 5.22: ray tracing of the microstructured glass.

EMBEDDED MICROSTRUCTURE	
Number of panes	2
PMMA thickness [µm]	620
Concentrator length [µm]	550
Sub segments	25
Mirror at focus	0,6
Period height [µm]	200
Incoming focus angle [°]	10
Focus offset [%]	30
Horizontal offset [µm]	10

Table 5.12: properties of the microstructured glazing (first optimization in Athens).

As it can be noticed from Figure 5.23, this geometry for the micro-mirrors is not suitable. The sun elevation in Athens varies in a range going from 28,6° to 75,5°. The transmittance is not sufficiently high during the cold months; the

maximum value is 38% when the incidence angle is 45° (corresponding to March or October). During December, January and February the transmittance vary between 13% and 24%. Moreover, this geometric configuration is not able to provide a reasonable level of daylighting into the room.

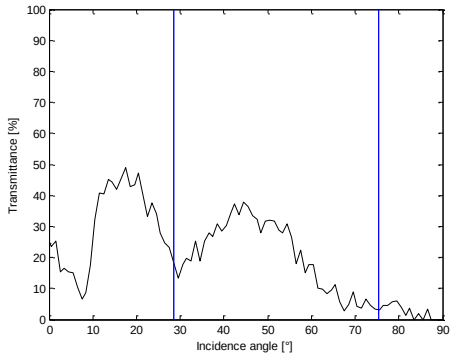

Fig. 5.23: total energy transmittance of the embedded microstructured glazing (first optimization) at different sun elevation angles. Blue lines indicate the solar altitude at noon on solstices for Athens.

Consequently, a new microstructure is obtained (Figure 5.24), changing the geometry, in order to obtain a marked seasonal variation of the total transmittance. The PMMA thickness is higher than the optimised structure in Lausanne (820 μm instead of 620 μm). The incoming focus angle is slightly increased: 45%, while for Lausanne was 40%.

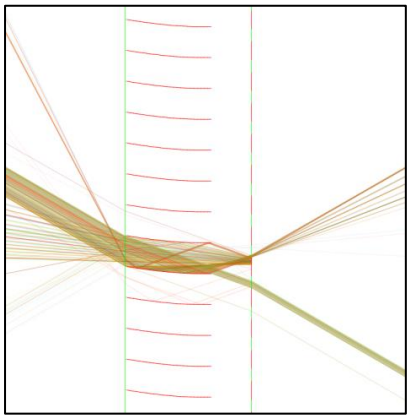

Fig. 5.24: ray tracing of the microstructured glass.

EMBEDDED MICROSTRUCTURE	
Number of panes	2
PMMA thickness [µm]	820
Concentrator length [µm]	550
Sub segments	25
Mirror at focus	0,35
Period height [µm]	200
Incoming focus angle [°]	45
Focus offset [%]	30
Horizontal offset [µm]	10

Table 5.13: properties of the microstructured glazing (second optimization in Athens).

In Figure 5.25 the total energy transmittance is illustrated. In the winter solstice, corresponding to the minimum incidence angle (28,6° in Athens), the transmitted energy is 48%. Then it increases until to reach a peak amounting to 74% at 37,6°. This range of incidence angles corresponds to the coldest months (from November to the middle of February). A significant decrease of transmittance takes place after this peak.

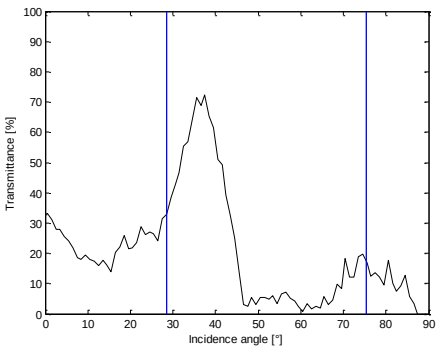

Fig. 5.25: total energy transmittance of the embedded microstructured glazing (second optimization) at different sun elevation angles. Blue lines indicate the solar altitude at noon on solstices for Athens.

The advantage is that, in spring and partially in autumn, when the sun elevation is between 46° and 60°, the early overheating is avoided because the transmittance is low (not exceeding 10%). During summer the transmitted energy can reach 20% at certain incidence angles, remaining quite low.

This effect can be noticed in Figure 5.25. The annual cumulated loads are reduced with this new geometry from 29,7 *kWh/*m2 to 19,4 *kWh/m²* (about 35%).Cooling loads are significantly reduced with the new geometry of the microstructured glass in Athens. With the optimization in Lausanne, cooling loads are required almost all over the year (more than 29 *kWh/m²*). The new optimization allow to reduce the cooling until 15 *kWh/m²*. There is also a need for heating during the cold season, amounting to 4,3 *kWh/m²*. The main part of the annual thermal loads are always due to the need for cooling but this requirement is greatly reduced.

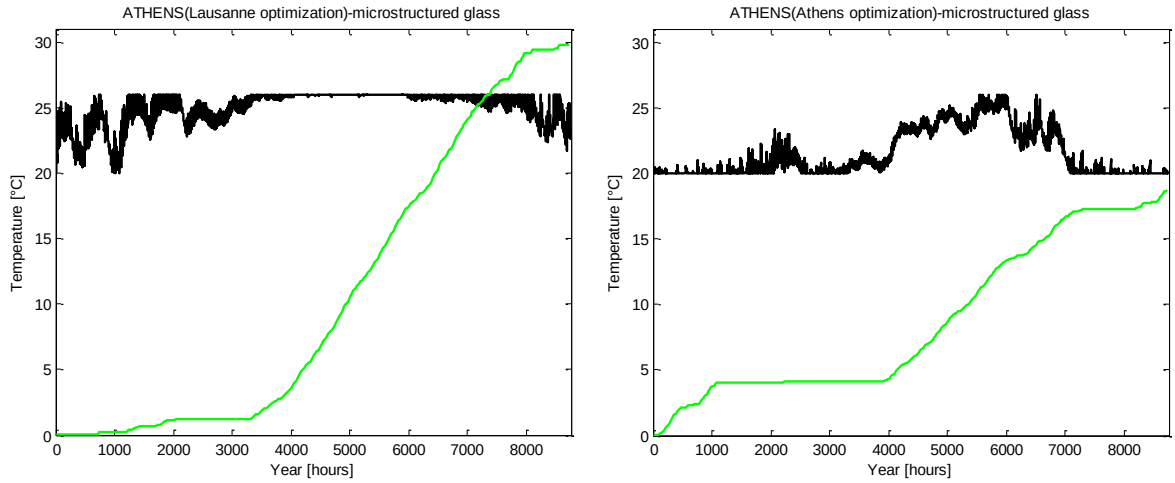

Fig. 5.26: annual thermal loads in Athens with the optimized microstructured for Lausanne and for Athens.

This configuration of the microstructured glass brings to the minimization of the thermal loads in Athens, that result equal to 19,4 *kWh/m²*.

However, a further optimization of the microstructured glass is needed, because the optimized sun protective glass in southern locations requires a lower amount of annual thermal gains (17,6 *kWh/m²*). In this way, the saved energy can significantly increase in a range of low latitudes (below 44°N). In these southern regions, the direct irradiance reaches high levels most of the months, usually overcoming 100 W/m² from March to September. The new proposed geometry is characterized by a non-parabolic shape, that allows to transmit solar radiation mainly for low elevation angles. In Figure 5.27 the comparison between the elevation angle dependent energy transmittance of the two different configurations can be observed. This optimized geometric configuration of micro-mirrors blocks radiation between 45° and 65°. The rest is maintained for view towards outside, daylight and thermal gains in winter months.

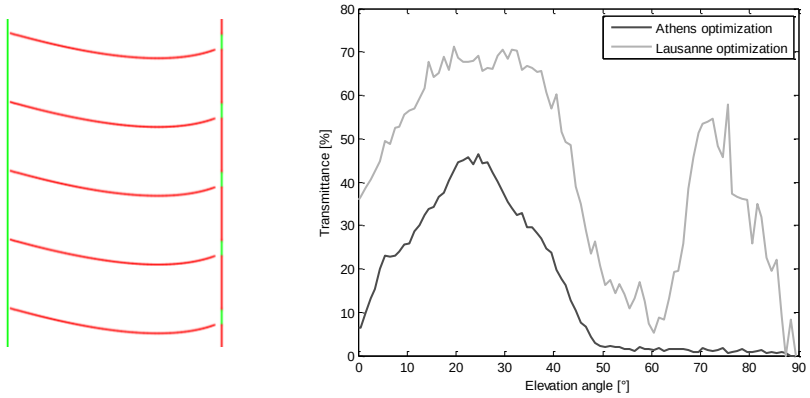

Figure 5.27: (a) geometric configuration of the embedded micro-mirrors optimized in Athens. (b) solar energy transmittance of the optimized microstructured glass in Lausanne and Athens, at different sun elevation angles. Blue lines indicate the solar altitude at noon on solstices for Lausanne.

In Athens as reference location, the sun elevation at noon ranges from 29° to 75°. During winter a solar transmittance between 37% and 20% is sufficient to help the heating system, as it can be noticed in Figure 5.27. Furthermore, this geometric configuration allows a significant reduction of the cooling loads in summertime. The blocking range is larger than in the case of the Lausanne optimized microstructured glass, covering all the sun incidence angles above 50°. Therefore, the transmittance during spring, summer and autumn is very low, not surpassing 3%. In this way, the reduction of the risk of building overheating and of the cooling requirement is guaranteed, especially during the hot season. in order to quantify the potential energy savings in comparison with the microstructured glass.

Also the optimization of the sun protective glass was performed in Athens. Figure 5.28a shows the annual thermal loads and the cooling loads with the sun protective glass, varying the transmittance at normal incidence angle. The two dots correspond to the total thermal loads and the cooling loads obtained using the microstructured glass. As the transmittance rises, cooling loads are increasing; when the transmittance is higher than 50%, the total annual loads coincide with the cooling consumption. The minimum amount of thermal loads (equalling 17,6 kWh/m^2) is reached for a transmittance equal to 24,5%. Concerning the sun protective glass, heating loads are dominant only if the transmittance is lower than 20%. The saved energy in Athens, comparing the novel CFS glazing envelope with the sun protective glass, amounts to 23%.

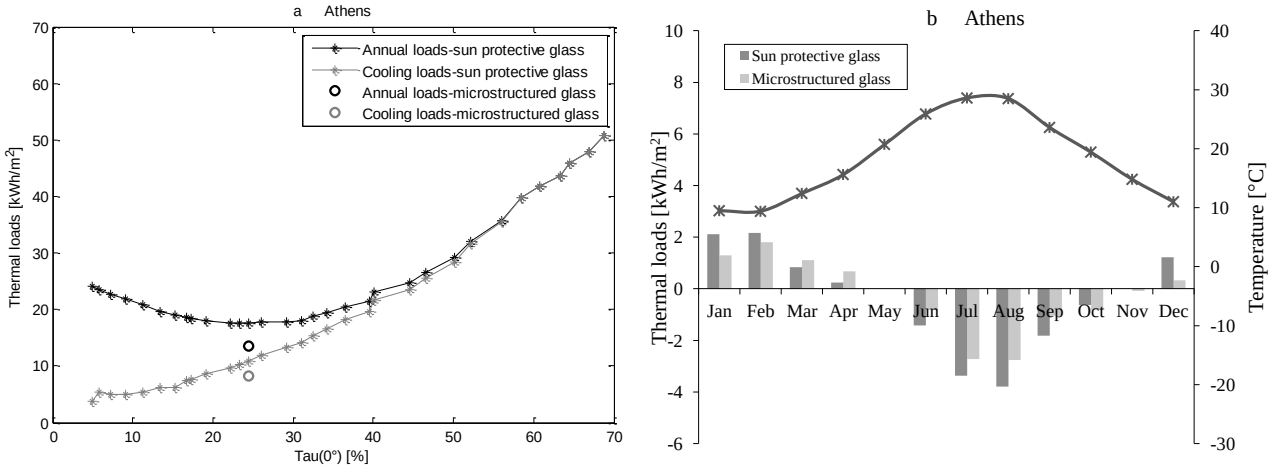

Figure 5.28: (a) annual thermal loads and cooling loads varying the solar energy transmittance of the sun protective glass in Athens; the dots represent the annual thermal loads and the cooling loads of the microstructured glass. (b) mean monthly temperature and cooling and heating loads during the year in Athens using the sun protective glass and the microstructured glass.

In Figure 5.28b monthly thermal loads required in the Greek location, using the optimized standard glass and the optimized microstructured glass in Athens, are shown. In addition, on the secondary axis the mean monthly temperature in Athens is displayed. Both the optimized glazing envelopes in Athens cause a need of heating from December until April. However the loads during these months never overcome 2 kWh/m^2. Despite the amount of needed heating in winter, the use of the suitable geometry for southern locations has the advantage to significantly reduce the cooling loads, in summer and autumn. In June, July, August and September the required air conditioning with the new design is reduced. During June and September the reduction of the cooling consumption is even above 40%. Therefore, the new optimized microstructured glazing can be a potential solution, in order to adapt to locations in which the climatic conditions are characterized by high temperatures and dominant direct irradiance, around 40°N of latitude. This suggestion can also be a suitable design for the future years, in a perspective of climate change.

Once determined the optimal geometry of the microstructures for the reference city of Athens, the obtained annual thermal loads in the Greek location, for all the three considered glazing envelopes, are shown in Figure 5.29.

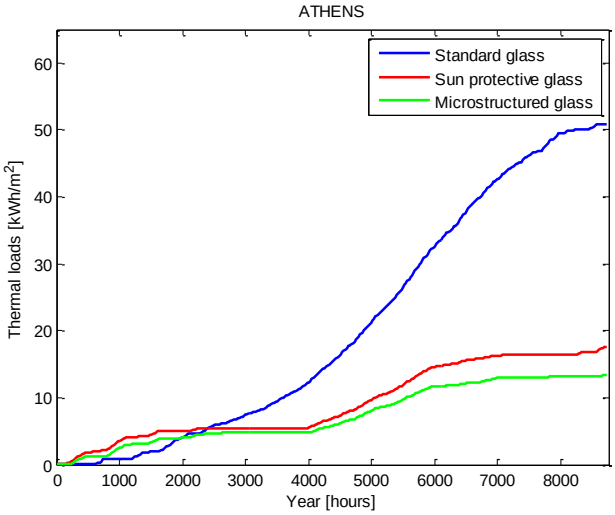

Fig. 5.29: cumulated thermal loads in Athens for the three glazing envelopes.

Thermal loads with the standard double glazing are always the same: 50,8 kWh/m^2. However, the reachable loads with the sun protective glass and the microstructured glass are lower (17,6 kWh/m^2 and 13,5 kWh/m^2, respectively). The saved energy by the heating and cooling consumption, using the new geometric configuration of the embedded micro-mirrors and the optimized sun protective glass, is about 23,4% and 73,5% respectively.

Embedded microstructured glazing can be a suitable solution, if their geometric characteristics are specifically optimized for particular range of latitudes. This analysis shows that the savings that are achieved by the installation of the microstructured glass are relevant respect to the case of the sun protective and the standard glass. However the geometric configuration has to be adapted, depending on the location latitude. In general, the microstructured glass is convenient from the energetic point of view.

In conclusion this novel complex fenestration system could be a potential solution for a relevant reduction of overheating in buildings located at low European latitudes, helping to decrease the cooling energy consumption, which is likely expected to grow more and more in the future years. At the same time, it could help to reduce the heating consumption in the northern locations, better exploiting the solar gains in winter.

5.4.4 From large scale to small scale

In order to obtain a confirmation about the advantage of the embedded microstructures, focusing on the link between climate and energy savings, it is interesting to study the thermal performance of the glazing envelope in a small scale. In this paragraph, results concerning Switzerland are presented. Simulations have been performed in thirteen Swiss locations, situated in a relatively small range of latitudes, going from 46°N (Lugano) to 47,7°N (Schaffhausen). Figure 5.30 shows the map of the chosen locations and in Table 5.14 their relative latitude, longitude and altitude.

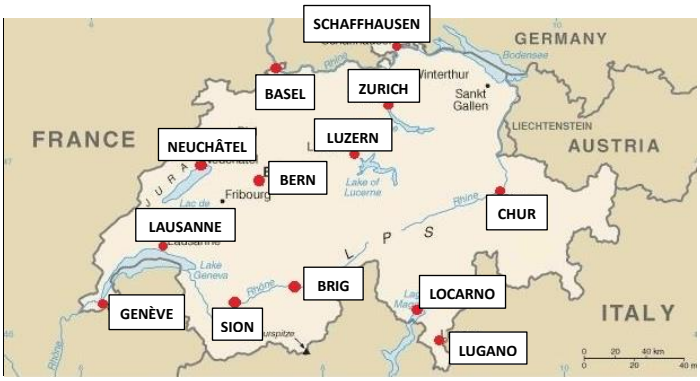

Fig. 5.30: map of the thirteen chosen locations in Switzerland at different latitudes.

	Lugano	*Locarno*	*Sion*	*Genève*	*Brig*	*Lausanne*	*Chur*	*Bern*	*Neuchâtel*
Latitude [°]	46,004	46,173	46,219	46,245	46,303	46,512	46,870	46,928	47,000
Longitude [°]	8,960	8,787	7,330	6,124	7,843	6,667	9,531	7,420	6,954
Altitude [m]	273	366	482	420	640	461	555	565	485

	Luzern	*Zurich*	*Basel*	*Schaffhausen*
Latitude [°]	47,036	47,378	47,541	47,69
Longitude [°]	8,301	8,566	7,583	8,620
Altitude [m]	456	556	316	437

Table 5.14: considered Swiss locations for the evaluation of the influence of latitude on the thermal performance of the glazing envelopes, with the corresponding latitude, longitude and altitude.

Simulations have been performed for each location, with the geometric configuration optimized in Lausanne, suitable for northern and central European latitudes.

Figure 5.31 shows the obtained annual thermal loads at different Swiss latitudes. Cumulated loads are between 14 kWh/m^2 (in Locarno with the microstructured glazing) and 34 kWh/m^2 (in Zurich with the sun protective glazing). In general, the microstructured glass bring the lowest annual loads. The standard glass is the worst performing envelope for all the locations, except in Bern, Luzern and Zurich. Low values of annual loads can be found until a latitude of 46,9°N (Chur). Until this latitude, cumulated thermal loads with the microstructured glass are between 14 kWh/m^2 (in Lugano) and 19,4 kWh/m^2 (in Lausanne). The only exception in this range of latitude is Genève, for which the thermal loads amount to 21,2 kWh/m^2. After the latitude corresponding to Chur, there is a significant increase of the loads: Bern (23,1 kWh/m^2), Neuchâtel (24,8 kWh/m^2), Luzern (26,1 kWh/m^2), until to reach 31,2 kWh/m^2 in Zurich with the embedded microstructured glazing. Basel turns out to have low thermal loads (23,3 kWh/m^2), in comparison with the locations situated in the highest range of latitudes (from 47°N). The reason is that Basel, has a higher direct irradiance in winter, compared with Luzern and Zurich: in January the direct irradiance is equal to 17 W/m^2 in Basel, 12 W/m^2 in Zurich and 10 W/m^2 in Luzern. Therefore, Zurich and Luzern have a sky that in winter is more overcast than in Basel. Additionally, the monthly mean temperatures in Basel are at least higher of 0,7°C than in Zurich and Luzern. The last location (Schaffhausen), situated at 47,7°N, has higher annual loads than Basel, increased by 16%. This percentage increase is mainly due to the difference of temperature between the two locations, because the irradiance behaviour all over the year is similar: in summer there is a difference of 0,5°C between Basel and Schaffhausen, while in winter around 1,3°C-1,5°C.

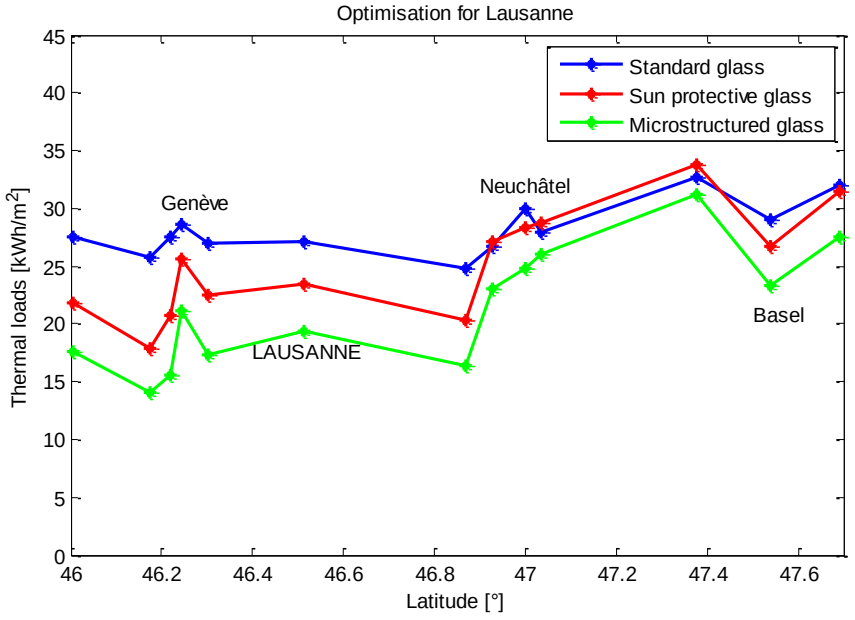

Fig. 5.31: annual thermal loads at different Swiss latitudes and for the three glazing types.

An accurate analysis of the meteorological variables is needed, in order to justify the resulting thermal loads.

For example, concerning Bern, Luzern and Zurich, the inefficient performance of the sun protective glass can be explained through the climatic conditions. The temperatures in these three locations, during summertime are the lowest of Switzerland (amounting between 1,5°*C* and 18,7°*C* in June, July and August). Additionally, as it can be noticed in Figure 5.32, the predominant portion of the global horizontal irradiance is the diffuse, except in August, where the direct slightly overcomes the diffuse. Therefore, expect in August, the distribution of the sky is mainly overcast. For this reason, the use of the sun protective glass is not decisive, in order to reduce the annual thermal loads.

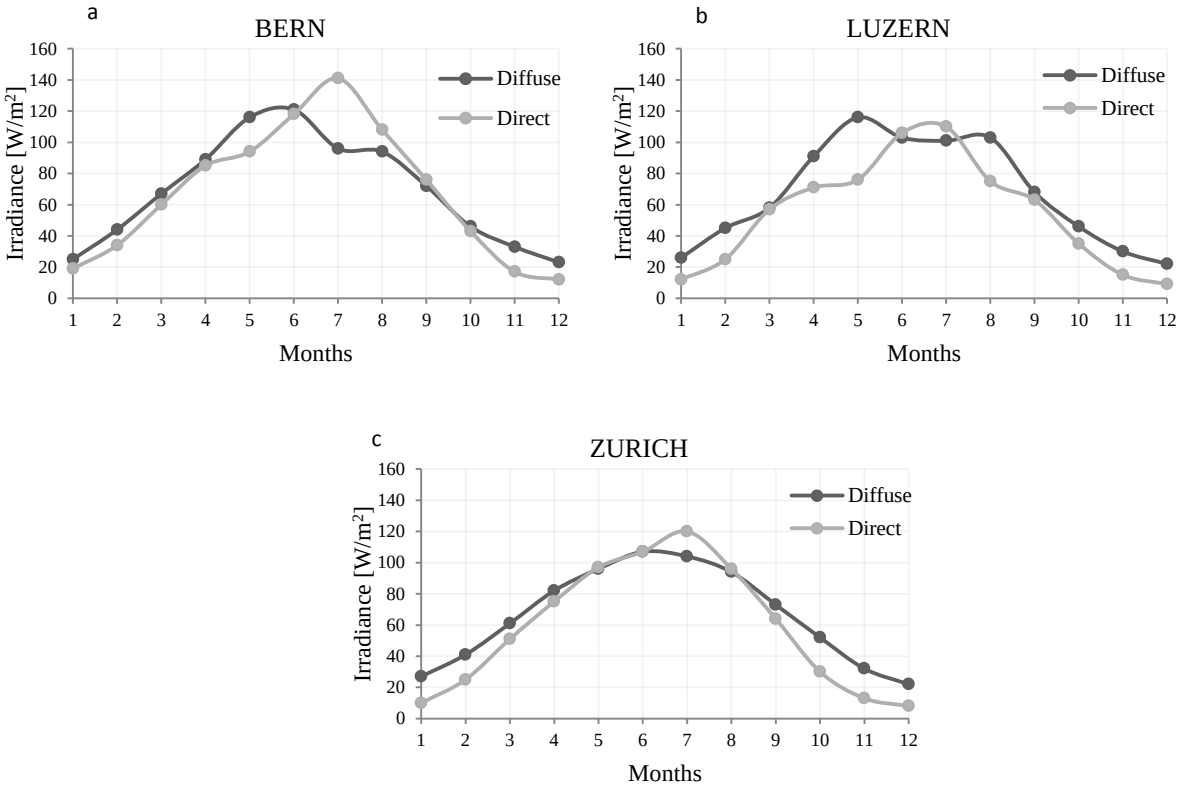

Fig. 5.32: diffuse and direct horizontal irradiance all over the year in Bern (a), Luzern (b) and Zurich (c).

Figure 5.33 illustrates the variation of the irradiance values with the latitude. Both the direct and diffuse irradiance are shown, for two summer months (June and July) and two winter months (January and December).

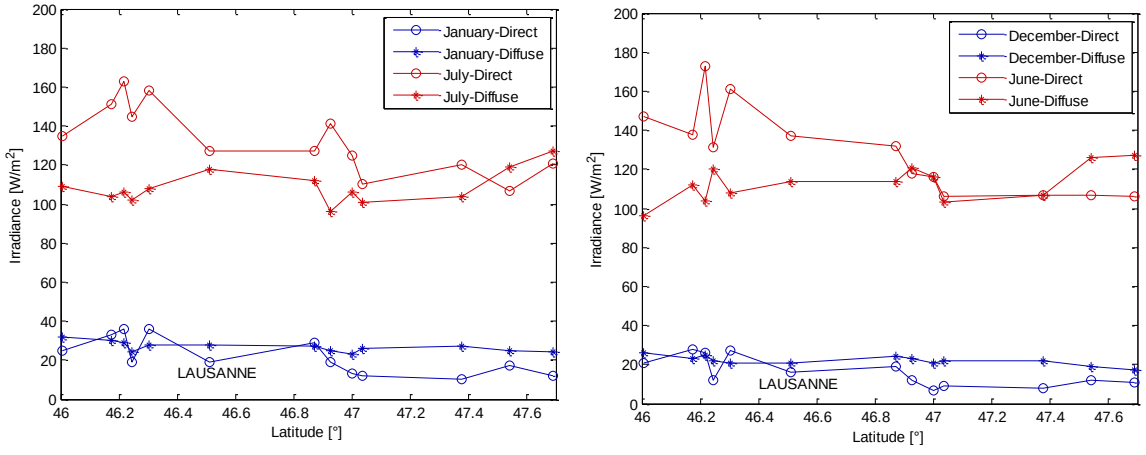

Fig. 5.33: diffuse and direct irradiance at different Swiss latitudes in the months of January and July (a) and December and June (b).

Concerning summertime, the direct radiation is higher than the diffuse (except in the northern locations of Basel and Schaffhausen) in July, while in June the diffuse and the direct part of the radiation have almost the same value in Bern, Neuchâtel, Luzern and Zurich. In general, the diffuse portion of the radiation follows an opposite behaviour, compared with the direct irradiance: when the direct part is increasing, the diffuse decreases. During winter, the diffuse irradiance slightly decreases, varying the latitude: it goes from 32 W/m^2 (Lugano) to 24 W/m^2 (Schaffhausen) in January and from 26 W/m^2 to 17 W/m^2 in December. From a latitude of 47°N, the difference the diffuse and the direct irradiance is relevant, in winter. Consequently, for these locations, the heating demand should be higher than in the lower range of latitude.

It can be noticed that Genève has the lowest direct irradiance, among the cities in the lowest range of latitudes (until Lausanne). The direct irradiance in June and July amounts to 131 W/m^2 and 145 W/m^2, respectively. In the adjacent cities of Sion and Brig the values of the direct irradiance are lower: 173 W/m^2 and 163 W/m^2 in June, 161 W/m^2 and 158 W/m^2 in July. Consequently, the cooling loads should be lower. Moreover, the direct irradiance is lower even during winter in Genève. Therefore the heating loads are expected to be significantly higher in this location. This effect can be observed in Figure 5.34: cooling loads are reduced in Genève, in comparison with the lowest latitudes. The reduction of the cooling demand is about 41%, compared to Sion. On the other hand, the heating requirement in Genève is high for the range of latitudes: 17,3 kWh/m^2, while in Sion and Brig amounts to 11,2 kWh/m^2 and 13,1 kWh/m^2, respectively. Then, it can be observed that the only location in which the cumulated cooling loads (8,6 kWh/m^2) are higher than the heating loads (5,4 kWh/m^2) is Locarno. This location also presents the lowest annual thermal loads (14 kWh/m^2), because of the high levels of irradiance and high mean temperatures in winter (3,6°C and 4°C in January and December). Additionally, it can be noticed that during winter, Locarno, Sion, Brig and Chur have the direct irradiance higher than the diffuse. Consequently, they present lower heating loads compared with the other locations. Concerning Luzern and Zurich, in winter, they have a higher portion of diffuse irradiance than the direct (around 10 W/m^2 more). Therefore, the sky is mainly overcast and the solar gains are not sufficient to significantly reduce the heating demand. Consequently, as it can be seen from the Figure 5.32, in Luzern and Zurich the amount of heating loads is the highest, equal respectively to 25 kWh/m^2 and 30 kWh/m^2. Due to the fact that, during summer, the direct irradiance is lower compared with the other locations, Luzern and Zurich present also the lowest cooling requirement in Switzerland.

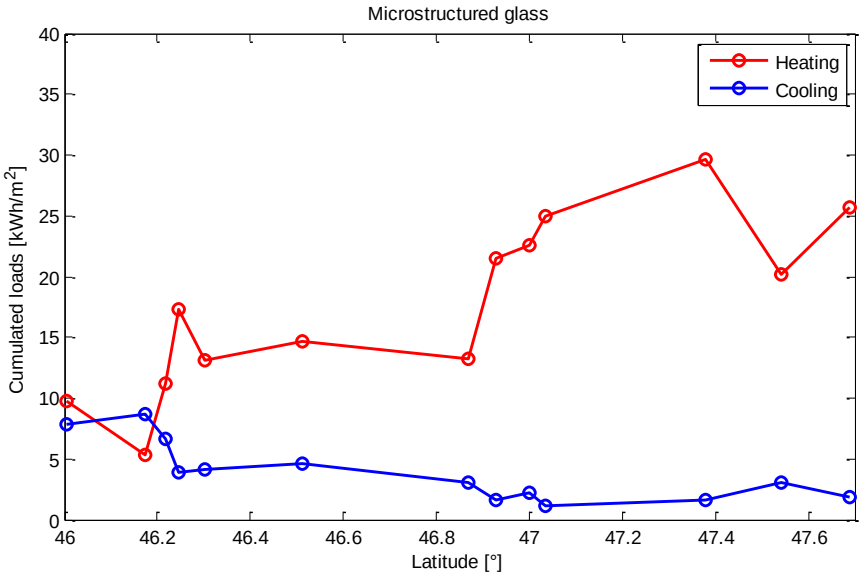

Fig. 5.34: heating and cooling cumulated loads during the whole year at different Swiss latitudes.

Relative energy savings in comparison with the reference glazing envelopes have been calculated and results are displayed in Figure 5.35.

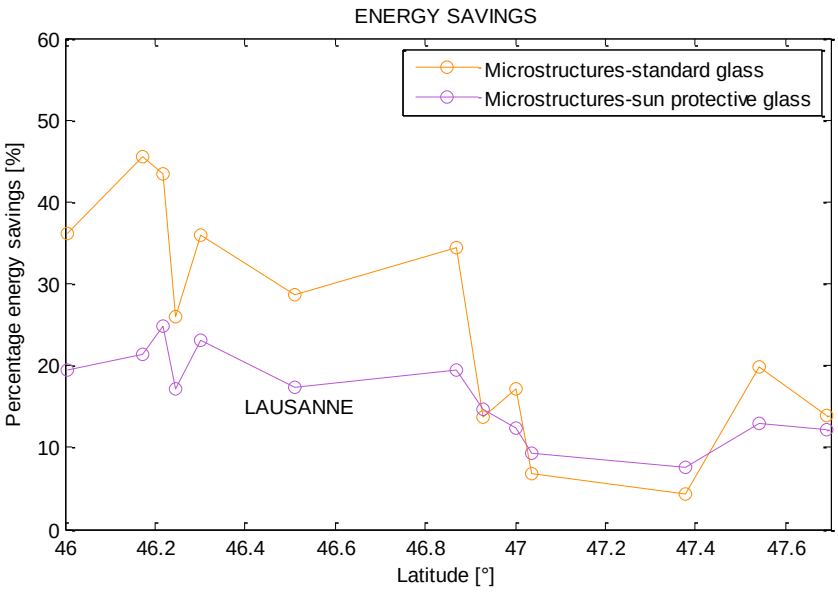

Fig. 5.35: percentage energy savings at different Swiss latitudes, in comparison with the standard double glass and the sun protective glass.

Energy savings compared to the sun protective glass are relevant: until a latitude of 46,9°N they are between 14,8% and 24,8%. The latter is the highest reached value (in Sion). Then there is a slight decrease of the saved energy and in Luzern and Zurich, relative savings compared to the standard glass are lower than energy savings compared with the sun protective glass. Percentage savings in these two locations are 6,7% and 4,4%, respectively. It can be pointed out that in Locarno, the location with the lowest thermal loads, energy savings are not the highest only in comparison with the standard glass (45,5%). Compared with the sun protective glass, in Locarno, 21,4% of the energy can be saved.

It is confirmed by this study, that the microstructured glass can be a valid solution, bringing to significant savings, especially when the distribution of the sky is not mainly overcast all over the year.

5.5 Influence on thermal loads of the heating/cooling system

In this chapter the influence of the reversible heat pump efficiency on the glazing envelope performance is investigated. The previous parametric study was set with a non-realistic value for COP of the heat pump, to evaluate effective thermal loads with balanced heating and cooling and allow the study to be focused on the performance of the window. This hypothesis was reasonable for this first aim. However, the evaluation of the thermal loads varying the heating/cooling system efficiency for a particular location is necessary. This allows to quantify how much the energy savings increase, depending on the reversible heat pump efficiency. For the microstructured glass optimized for Lausanne, the study of the COP variation was performed.

5.5.1 Reversible heat pump performance

The illustration of a reversible heat pump driven by electricity is used to describe the working principle (Figure 5.36). The working principle of this device is to extract heat from one place and transfer it to another, by circulating a refrigerant through a cycle of evaporation and condensation. It can be seen from the scheme that, for the heating mode, the compressor pumps the refrigerant between two heat exchangers. In the first one the refrigerant is condensed at high pressure, releasing the absorbed heat in the cycle. Then, the heat transfer fluid flows through an expansion device and it reaches the evaporator, that is the second heat exchanger, where it evaporates at low pressure, absorbing heat from the surrounding.

Reversing the direction of the cycle and the function of the heat exchangers we obtain the cooling mode in which the building acts as a heat source and the external environment as an heat sink.

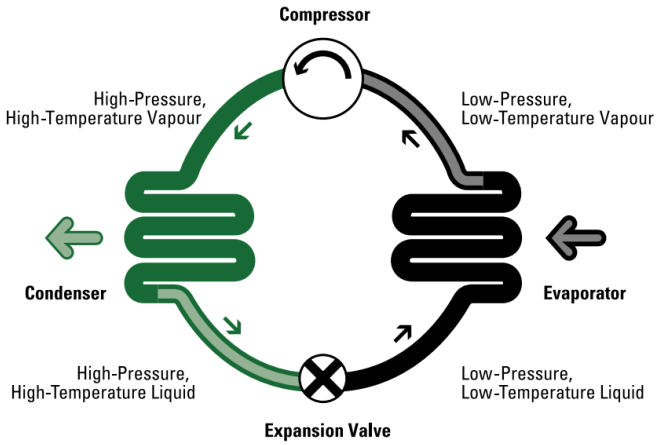

Fig. 5.36: basic working principle of a heat pump [*EnerGuide, 2004*].

In Figure 5.37 the scheme of the thermal plant is shown, both in the heating and in the cooling mode. On the left the heat pump is installed; on the right the air conditioning system is connected to the evaporator.

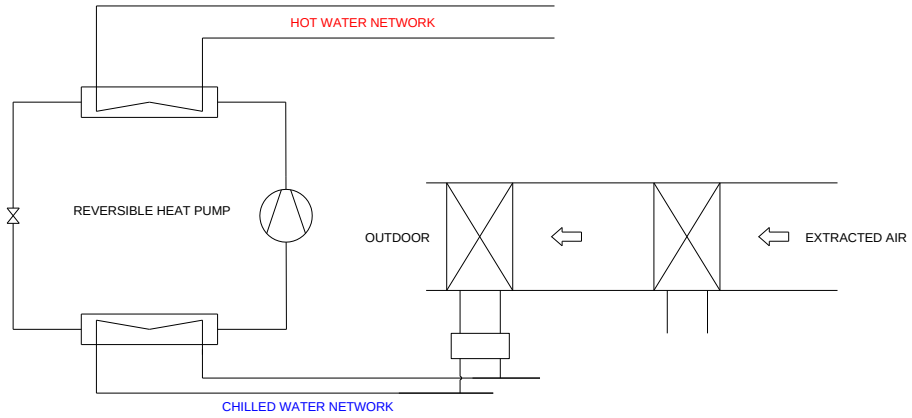

Fig. 5.37: scheme of the heating and cooling system of the reference office room.

The basic components of the loop are the same in both the operational modes. In the heating cycle the condenser is represented by the heat exchanger that provides heat to the radiators. After being compressed, the heat transfer fluid goes in the evaporator that slightly cools the hot water coming from the boiler and finally there is the expansion in the valve. In the cooling cycle the function of the two heat exchangers is exchanged and the evaporator cools the air for the air conditioning system.

Heat pumps are characterized by the coefficient of performance (COP), that is defined by the ratio of the useful thermal energy delivered by the heat pump itself and the electric energy consumption. The COP is an important indicator to evaluate the performance of different heat pump technologies. The value of this coefficient is provided by the manufacturers of the heating/cooling system.

There are different kind of reversible heat pumps and each of them have some advantages and drawbacks. Concerning the typology of device, it has to be considered that an air to air or air to water heat pumps, where in both cases the source of heat is the outdoor air, have the drawback that consists in extracting heat from a source (the outside ambient) with a variable temperature and humidity during the year, resulting in a waste of efficiency. For this reason, usually the installation of a water to water heat pump, where the source is an aquifer, or of a ground source

heat pump, with the ground that remains at almost constant temperature all over the year, leads to better performance, thanks to the fact that the heat source undergoes less temperature changes.

The first parametric study was based on the evaluation of the performance of different kind of glazing envelopes at different latitudes, given a particular HVAC system. Theoretical COP values have been assumed equal to 1 for cooling and heating, in order to focus on the glazing envelope performance, considering effective annual thermal loads. However, it is interesting to perform all the simulations considering the same location and changing the performance of the heating/cooling system, in order to evaluate the influence of the heat pump efficiency on the thermal energy savings. The efficiency of the heating and cooling system significantly affects the smart management of the building energy consumption. Indeed, the variation of the COP values of the reversible heat pump has an influence on thermal loads. Lausanne was considered as a reference location to carry out simulations, because the geometry of the microstructured glass was optimised in this location for a middle range of latitudes.

COP values of the reversible heat pump were considered in a wide range both for heating and cooling: from 0,5 to 7. In this way, a general overview on the thermal loads trend can be observed.

Thermal loads were obtained varying the COP for the heating mode. Different curves were plotted at different COP for cooling mode. Considering the microstructured glass optimized in Lausanne, the parametric curves representing thermal loads depending on the COP values are shown in Figure 5.38.

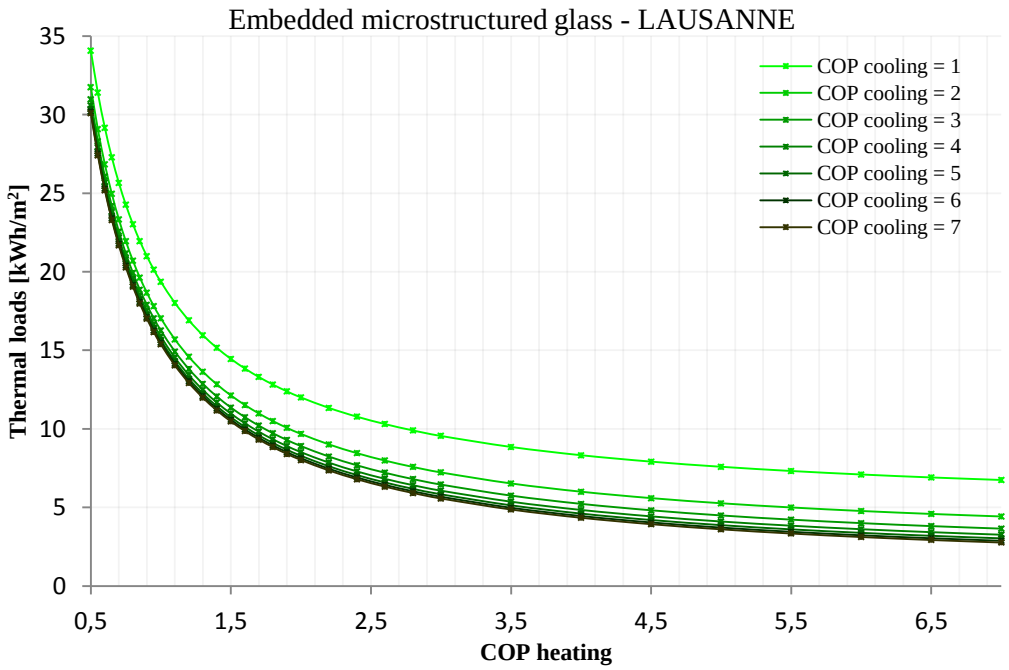

Fig. 5.38: COP influence on the thermal loads in Lausanne for a microstructured glass.

The lower the COP, the higher the annual thermal loads. When the COP is very low (below 2), the thermal loads undergo a relevant decrease: from around 30-34 kWh/m^2 to 8-12 kWh/m^2, depending on the COP for cooling. Furthermore, in this low range of COP, the decrease of thermal loads is higher for the heating mode than for the cooling mode. If the system is efficient, the annual consumption is strongly reduced. However, the reachable reduction of energy consumption with COP values larger than 3 is not significant as much as the potential decrease of thermal loads improving the COP in a lower range. For example, varying the COP for heating from 4 to 5, annual loads vary from 4,9 kWh/m^2 to 4,1 kWh/m^2 considering a COP for cooling equal to 4. Therefore, a reasonable COP value both for the heating and the cooling modes should be found, as a compromise between a good efficiency and an acceptable cost of the HVAC system. However, because heating in Lausanne is the dominant part of the annual loads, it is more important to have a good COP for the heating mode.

To have an idea of the different weight that cooling and heating can have on the thermal loads, in a particular location, it is necessary to plot the cooling COP dependence on thermal loads, for different values of heating COP. This evaluation is shown in Figure 5.39. it can be noticed that the curves is always decreasing as the COP for cooling rises. However, the variation is less relevant varying the cooling COPs; in fact the slope of the curve is less accentuated.

The distance between the heating COP curves is higher than the previous case. For example, installing a reversible heat pump with an heating COP equal to 2 instead of 1, the enrgy savings can be more than 5 kWh/m^2, while the difference between the cooling COP curves is around 2 kWh/m^2.

From the comparison between the two curves, it can be noticed that in Lausanne the heating loads have a bigger impact than the cooling loads for reasonable COP values of the heat pump, among which the range of COP from 2 to 5 is considered reasonable.

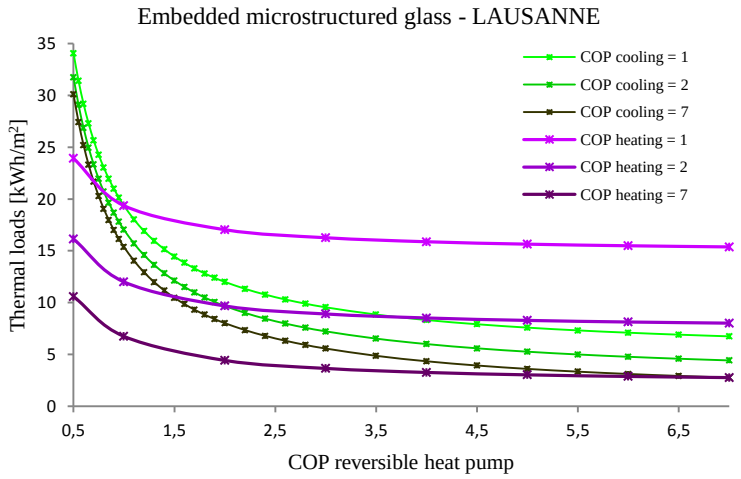

Fig. 5.39: difference between the heating and cooling COPs behaviour on the thermal loads in Lausanne for a microstructured glass.

The same study was performed considering the sun protective glass envelope for the building. Results are shown in Figure 5.40.

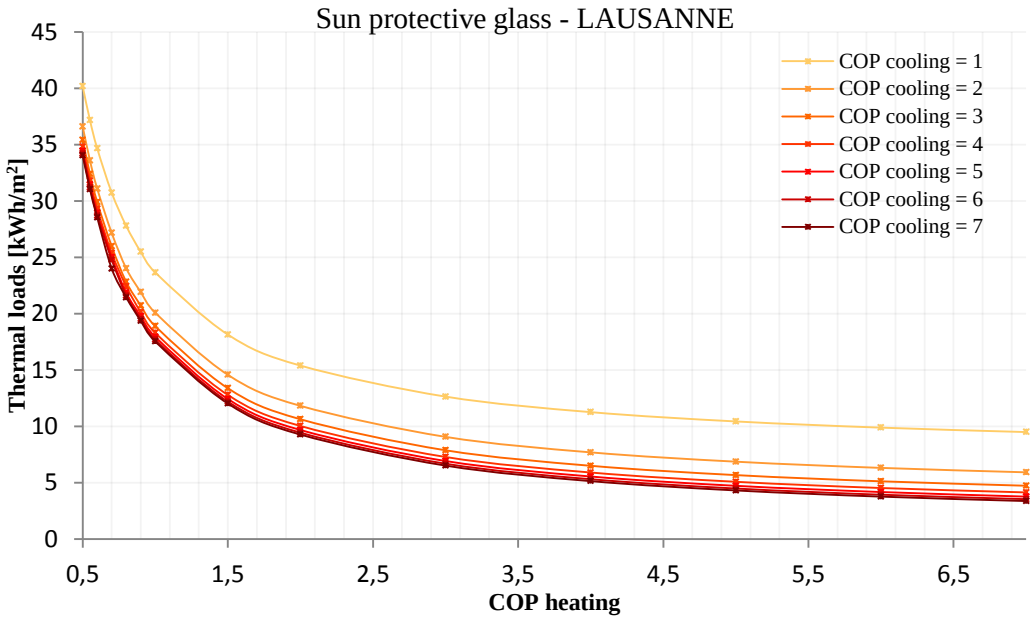

Fig. 5.40: COP influence on the thermal loads in Lausanne for a sun protective glass.

In the case of the solar glass the general trend of the curves is the same and the difference between the thermal loads is relevant for low values of heating COPs, but for highest values (COP equal to 7) is less than 1 kWh/m^2. The only difference is that the thermal loads are slightly higher in comparison with the microstructured glass.

The hyperbolic trend of the coefficient of performance basically depends on the climatic conditions. Focusing on the reference COP values of the first parametric study (heating and cooling COP equal to 1), the histogram below (Figure 5.41) shows the influence of the typology of glazing envelopes on the thermal loads.

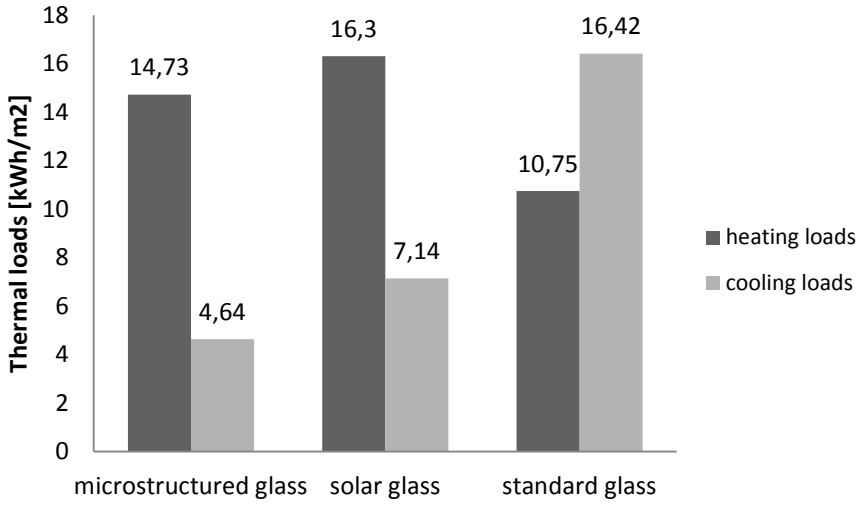

Fig. 5.41: heating and cooling demand in Lausanne for the three glazing envelopes, considering COP=1 for heating and for cooling.

In Lausanne, the predominant part of the thermal loads all over the year is intended for heating. The only exception is the standard double glass that brings to a relevant increase of the total thermal loads, especially to supply the cooling demand. In fact the standard glass leads to 40% of heating consumption and 60% cooling consumption by the reversible heat pump system. Instead, both for the sun protective glass and the microstructured glass the cooling demand is less than a half of that for heating. The innovative glazing envelope is the most convenient because it allows to obtain an higher value of energy savings during the year, reducing both cooling and heating consumption, respect to the sun protective glass. The microstructured glazing allows heating loads to decrease of 10% and cooling loads are reduced of about 35%, in comparison with the sun protective glass.

5.5.2 A Swiss case study

In this subchapter, the installation of a of heat pump with realistic COP values is supposed in Lausanne, in order to quantify the possible percentage energy savings for the reference office room.

Concerning the typology of reversible heat pump, it has to be considered, as previously discussed, that an air to air or air to water heat pump, where the source of heat is the outdoor air, has the drawback that consists in extracting heat from a source (the outside ambient) with variable temperature and humidity during the year, resulting in a waste of efficiency. Therefore, a Ground Source Heat Pump (GSHP) represents a technically viable technology for heating, cooling and domestic hot water in buildings. This heating/cooling system offers several interesting characteristics for the potential user, such as lower electrical demand and maintenance requirements than conventional systems. Consequently, it brings to lower annual costs. From a non-economical point of view, the GSHP offers competitive levels of comfort compared with standard technologies, reducing noise levels and visual contamination and guaranteeing savings of greenhouse gas emissions and reasonable environmental savings. The Environmental Protection Agency (EPA) recognized ground source heat pumps among the most efficient and comfortable heating and cooling systems available today [*Urchueguìa, 2008*].

Climatic conditions in Switzerland are suitable for these heating and cooling systems. There is a long steady heating period with a ground temperature of 10°*C*-12°*C* at a relatively shallow depth. For this reason, it is supposed to install a GSHP reversible heat pump, where the heat source is the ground, that remains at pretty constant temperature over the year. The study was performed for the reference office room. However, it has to be considered that usually in commercial buildings the HVAC system is designed to provide heating and cooling to several offices and not only one. This is only a way to have a realistic example with quantitative data and results.

In Figure 5.42, the scheme of the GSHP installed is showed, with the network of pipes running underground and forming a closed loop. The steady temperature conditions around 5-10 metres of depth allow the heat pump operate efficiently.

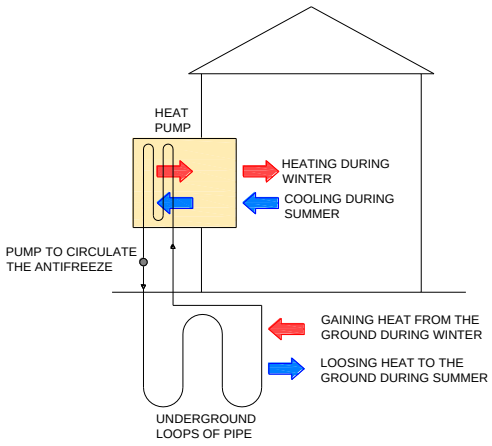

Fig. 5.42: GSHP scheme for the reference office room. The function of reversibility is illustrated.

Figure 5.43 shows the two operational modes of the reversible heat pump.

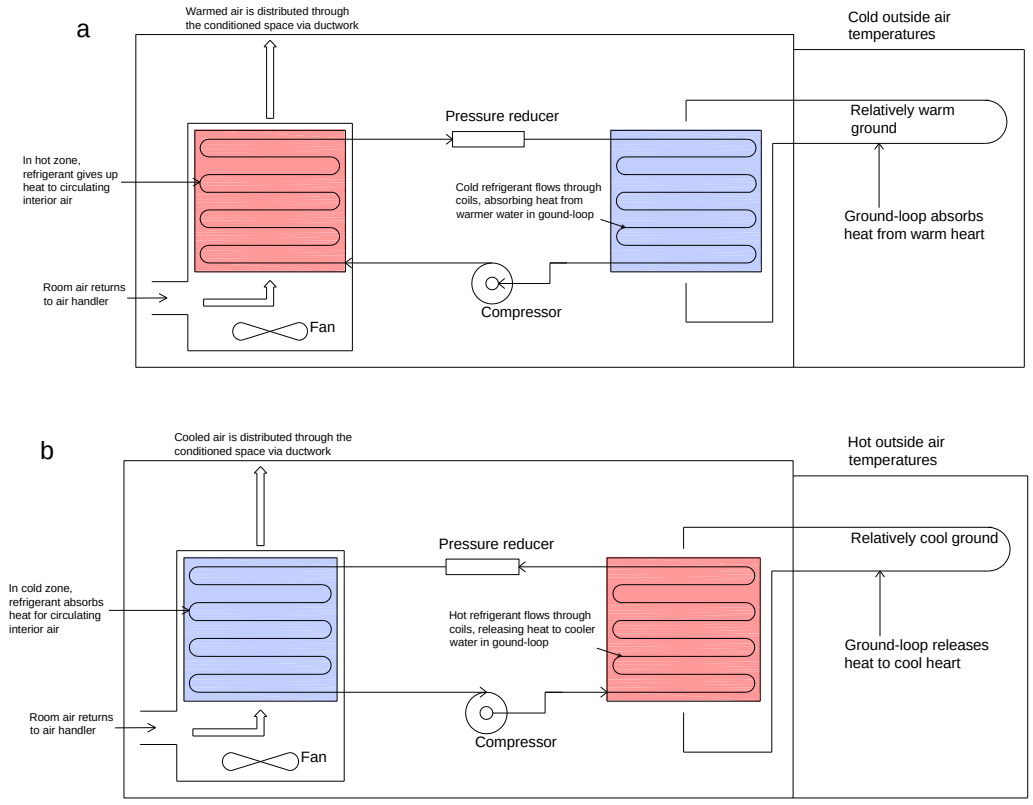

Fig. 5.43: the two operational modes of the reversible heat pump. (a) the heating cycle and (b) the cooling cycle of GSHP system.

During wintertime, an anti-freeze liquid solution, such as propylene glycol mixed with water, which serves as the heating medium, is pumped through the pipes. In this way it is heated up to roughly the ground temperature. This liquid solution enters a heat exchanger which allows the gained heat energy from the ground to be transferred to the heat pump, which then transfers the energy indoors, in order to heat the building. The anti-freeze solution makes its way back underground to gain heat once again from the ground, and the cycle repeats.

During summertime the GSHP can operate in reverse, as a cooler (air conditioner). Indeed, instead of gaining heat from the ground, the anti-freeze solution, that now acts as a cooling medium, releases heat to the ground. As the fluid makes its way back in the cooled state, it enters a heat exchanger which allows the heat energy from the inside of the building to be transferred outside, by way of the heat pump. This process enable the building to get cooler inside [*EnerGuide, 2004*].

The coefficient of performance of the installed GSHP is assessed to be 3 for the heating and 3,5 to supply the cooling demand. These values indicate that the heat pump system has an higher efficiency to cool the office room, respect to the heating supply. The temperature of the ground is supposed to be around 10°*C* all over the year.

The resulting thermal loads are equal to 6,2 kWh/m^2 in the case of the microstructured glazing and for the solar glass and standard double glass are approximately the same, 7,4 kWh/m^2 and 8,3 kWh/m^2. The chart below (Figure 5.44) shows the percentage thermal loads for each kind of glazing envelope. The installation of the novel CFS technology brings to significant savings, in comparison with the two other glazing envelope applications. Therefore, considering COPs values of 3 for heating and 3,5 for cooling, energy savings in Lausanne, in comparison with the sun protective glass, are still relevant, amounting to 16% (instead of 17%).

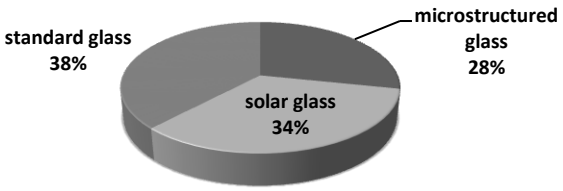

Fig. 5.44: percentage annual thermal loads [kWh/m^2] for the Swiss case study.

It is important to evaluate how these thermal loads are distributed during the year, because they can be used for the heating or for the cooling demand in different amounts, mainly depending on the type of climate. As it can be expected, in Lausanne they are used for 72% in order to heat the office room (in the case of the sun protective glass).

The economic evaluation was performed, calculating the electric consumption of the office room to satisfy the annual heating and cooling demand. Knowing the COP values of the GSHP and the provided energy to the office, the need of electricity can be obtained by (5.1) and (5.2). In Switzerland the cost of electricity for commercial buildings is equal to 0,1911 CHF/kWh_{el}, corresponding to 0,156 $€/kWh_{el}$ [*DATEC, 2011*].

In winter, when only the heating demand Q_h has to be satisfied, the electricity consumption Q_{el} has been evaluated through the following equation:

$$Q_{el} = \frac{Q_h}{COP} \quad (5.1)$$

During the hot season, when there is the need of cooling supply Q_c, the electricity consumption Q_{el} has been evaluated through the following equation:

$$Q_{el} = \frac{Q_c}{COP} \quad (5.2)$$

In this way, the annual specific electricity consumption for the reference office room has been calculated, taking into account the weight that cooling and heating assume from an economic point of view (Figure 5.46). It can be noticed

that both for the energetic and the economic point of view, the embedded microstructures lead to significant percentage savings. The economic savings using the microstructured glass amount to 15,5% and 21,3%, comparing the sun protective glass and the standard glass, respectively. Considering the solar glass and the standard glass, results are approximately the same. For the microstructured glass the cooling demand brings to lower costs respect to the heating demand, counting about 19% on the annual electricity consumption.

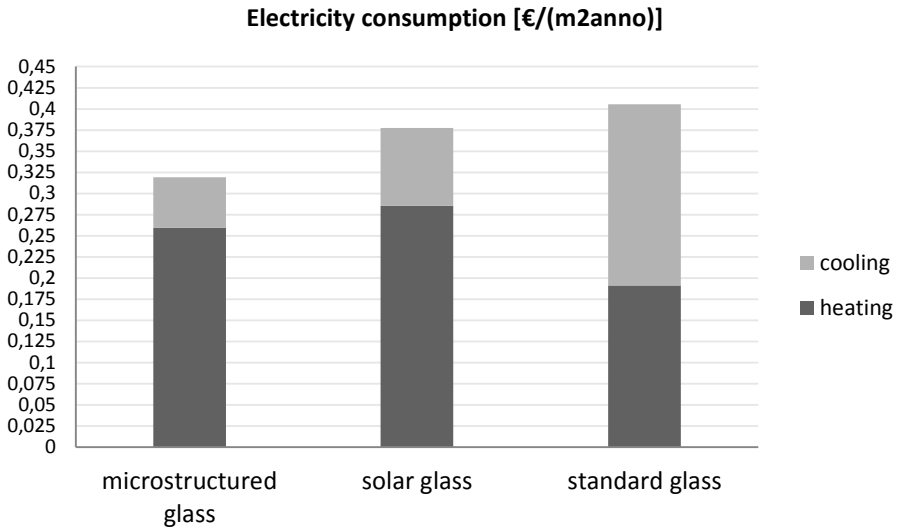

Fig. 5.45: annual electricity consumption for the three different glazing envelopes.

In this case study, the capacity of the heat pump has not a big size because the reference office has a floor area of 29,5 m^2, relatively small. However, the percentage economic savings are relevant and for installation of GSHP in whole buildings with several office rooms and the entire microstructured glazing façade, the amount of saved money during the year becomes very significant.

5.6 Previsions for the future

In general, especially concerning locations in southern regions of Europe, windows can lead to high solar gains, strongly influencing the annual energy consumption. In particular, with the global warming and the increase of average temperatures, a problem of overheating can occur for a higher range of latitudes. Consequently, the general trend for the energy consumption is the reduction of heating loads and the increase of cooling. The changes on thermal loads induced by global warming will vary depending on locations but also on the building envelope. The estimation of the future energy consumption of buildings is becoming more and more important, in order to plan a smarter energy management.

This chapter investigates the future thermal loads for heating and cooling, in order to evaluate the total energy consumption during the year. The aim is to evaluate if the performance of the novel CFS technology for glazing envelope is suitable also in a global warming scenario. The overall effect of the global warming on the energy demand depends on the meteorological parameters, as well as on the type of building. Considering the reference office room previously analysed, the microstructured glass optimized in Lausanne is considered, in order to evaluate its performance at different latitudes. In Figure 5.46, the list of the twenty-one European locations is displayed, with the corresponding extreme latitudes (Athens and Bergen). Meteorological data for the probabilistic future climate projections are provided by the Meteonorm database [*Meteonorm, 2014*], as the data for the current climatic conditions. Projections until 2050, following the A1B scenario produced by the Intergovernmental Panel on Climate Change (IPCC) were selected, considering an albedo of 0,2. The IPCC is a scientific intergovernmental group established by the World Meteorological Organization (WMO) and the United Nations Environment Programme (UNEP) to assess the scientific, technical and socio-economic information relevant for the understanding of the risk of

human induced by climate change. The A1B scenario is one of the Special Report on Emissions Scenarios, belonging to the A1 group. The A1 storyline describes a future world of very rapid economic growth, global population that peaks in mid-century and declines thereafter and the rapid introduction of new and more efficient technologies. This scenario is distinguished in three groups that describe alternative directions of technological changes in the energy system: fossil intensive (A1FI), non-fossil energy sources (A1T) and a balance across all sources (A1B) [*IPCC, 2000*].

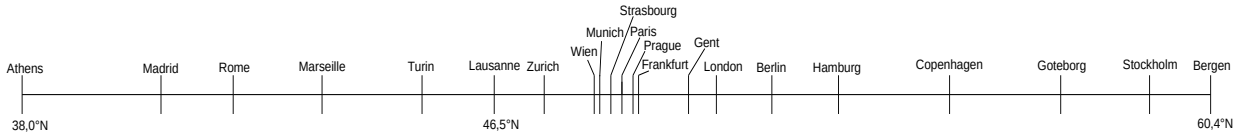

Fig. 5.46: list of the twenty-one chosen European locations; the range of latitude is between 38°N (Athens) and 60,4°N (Bergen).

The 20th century has been marked by a global warming of the Earth of about 0,6 to 0,9 *°C* [*Le Treut, 2003*]. In Figure 5.47 the expected increase of the mean monthly air temperature in January and July during 2050 is displayed. Both in summer and winter, the increase of temperature is larger for the low range of latitudes (until 48°N). The difference of temperature for these locations stands between 1 *°C* and 2,7 *°C*. The highest difference of temperature is expected in Turin, where in July amounts to 2,7 *°C* and in January to 2,3 *°C*. Locations situated in the continental region, such as Paris, Frankfurt and Munich, are characterized by a small increase of temperatures, in comparison with the other locations. In the north of Europe, when the latitude is higher than 54°N, the increase of temperature is relevant in winter (about 1 *°C*), while in summer is smaller (around 0,5 *°C*). Moreover, considering huge urban areas (UHI), that are expected to grow up, the increase of the ambient mean temperature could be even more relevant.

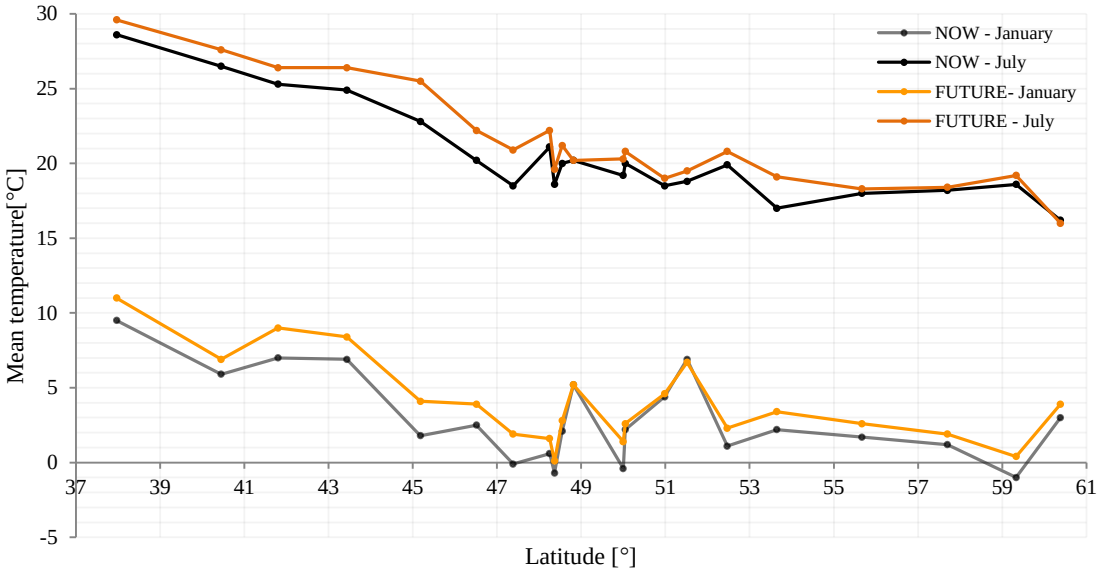

Fig. 5.47: monthly mean temperature increase varying the latitude in January and July.

The future climate projections provide also data about the global horizontal and the diffuse irradiance. The difference of global horizontal irradiance between the current situation and the future is not significant as the rise up of temperature. The global irradiance slightly decreases, except for southern locations, such as Madrid, Rome and Marseille that see a general increase all over the year.

The magnitude of these climatic change can vary depending on the region and on the season. However, the overall influence on the energy consumption depends on the local and seasonal meteorological variables, as well as on the type of glazing envelope. The performance of the building glazing envelopes has been evaluated through the Monte Carlo based ray tracing program [*Kostro, 2014*]. Simulations have been carried out for the same range of latitudes going from Athens (38°N) to Bergen (60,4°N).

In Figure 5.48 obtained thermal loads for the microstructured glass are shown. It can be noticed that the increase of the annual loads is significant for southern European locations. From Athens to Lausanne the expected thermal loads stand between 22,6 kWh/m^2 (in Turin) and 37 kWh/m^2 (in Athens). In the nowadays climatic conditions, for this range of latitudes, the cumulated loads are from 16,7 kWh/m^2 and 29,7 kWh/m^2, corresponding to the same cities. From Zurich (47,4°N) to Berlin (52,5°N), the loads are slightly higher in the future scenario, except in Prague, where they decrease of 1,7 kWh/m^2. At these latitudes, the highest difference between the future and the current situation is in Frankfurt, with an increase of 3 kWh/m^2. The northern locations (from Hamburg to Bergen) are characterized by a decrease of the annual thermal loads, more accentuated in Copenhagen, Goteborg and Bergen, where the difference is around 2,5 kWh/m^2.

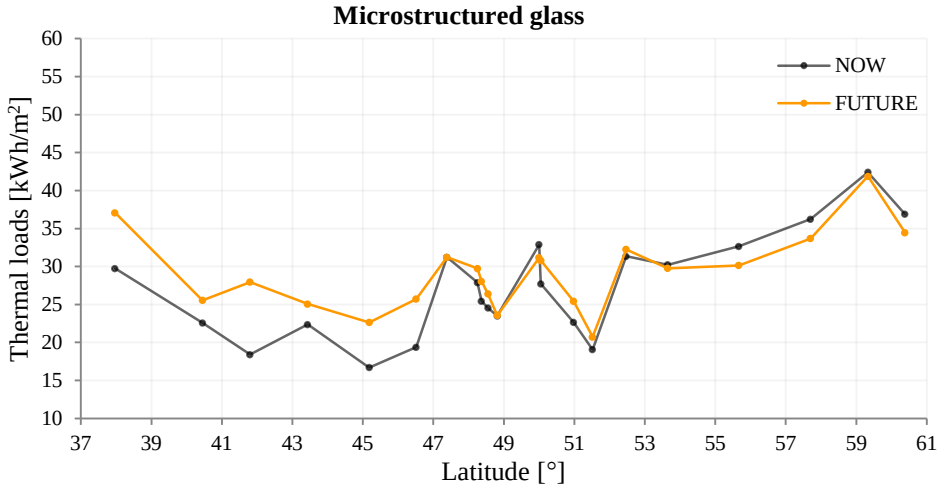

Fig. 5.48: annual thermal loads at different latitudes for the microstructured glass in the current situation and in the future.

In conclusion, three ranges of latitudes can be distinguished: in southern locations the annual loads are increased (until around 47°N), in the continental region the variation is not significant and in the north of Europe the thermal loads are slightly decreased (above 53°N). This is due to the fact that the increase of the average temperature is more relevant in southern locations. In the continental region the expected climatic change is less sensitive. Moreover, in locations situated at latitudes higher than 53°N, the increase of temperature is larger in winter than in summer. Consequently the cooling consumption is not importantly increasing in the north of Europe, while the heating loads slightly diminish because of the increase of temperatures during the cold season. In general, with the global warming effect, the energy consumption for heating decreases. On the other hand, the need for cooling rises up. In Figure 5.49 the cumulated loads in Lausanne are shown with the microstructured glass and the sun protective glass.

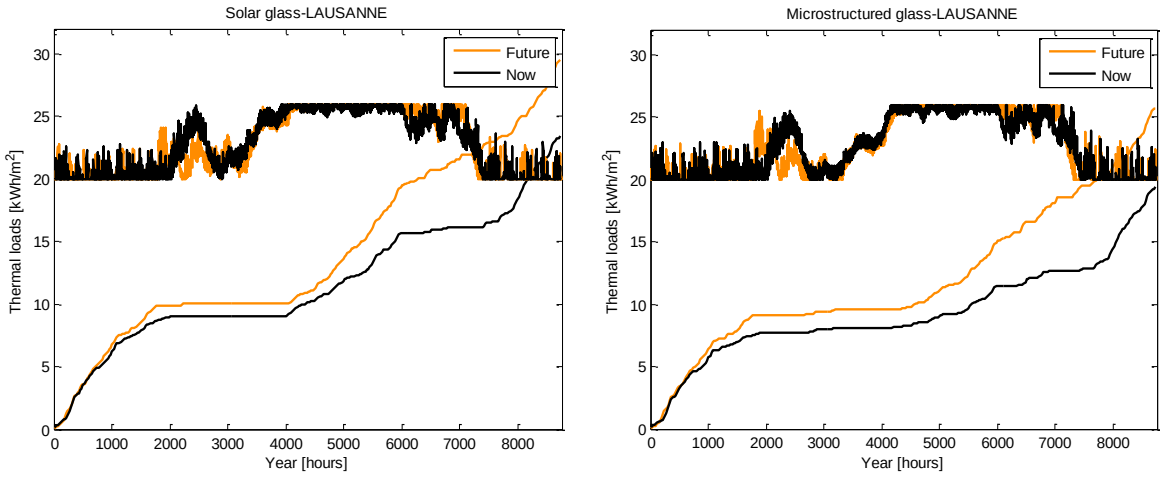

Fig. 5.49: annual loads in Lausanne for the sun protective glass and the microstructured glass in the future and current situation.

In both cases, looking at the future, the thermal loads increase: with the sun protective glass they are 23,4 kWh/m^2 and become equal to 29,5 kWh/m^2, undergoing an increase of 20,7%. With the embedded microstructures the expected increase of annual loads is about 24,7%, going from 19,4 kWh/m^2 to 25,7 kWh/m^2. Even if the percentage increase in the future of the energy consumption is higher with the microstructured glazing than with the sun protective glass, the first one remains the most advantageous glazing envelope. It can be noticed that the period for cooling is almost the same (from June to the end of September), comparing the current and the future situation. However, the slope of the curve of cooling loads is significantly increasing in the projections of 2050. The heating is excepted to increase of 8% and 12%, with the sun protective glass and the microstructured glass respectively. The rise up for cooling is much more relevant: 40% and 48%, respectively.

Relative energy savings in comparison with the sun protective glass for all the considered European locations have been quantified (Figure 5.50).

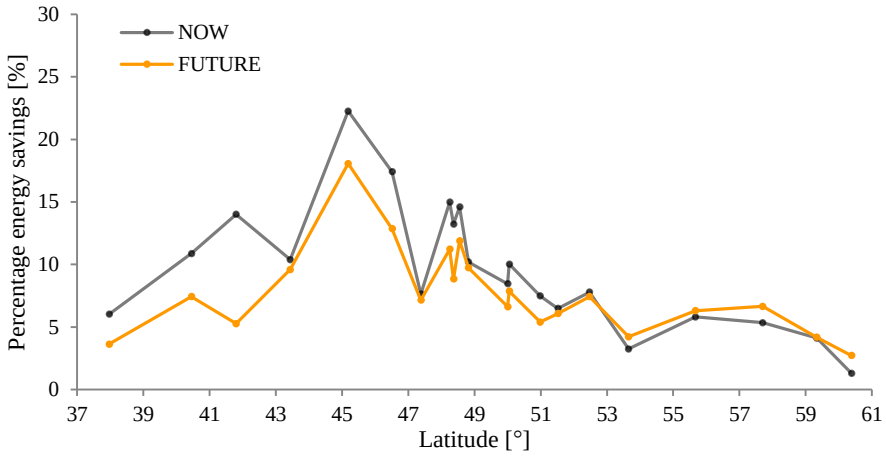

Fig. 5.50: percentage energy savings at different latitudes for the microstructured glass, in comparison with the sun protective glass in the current and future situation.

The curve representing the energy savings has the same shape in the future and present climatic scenario, with the exception of Rome, that will be described in more detail in the following paragraph. Until a latitude of 52,6°N, relative energy savings are decreasing in the future climatic conditions. Especially southern locations are characterized by a considerable reduction of the saved energy; in Athens they diminish from 6% to 3,6% (40% of reduction) and in Lausanne the decrease is about 26%. In the north of Europe, where the latitude is above 53°N, relative savings are increasing, except in Stockholm, where they remain almost the same, rising from 4,1% to 4,2%. In Hamburg the increment is of 23%, in Copenhagen around 8% and in Goteborg is 20%. As last, in Bergen energy savings are expected to grow from 1,3% to 2,7%.

A particular case is the location of Rome. In this city, the energy savings are expected to be significantly reduced, from the current 14,0% to the future 5,3%. The reason can be explained observing Figure 5.51. As it can be noticed, in Rome the direct irradiance is expected to significantly increase in the future decades.

During summertime, the increase the direct irradiance is about 30%, causing a considerable amount of solar gains. In winter the direct horizontal radiation increases between 14% and 40%, depending on the month. The diffuse irradiance is slightly decreasing during the hot season. Consequently, the global irradiance is increased all over the year. The increased temperatures combined with the rise of the direct portion of the irradiance induce the overheating of the building. In Figure 5.51c, it can be noticed that, according to the IPCC projections, there is a first need of cooling from the end of January until April. In these months, the transmitted energy through the microstructured glass is around 70% (Figure 5.51b). When the direct transmittance is between 30% and 11% in spring, there is no need for cooling. Then the cooling requirement is starting again in the end of May, lasting until December. In Rome, the amount of heating is drastically reduced in a future scenario (of about 81%), while the cooling loads are

increasing of 43,6%. In a future scenario of global warming, the annual thermal loads in Rome are increased by 34%, going from 18,4 kWh/m^2 to 27,9 kWh/m^2.

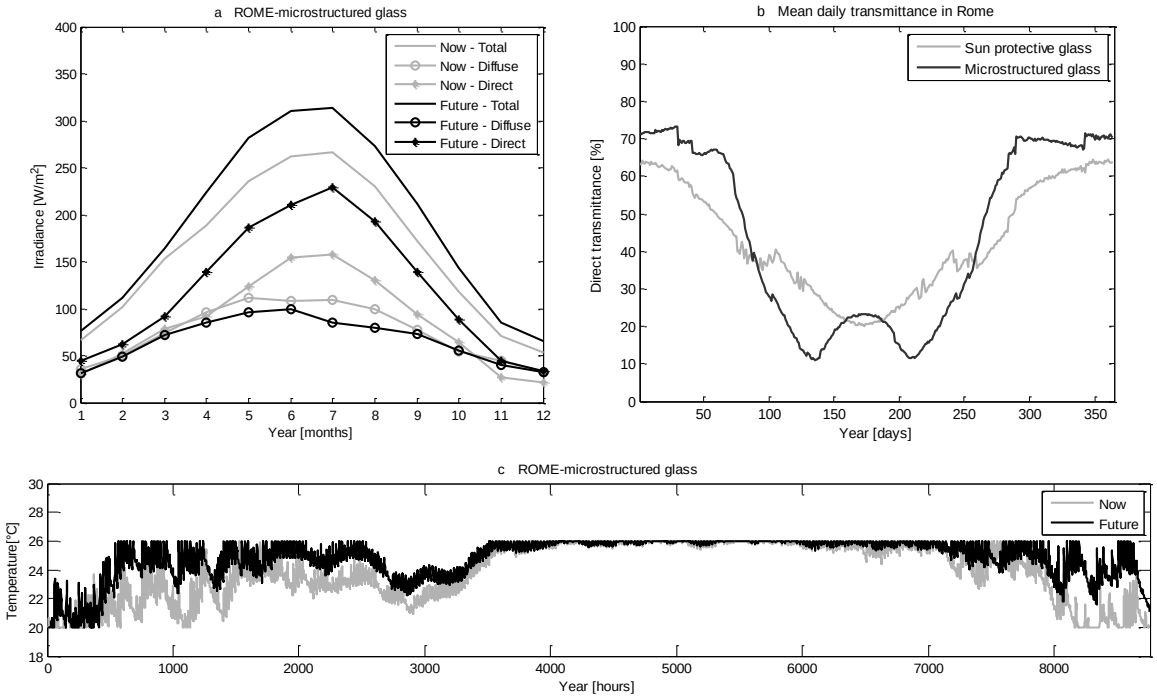

Figure 5.51: (a) global horizontal, diffuse and direct irradiance in Rome (b) daily direct transmittance in Rome with the sun protective glass and the microstructured glass and (c) mean hourly temperatures in Rome for the microstructured glass in the current and in the future scenario.

Another exception among the southern European locations is Marseille, where the saved energy is almost the same, passing from 10,4% to 9,6%. The reason is that in the current meteorological conditions the irradiance levels are already high: in July the mean global horizontal irradiance is currently 305 W/m^2, while equal to 304 W/m^2 in the future. Therefore, in this location, the climatic conditions are comparable in the future and in the present. In this case, as well as it is expected to happen in Rome in 2050, the overheating problem exists with the nowadays climatic situation, starting from spring. Both in the current and in the future years, a high amount of solar gains get in the building, before the sun elevation angle reaches the blocking range of the embedded microstructures.

In the north of Europe, where the latitude is above 53°N, relative savings are increasing, except in Stockholm, where they remain almost the same, rising from 4,1% to 4,2%. In Hamburg the increase is of 23%, in Copenhagen around 8% and in Goteborg 20%. Finally in Bergen energy savings are expected to grow from 1,3% to 2,7%.

However, despite the variation of the meteorological conditions, at all the latitudes energy savings still exist using the microstructured glass, optimized for Lausanne. Using hourly climatic data for a forty year period, it can be affirmed that the climate change impact is more acute in southern European regions, where the need for cooling is more important. In this range, the microstructured glass optimized in Athens will perform better.

The variation of the energy savings all over Europe can be explained by the change in distribution of thermal loads between cooling and heating. The expected cooling and heating loads are shown in Figure 5.52 and 5.53, respectively. In general the need for cooling (Figure 5.52) is increasing for all the locations, except in Zurich, Paris, London and Goteborg, where it is almost maintained. The highest amount of cooling loads takes place in southern locations, more sensitive to the climate change. In Athens cooling loads currently amount to 29,7 kWh/m^2, while in the future they are reaching 36,4 kWh/m^2. The increase of the cooling consumption is smaller at higher latitudes, among which there is a peak in Berlin, where the cooling loads are expected to vary from 5 kWh/m^2 to 8 kWh/m^2 (increasing about 37,5%). In general, results shows that there is a large increase of cooling consumption, more accentuated at lower latitudes.

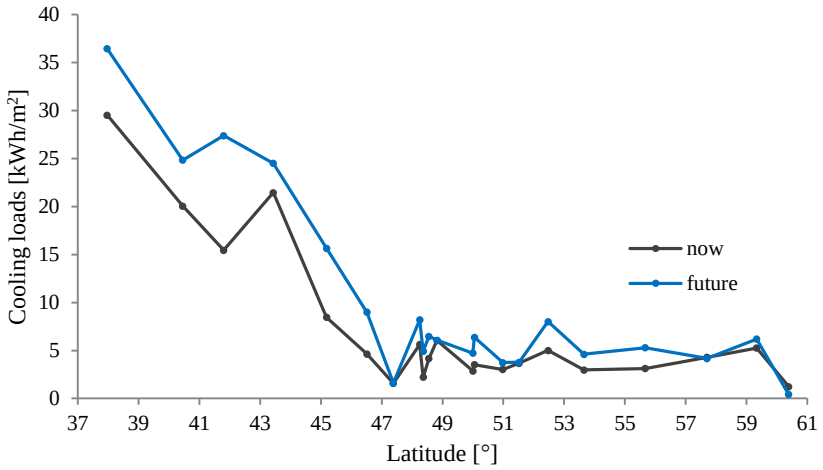

Fig. 5.52: current and expected cumulated cooling loads at different latitudes.

In Figure 5.53, the annual amount of heating loads, varying the latitude is shown. Two exceptions in south of Europe are Madrid and Rome, where they significantly decrease. In Madrid the need for heating is expected to diminish from 2,5 *kWh/m²* to 0,7 *kWh/m²* (of about 72%), while in Rome from 3 *kWh/m²* to 0,55 *kWh/m²* (down to 81%). For the other locations, situated in the range of latitude between 43°N and 52°N, the heating consumption is not importantly changing, according to the future projections and it remains almost the same. At high latitudes (above 52°N), heating loads are decreased. The highest amount of heating loads is in Stockholm, equal to 37,1 *kWh/m²* in the current situation and 35,7 *kWh/m²* in the future scenario.

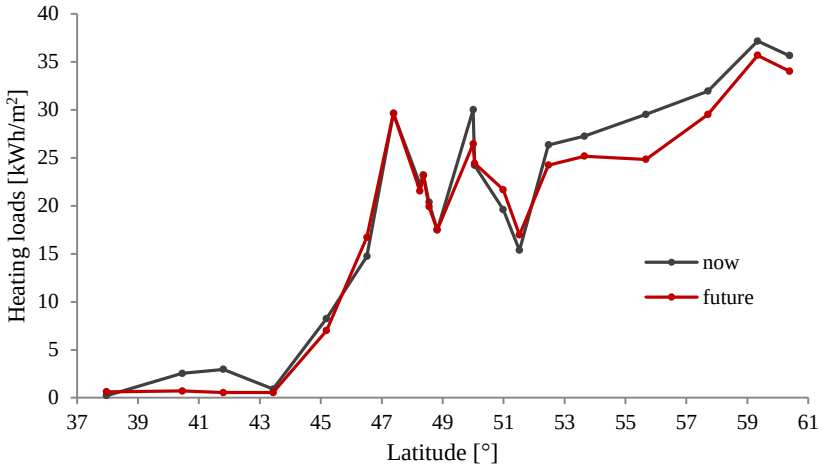

Fig. 5.53: current and expected cumulated heating loads at different latitudes.

Heating energy requirements are expected to decrease, according to the projections in 2050, especially in southern climatic conditions. This reduction depends on the location and it is negligible in the continental European region (including cities like Zurich, Wien, Munich and Strasbourg). At high latitudes (above 52°N) heating loads will decrease by around 4%-16%. This general change is strictly linked to the effect of global warming on thermal loads and to the expected increase of the Urban Heat Island effect. The urban growth will be accentuated in the mid of the century. In this period the A1B scenario foresees that there will be the peak of population increase. Consequently urban centres will become larger and larger; the air temperature in this area will increase.

Climate change is expected to shift up the annual space conditioning loads and to shift down the heating requirements. In the future, the dominant part will be for cooling, until a latitude of about 45°N. For example, currently, in Turin cooling and heating loads are almost balanced (8,2 *kWh/m²* for heating and 8,5 *kWh/m²* for

cooling). While in 2050 the need for cooling will be about 15,6 kWh/m^2 and the need for heating 7 kWh/m^2. From the latitude of Lausanne, the main part of the annual loads will remain for heating.

In conclusion, this study investigates the impact on heating and cooling demand, depending on the glazing envelope, considering a climate change scenario. Focusing on the microstructures performance, it can be affirmed that climate change can significantly alter the heating and cooling requirements. However, this novel complex fenestration system remains a potential solution even in a future climatic scenario, contributing to the reduction of overheating in buildings. The analysis shows that the predicted energy consumption is growing for southern European locations, due to the relevant increase of the cooling demand. As the latitude rises, the majority of thermal loads decrease; for latitudes above 53°N they are getting lower than the current situation, because the heating consumption will decrease, without a significant increase of cooling loads. All over Europe, expected energy savings in comparison with a sun protective glass are in a range between 3% and 18%.

A microstructured window allows to reach energy savings, compared with conventional glazing envelopes, despite the perspective of global warming. Such CFS system helps to decrease the cooling energy consumption, which is expected to grow more and more in the incoming years. This advantage becomes an increasingly important aspect to be considered, alongside that of daylighting. The microstructured glass optimization in Athens can potentially be a good solution in the region affected by high cooling requirements, that in the future will include a higher range of latitudes.

6 Assessment of building performance

This second parametric study examines the dependence of the annual thermal loads on the thermal properties and the geometric characteristics of the reference room.

Firstly, the change of the thermal properties of the building is considered. Three types of stratigraphic layout of the exterior wall have been defined, with different thickness of insulation.

In the second part, the influence of the area of the window on the thermal loads is investigated. The parameter that allows to evaluate this trend is the percentage glazed area varying the total wall area: the so called window to wall ratio (WWR).

Simulations have been performed considering both the optimized microstructured glass for Lausanne and for Athens, in order to evaluate the impact on energy savings of the different geometry of the micro-mirrors.

6.1 Building configurations

In this study, the energy performance of different glazing envelopes has been evaluated. The considered window glazing types are the sun protective glass, the standard double glass and the microstructured glass with the optimized geometry for Lausanne and for Athens. The geometric configuration of the office is maintained: the dimensions of the room are always the same (29,5 m^2 x 2,8 *m*) and the window to wall area ratio is fixed at 40%, as in the first parametric study.

Three different building configurations were proposed for the analysis. Due to the fact that the reference office room has only an exterior wall, the variation of the thermal properties of the building is referred to this specific façade. For the first type of building (called the non-insulated building), the exterior wall was assumed to be constructed with the outdoor and indoor sides made of brick, with thickness of 12 *cm* and 20 *cm* respectively. In the middle space there is air. The resistance of the air is equal to 0,14 m^2K/W, considering the thickness of the layer (8 *cm*) according to UNI EN ISO 6946. This configuration corresponds to an old building and currently, especially for middle and high latitudes, is no longer accepted for new constructions. However, it is interesting to evaluate the consequence that a non-insulated building can have on the thermal loads. The second type of building is moderately insulated; the air is replaced with 8 *cm* of insulation material (rock wool), drastically reducing the U-value of the wall of about 75%. The third type of building corresponds to the considered well-insulated building for the first parametric study. Therefore the exterior wall has 12 *cm* in addition of insulation and wood instead of brick. In this way the U-value result very low, equal to 0,15 W/m^2K (reduced of 61% respect to the moderate insulation).

In the table below (Table 6.1) the stratigraphic layout of the exterior wall is shown:

	Non insulated			**Moderately insulated**			**Well insulated**		
	brick	air	brick	plaster	insulation	brick	plaster	insulation	wood
Thickness [m]	0,20	0,08	0,12	0,02	0,08	0,30	0,02	0,20	0,20
Conductivity [W/mK]	0,89	-	0,89	0,40	0,04	0,89	0,40	0,04	0,13
Density [kg/m^3]	1920	-	1920	1000	40	1920	1000	40	500
Specific heat [J/kgK]	790	1005	790	1000	840	790	1000	840	1600
U-value [W/(m^2K)]	**1,50**			**0,39**			**0,15**		

Table 6.1: stratigraphic layout of the three chosen exterior walls.

Based on these three types of buildings, simulations have been performed in order to determine the annual thermal loads in Lausanne and Athens. Firstly the variation of the thermal transmittance of the window was considered. Then,

a second analysis was carried out, changing the glazed area for different window U-values. Energy savings were the final result of the study. In the following chapters these two analysis have been performed and evaluated.

6.2 U-value variation of the window

The thermal transmittance of the window (called U-value), is an important parameter. It indicates the level of insulation of the glazing envelope, that is the weakest element of the building in terms of heat losses. The lower the U-value, the better is the insulation of the window. The U-values of the window glazing have been decreased throughout the years from 3 W/m^2K to 1,6 W/m^2K and further down 1,2 W/m^2K for double glazing with low-e coatings and noble gas filled. Especially in northern climates, the construction of well-insulated buildings is important to reduce the energy use for heating. For this reason, European legislation fixed thresholds on the U-value of the window. Consequently the low-e coatings windows are becoming more used, because they allow to reach lower values of transmittance. Typical U-values for a standard double glass with 25 mm thickness are around 2,9 W/m^2K without low-e coating and until 1 W/m^2K with low emissivity properties. Nowadays lower values are required, especially in northern locations [*SINTEF, 2007*]. Therefore, taking into account that also a sun protective glass and a microstructured glass were considered, a reasonably wide range for the transmittance is chosen between 0,5 W/m^2K and 3,5 W/m^2K, in order to perform simulations.

In Figure 6.1 the cumulated annual thermal loads varying the U-value of the window are shown in Lausanne, considering the optimization of the embedded microstructures for this location.

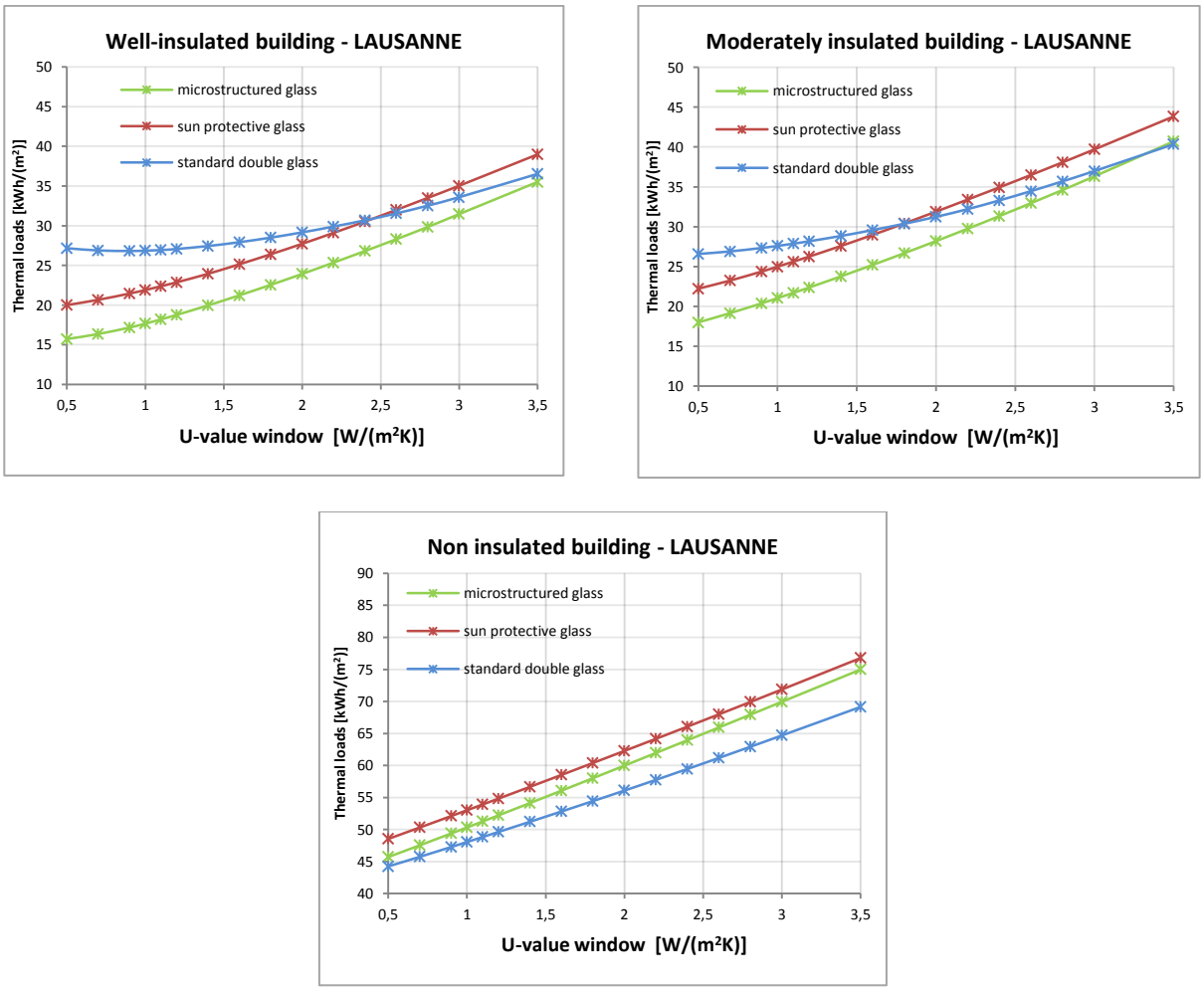

Fig. 6.1: cumulated thermal loads in Lausanne varying the U-value of the window for the three different building configurations.

Concerning the well-insulated building, the embedded micro-mirrors allow the window to have the best performance. The difference between the annual thermal loads with the sun protective glass and the microstructured glass slightly decreases with the increase of the U-value. With a U-value of 0,5 W/m^2K the saved energy is of 21%, while considering a U-value of 3 W/m^2K it goes down until 10%. This means that if the thermal performance of the window becomes worse, the advantage of the installation of the embedded microstructures diminishes, but still is relevant. The trend of the standard glass is parabolic and it performs better when the U-value is around 1 W/m^2K. Moreover, for thermal transmittances above 2,5 W/m^2K, the conventional glazing envelope is more favourable in comparison with the sun protective glass, because the thermal loads are becoming more and more closed to the annual loads of the microstructured glass. For high U-values, the solar glass has not a good performance. This is because of the relevant increase of the heating loads, that start to be around 10 kWh/m^2, until reaching 35 kWh/m^2 for the maximum U-value, as it can be noticed in Figure 6.2. Looking at the sun protective glass, as the thermal transmittance of the window rises, the distance between the curves of the heating and the cooling loads increases. The cooling loads goes slightly down while the U-value rises and there is not a compensation between cooling and heating. The reason is that the sun protective glazing has the goal to keep away the solar gains from the building, but if the window has not a good insulation (low U-value), the demand for the heating significantly increases during winter. This happens especially in locations at latitudes above 45°N, where the need to reduce the solar gains is limited to a shorter period of the year because of the climatic conditions. The trend of heating and cooling loads for the double standard glass is different: cooling loads are more relevant in comparison with the case of the sun protective glass (for low U-values they are doubled). On the other hand, heating loads are lower of about 39% for 0,5 W/m^2K of and 22% for higher U-values. For the double standard glass there is a point in which the cooling loads have the same value of the heating loads. It is around a U-value of 1,8 W/m^2K. Also for this conventional glazing with the increasing of the thermal transmittance, the need of cooling decreases, while the need for heating rises, because the losses towards outside become more relevant. For this reason, the resulting curve of the cumulated thermal loads has a parabolic shape. The microstructured glass present the same trend of the sun protective glass and it is able to further reduce the thermal loads.

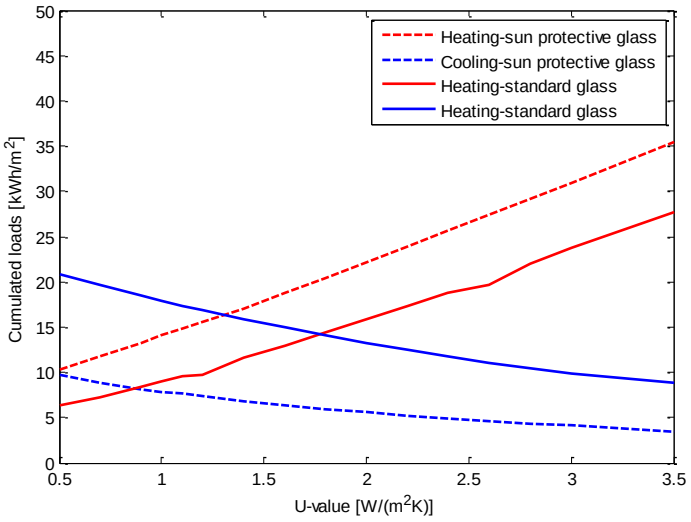

Fig. 6.2: cooling and heating loads trend for the sun protective glass and the double standard glass in Lausanne for a well-insulated building.

Considering the moderately insulated building, the trend of the annual thermal loads is roughly analogue to that of the well-insulated building. One difference is that the slope of the three curves is higher, bringing to the same value of thermal loads for the microstructured glazing and double standard glazing, equal to 40 kWh/m^2 for a 3,5 W/m^2K U-value. Moreover, the performance of the sun protective glass is even worse than in the case of the well-insulated building: above 1,7 W/m^2K the standard double glass performs better. The microstructured glass results the most advantageous glazing envelope until a U-value of 3 W/m^2K.

The situation for the non-insulated building is completely different. In this case the needed annual loads undergo a significant increase in comparison with the other two building configurations, starting around 45 *kWh/m²* for low U-values until 75 *kWh/m²*. The double standard glass has the best thermal performance and it is characterized by a non-parabolic trend. The microstructured glass brings to higher thermal loads in comparison with the standard glass for all the U-values. The reason is that if the building has not insulated walls, the heating loads become more relevant. Heating loads significantly increase as the U-value rises, while cooling loads remains roughly constant for all the types of glazing. Without insulation in the wall, microstructures cause more heating loads than the standard glass and lower cooling loads (around 0,5 *kWh/m²*). However, the increase of the heating with the microstructured glass is not compensated by the cooling loads brought by the standard glass. This is because for high latitudes the heating becomes more important and without insulation in the wall the standard glass keeps more solar gains in the room than the microstructured glass, during the winter season.

In general, the higher is the thermal transmittance of the window, the larger are the annual thermal loads. Moreover, better the building is insulated, less are the thermal loads all over the year. Because of the climatic conditions in Lausanne, all the buildings require to be constructed with an insulation layer in the exterior walls and the U-value of the window should not be too high. Therefore, the embedded micro-mirrors turn out to be the optimal solution for the thermal management, bringing to relevant energy savings.

Concerning the optimization of the micro-mirrors and of the sun protective glass for southern locations, the same analysis was performed. In particular, simulations have been carried out for the geometry of the embedded microstructures optimized in Athens, following the first parametric study. In Figure 6.3 results are shown in Athens, varying the U-value in the same range considered for Lausanne: from 0,5 *W/m²K* to 3,5 *W/m²K*.

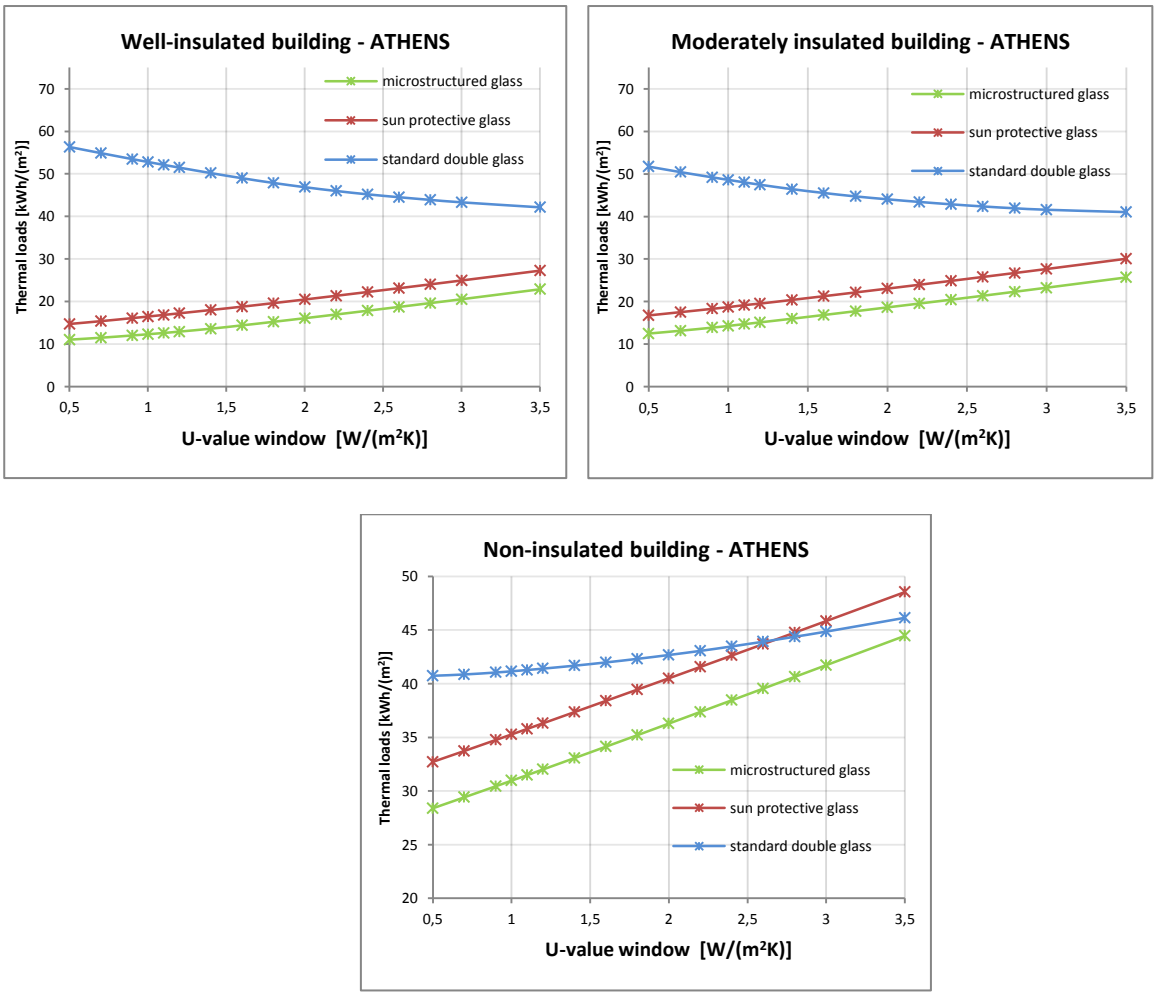

Fig. 6.3 : annual thermal loads in Athens varying the U-value of the window for the three different building configurations.

For a well-insulated building, the standard glass is the worst performing glazing, especially for low U-values, starting to bring annual thermal loads equal to 56,3 *kWh/m²*. Indeed, the trend of the conventional glass is descendent with the increase of the thermal transmittance. This is due to the fact that if the window is well insulated considering a standard glass, solar gains will not be avoided, in a location in which cooling loads dominate the annual loads. Consequently, the requirement for air conditioning will significantly rise up. The sun protective glass has a linear trend, with thermal loads increasing as the U-value rises. Annual loads are equal to 14,7 *kWh/m²* for the lowest U-value and equal to 27,2 *kWh/m²*, when the U-value is the maximum (3,5 *W/m²K*). Concerning the embedded micro-mirrors, they present the best performance when compared with the other glazing envelopes. The trend is the same of the sun protective glass but the line is shifted down. The loads slightly increase, as the U-value becomes larger, because heating loads grow more than the cooling loads. Consequently, the advantage respect to the standard glass diminishes with the increase of the U-value and it is significant.

As in the case of Lausanne, the trend of the curves considering the moderately insulated building is similar to the well-insulated one. The main difference is that the standard glass brings to a decrease of thermal loads of about 8% respect to the case of the well-insulated wall. Therefore the energy savings decrease with a smaller thickness of insulation in the wall.

If the exterior wall is not provided with insulation, the resulting thermal loads with the standard glass are different, in comparison with the other building configurations. Concerning the sun protective and the microstructured glazing, the trend is always linear but the amount of thermal loads is significantly high. The distance between the two curves is around 4 *kWh/*m². As the U-value of the window rises, the standard glass curve is ascendant. The reason is that more heating loads are needed, if the window has a high value of losses and it is installed in a non-insulated building. As it can be seen in Figure 6.4, the heating consumption with the sun protective glass significantly increases for higher U-values. In a well-insulated building heating loads start to be equal to 3,6 *kWh/m²* and they reach 16,0 *kWh/m²* when the thermal transmittance is the highest (3,5 *W/m²K*). Cooling loads are almost constant for all the U-values and they remain the dominant part of the energy consumption until a U-value of 2,4 *W/m²K*. The standard glass brings no heating loads In the considered range of U-values, heating loads are increasing from 7,4 *kWh/m²* to 18,4 *kWh/m²*. This increase of the heating consumption is mainly due to the absence of the insulated layer in the exterior wall.

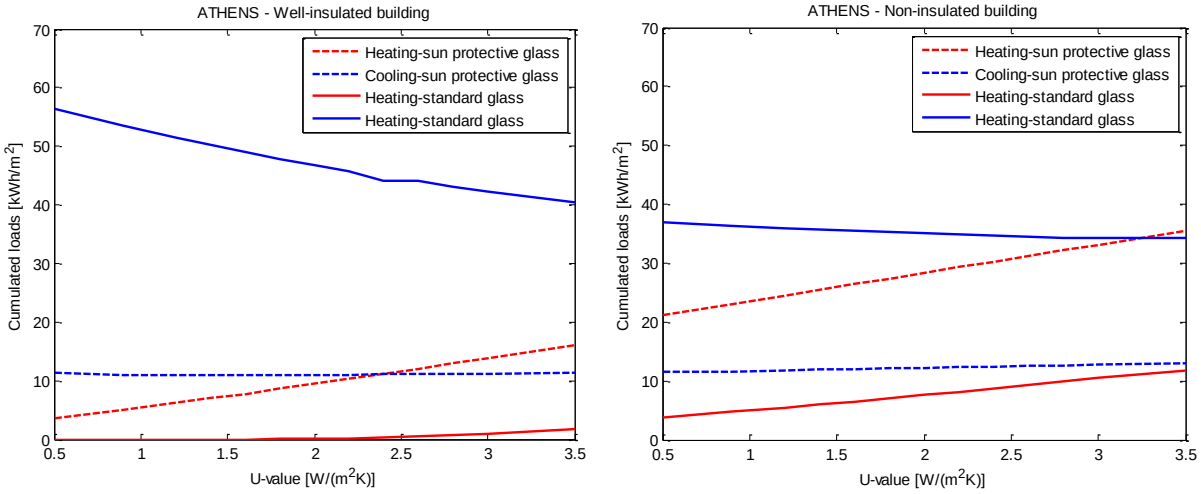

Fig. 6.4 : cooling and heating loads for the sun protective glass and the double standard glass in Athens for a well-insulated building (on the left) a non- insulated building (on the right).

However the amount of the annual thermal loads brought by the standard double glazing envelope is lower than in the case of an insulated building, for low thermal transmittance values. This is due to the fact that that cooling loads are reduced, since the building has more thermal losses towards the external environment. When the building is not insulated, cooling is the dominant part of the annual loads only with the use of the standard glass. For the sun protective glass, the heating requirement is higher than the cooling, as it can be noticed in Figure 6.4.

In general, results show that embedded micro-mirrors bring to an energetic advantage if the building is provided by insulation. Indeed, for a well-insulated building, in both the locations, the microstructured glass has the best performance, when compared with the two reference glasses. Annual thermal loads are found to be higher for increasing U-values. Therefore, the thermal transmittance of the window should be reasonably low (less than 1,5 W/m^2K), to minimize the energy consumption. As the U-value rises, the heating consumption becomes higher, especially in north locations. In the south of Europe, with higher U-values, the increase of the heating loads is less accentuated and the need for cooling remains almost constant or slightly decreases.

The calculated relative energy savings are displayed in Figure 6.4, concerning the well-insulated building.

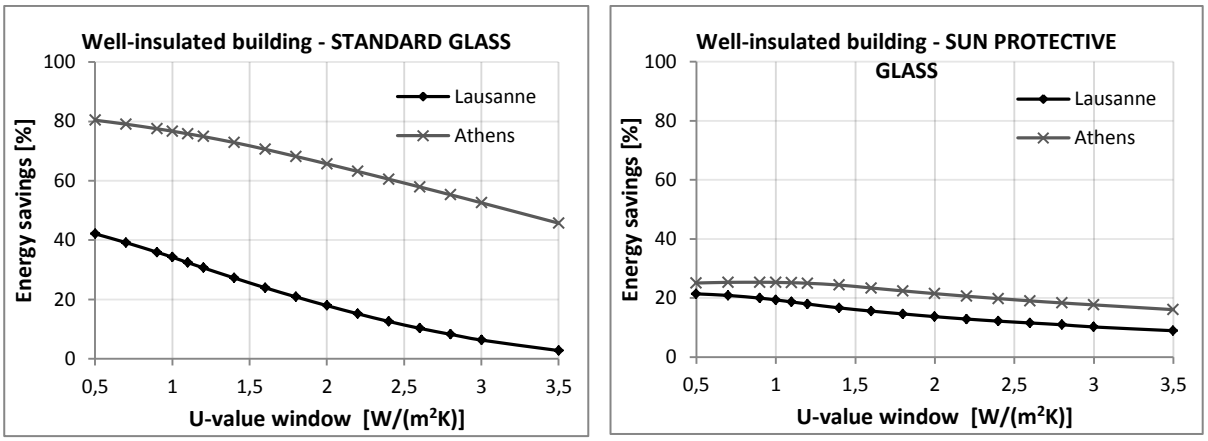

Fig. 6.5: percentage energy savings in Athens and Lausanne comparing the microstructured glass with the other two glazing envelopes, for a well-insulating building.

The first graph shows the effect of the variation of the thermal transmittance of the window on the energy saved by the microstructured glazing, in comparison with the standard double glass. The savings diminish for growing U-values. In Lausanne the decrease is relevant because the energy saved varies from 42% ,with the minimum U-value, to 3% when the U-value is 3,5 $W/(m^2K)$. This is due to the fact that heating loads becomes more and more dominant if the thermal transmittance of the window rises. In Athens, the trend of the energy savings is also descendent but in this case the cooling consumption mostly influences the total thermal loads. Especially with the use of a standard glass, in southern latitudes, the cooling loads are very high. With the increase of the thermal transmittance of the window, heating loads grow slowly. Therefore in this case the microstructured glass brings to high relative savings, starting up to 80% for low U-value, until 46%.

The second graph illustrates the relative energy savings of the microstructured glass, when compared with a sun protective glazing. It can be seen that in Lausanne the percentage energy savings goes from 21% to 9% if the U-value increases. In Athens savings are still higher than in Lausanne, but not importantly surpassing them. They start from 25% and going down to 16%.

Figure 6.6 shows the relative energy savings for a reasonable U-value, equal to 1,2 $W/(m^2K)$, considering all the building configurations. Regarding Lausanne, when the building is well-insulated, energy savings are 31% when compared with the conventional glazing and 18% when compared with the sun protective glazing. If the thickness of the layer of insulation decreases, the relative savings slightly diminish, as it happens for the moderately-insulated building. In this case savings are 20% and 15%, respectively in comparison with the standard glass and the sun protective glass. The significant energetic advantage of the microstructured glass is due to the important reduction of the cooling loads.

Concerning the absence of insulation in the wall, as previously mentioned, the use of the embedded micro-mirrors in the glass is not convenient if compared with the standard glass in Lausanne. If compared with the solar glass, the microstructured glass is advantageous only in Lausanne, bringing to 4% of saved energy. In Athens the use of the

microstructured glass leads to almost the same amount of thermal loads brought by the sun protective glass (around 20%).

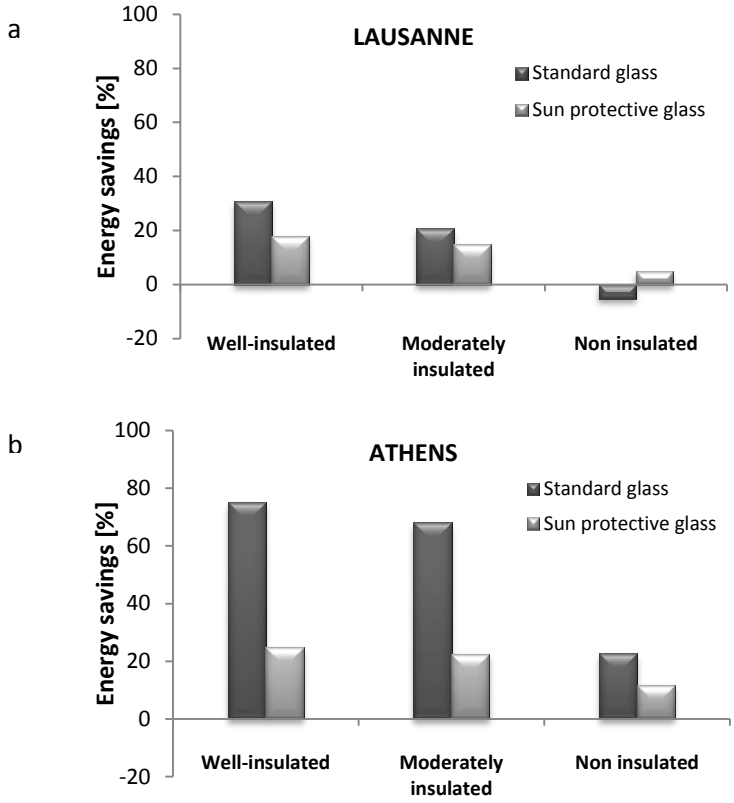

Fig. 6.6 (a) e (b): percentage energy savings for the considered building configurations in Lausanne and Athens, comparing the microstructured glass with the other two glazing envelopes.

Comparing the two histograms the saved energy in Athens is higher than in Lausanne for all the types of building. For the well and moderately insulated building, energy savings in comparison with the sun protective glass are almost three times higher than in Lausanne. Concerning the replacement of the microstructured glazing with the sun protective glazing, energy savings amount to 17% in Lausanne and 23% in Athens. In the non-insulated building, in southern locations, the use of the microstructured glass bring to lower energy savings, that are still around 8%. Therefore, energy savings are still quite relevant. The conventional double glass is not convenient in comparison with the other glazing envelopes. The sun protective glass remains less advantageous when compared with the microstructured glass. The difference in energy savings between the well-insulated and the moderately insulated building is not significant.

This study shows that there is a strong dependence of energy saved on the insulation of the building and on the type of glazing. The suitable choice of the thermal transmittance of the window can improve the smart management of the annual thermal loads. The use of the microstructured glazing is even more advantageous from the energetic point of view, if the thermal transmittance of the window is not too high (below 1,5 W/m^2K) and the building is properly insulated, depending on the range of latitude of the considered location.

6.3 Glazed area study

The energy efficiency of a building strongly depends on the façade construction. Nowadays, for aesthetic motivations, highly glazed buildings are more and more designed. Another reason is that a transparent façade allows to take advantage of the daylight, improving the visual comfort. Therefore, it is important to evaluate if a large glazed surface

can induce a significant amount of the energy consumption in the building. In this chapter, the influence of the window's area on the thermal loads is analysed.

All the geometric characteristics of the test office room are maintained, except the glazed surface. Simulations have been performed for the two conventional glazing envelopes and the microstructured glazing. The U-value of the window is chosen equal to 1,3 W/m^2K, as in the first parametric study. Due to the fact that, at medium-high range of latitudes, the buildings are provided with insulation in the wall, for Lausanne simulations have been carried out only considering the insulated building configuration. For Athens both the well-insulated and the non-insulated exterior walls are evaluated. The reason is that, in southern locations, the majority of the buildings are not provided with insulation.

The variation of the window size for the test room has been considered through discrete values window wall ratio (WWR). The chosen range for the WWR is from 5%, corresponding to a small window covering about 0,503 m^2 of the glazed façade, until 100% (the glazed area corresponds to all the façade wall).

In Figure 6.7 results are shown in Lausanne for the well-insulated building with the U-value of the exterior wall equal to 0,15 W/m^2K. In general, for all the glazing envelopes, annual thermal loads present a parabolic shape varying the window to wall ratio. If the glazed area is restricted, the heating loads are the dominant part of the loads. Increasing the surface of the window, cooling loads become more and more important, contributing to raise the energy consumption. The minimum of the parabolic curves corresponds to the value of WWR that represents the best compromise between heating and thermal loads. The double standard glass presents the best performance if the glazed surface is small, until a WWR around 24% and 31% when compared with a microstructured glass and a sun protective glass, respectively. However, in this range of WWR the trend of the sun protective glass and of the embedded microstructures brings to almost the same annual thermal loads. The difference between the obtained thermal loads with the conventional standard glazing and the other two glazing is negligible (around 2 kWh/m^2 on a total of 20-30 kWh/m^2). The optimal value of the WWR for a conventional glazing is around 20% (corresponding to 2 m^2). Increasing the area of the window, the standard glass is not advantageous anymore. For a completely glazed façade, thermal loads result high, equal to 95 kWh/m^2. The sun protective glass and the embedded microstructures bring to lower thermal loads. Annual loads start to 35,5 kWh/m^2 be equal for both these glazing envelopes. However, as the glazed area increases, the microstructured glass becomes more advantageous. In order to minimize the energy consumption, the optimal WWR value can be reached by the microstructured glazing and it is equal to 40% (corresponding to 19 kWh/m^2). When the façade is completely covered by the glazing, cumulated loads using the sun protective glass and the microstructured glass are respectively 60 kWh/m^2 and 52 kWh/m^2.

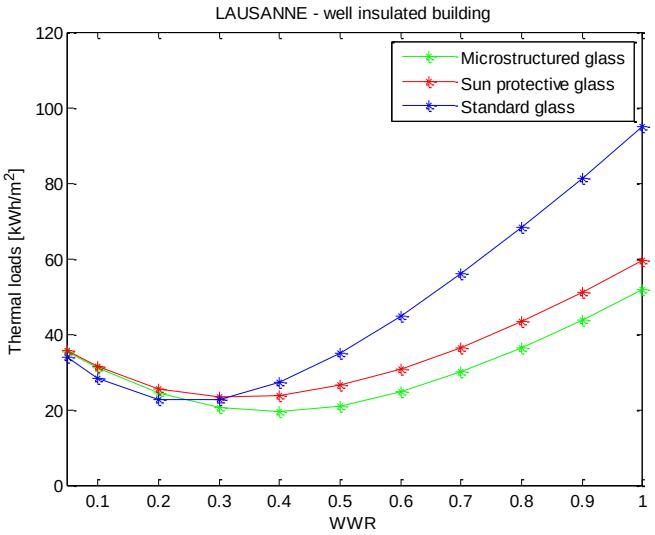

Fig. 6.7 : cumulated thermal loads in Lausanne, for a well-insulated building, varying the WWR.

In Figure 6.8 the cooling and heating loads at different window to wall ratio are shown in Lausanne, comparing the standard glass and the microstructured glass. The graph confirms the parabolic shape of the curves varying the WWR. Moreover, the use of the embedded micro-mirrors lead to higher heating loads than the standard glass, because they better exploit the gains coming from the solar radiation in winter. For this reason, when the WWR is less than 24%, the conventional glazing is slightly more convenient.

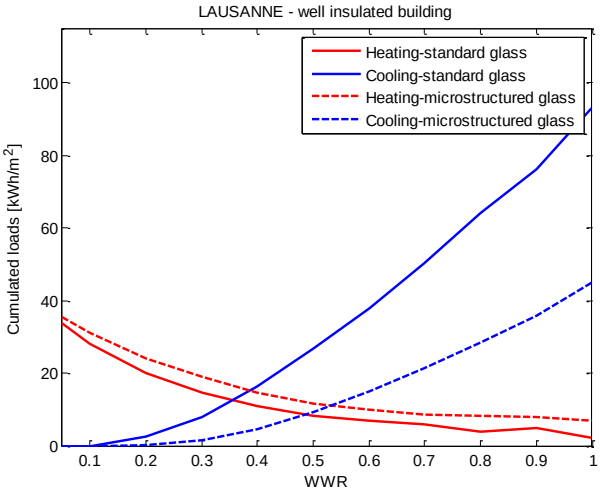

Fig. 6.8: cooling and heating loads for the standard double glazing and the microstructured glass in Lausanne for a well-insulated building.

Concerning Athens, two building configurations have been analysed, in order to evaluate the more advantageous case. In general the curve of the annual loads varying the glazed area has a parabolic shape, such as in Lausanne (Figure 6.9a).

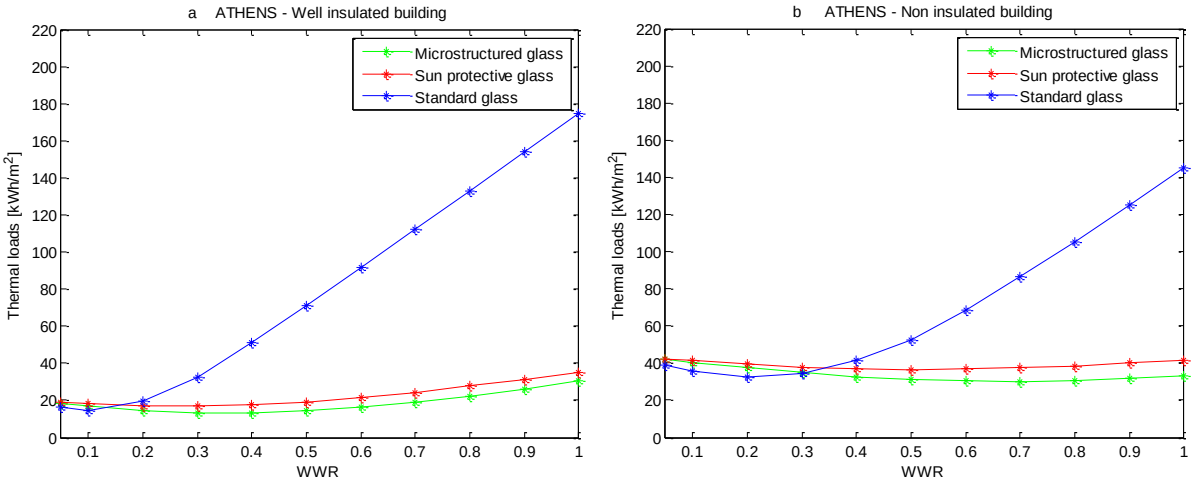

Fig. 6.9 : cumulated thermal loads in Athens, for a well-insulated building (a) and a non-insulated building (b), varying the WWR.

Firstly, if the building is well-insulated, until a WWR of 13% the standard glass is the most advantageous solution. This is due to the fact that, if the window is small in comparison with the façade, the solar gains in summer are limited and the need for heating in winter is relatively low thanks to the insulation of the wall. However, in this range of window to wall ratio, energy savings brought by the microstructured glazing in comparison with the sun protective glazing envelope are not so high (varying from 1% to 6%). The microstructured glass brings to a similar value of annual loads, in comparison with the sun protective glass until a WWR of 20% (around 16 kWh/m^2). After these values of glazed area the cooling loads start to play an important role in the energy balance of the building. The difference between the annual loads using the microstructured glass and the loads with the sun protective glass remains almost constant for all the glazed areas (4,5 kWh/m^2). Increasing the glazed area, the yearly cumulated loads become more and more

relevant, especially for the double standard glazing. When the building has the WWR reaching 100%, thermal loads brought by the standard double glass are high, equal to 174,7 kWh/m^2. Concerning the sun protective glass, the thermal loads with a complete glazed façade amount to 35 kWh/m^2. The embedded microstructures lead to the lowest energy consumption, amounting to 30 kWh/m^2. In this case the novel CFS technology induces significant saved energy (14% when the WWR is 1).

As shown in Figure 6.10, cooling loads in southern locations are significantly more relevant than the need of heating, except if the window area is small (WWR less than 30%) with the sun protective glass and the embedded microstructures. Above a WWR of 40%, using the microstructured glass energy savings are 74% in comparison with the standard glass and around 40% in comparison with the sun protective glass. On the other hand, heating loads are always low in comparison with the need of cooling. Moreover, they are more important when the window area is low, until a WWR of 10% for all the type of glazing. When the WWR is larger than 40% with the standard glass, heating loads become null. For the sun protective glass and the microstructured glass the heating consumption is not negligible until a WWR of 75%, but it is relatively low, starting from 16 kWh/m^2 until 0,6 kWh/m^2 when the façade is completely glazed. Even if the heating demand is higher in the case of the microstructured glass when compared with the reference glazing, cooling loads are reduced. The reason is that the microstructured glass better avoid the solar gains, thanks to the angular dependence of the transmittance. The suitable geometry of the micro-mirrors allow the seasonal variation of the total transmitted energy. In this way, the main part of the incoming radiation from the sun light can be reflected and the solar gains are reduced. However, when the WWR is larger than 50% the risk of overheating in the building increases. The reason is that if the glazed area is large, the need for cooling starts earlier (in spring).

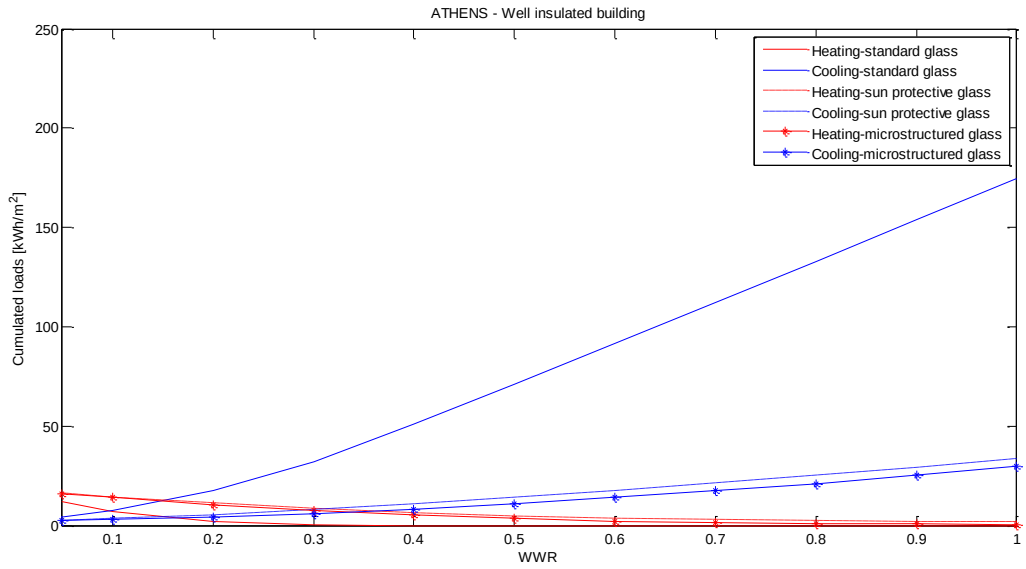

Fig. 6.10: cooling and heating loads for the standard double glazing, the sun protective glazing and the microstructured glass in Athens for a well-insulated building.

Secondarily, the absence of insulation in the wall has been considered (Figure 6.9b). In southern locations the non-insulated buildings are quite common. Windows sized under a 30% façade area have not advantage with the use of the microstructures or the sun protective glass. The situation is similar to that of the insulated building: until a WWR equal to 30% the microstructured glass is not the best-performing glazing in comparison with the standard glass. However, if the building is not provided with insulation, annual thermal loads are lower than the case of well-insulated building: when the façade is completely glazed the cumulated loads are 145 kWh/m^2 with the standard glass and 42 kWh/m^2 with the sun protective glass. The microstructured glass allow to greatly decrease the loads, reaching 33 kWh/m^2 for the WWR of 100%.

Simulations show that at low range of latitudes (south of Europe), if the exterior wall has not the insulation layer, the annual thermal loads are lower only using the standard glass. With the completely glazed façade, considering the

standard glass the percentage decrease is 17%. The reason is that, if the building is not insulated, the level of overheating is lower, because the losses through the wall are higher, mainly flowing outside. While, the layer of insulation keeps the energy caused by the excessive solar gains. Consequently the increase of cooling loads is more relevant for the insulated building. Concerning the sun protective glass and the microstructured glass, the insulated building present the highest amount of energy savings. If the wall is provided with insulation, using the sun protective glass the reduction of thermal loads is of 17% and using the microstructured glass equal to 9%.

Reachable energy savings with the microstructured glass have been calculated, in comparison with the two reference glazing. Results in Lausanne for a well-insulated building are shown in Figure 6.11. If the window area is small (until a WWR value equal to 25%), the use of embedded microstructures is not advantageous in comparison with a standard glazing envelope. In this range of WWR cooling loads are negligible for the standard glass and null for the microstructured glass. Therefore the dominant part of the thermal loads is determined by the heating consumption, that is slightly higher for the microstructured glass. However, starting from a glazed area of 2,5 m^2 (WWR equal to 25%), using the microstructured glass the energy is saved. Relative savings significantly increases until 45% for a window to wall ratio of 0,6. Then they assume a saturation trend, maintaining a value of 45% also for a fully glazed façade. In comparison with the sun protective glass, energy savings are null until a WWR of 10%. Increasing the window area, relative savings rise up until a WWR of 50%, reaching a value of 21% and then they slightly decrease until the fully glazed façade assuming a value around 13%. When the WWR becomes larger than 32%, relative savings brought by the comparison with the standard glass start to be higher than savings compared with the sun protective glass, because cooling loads significantly grow up.

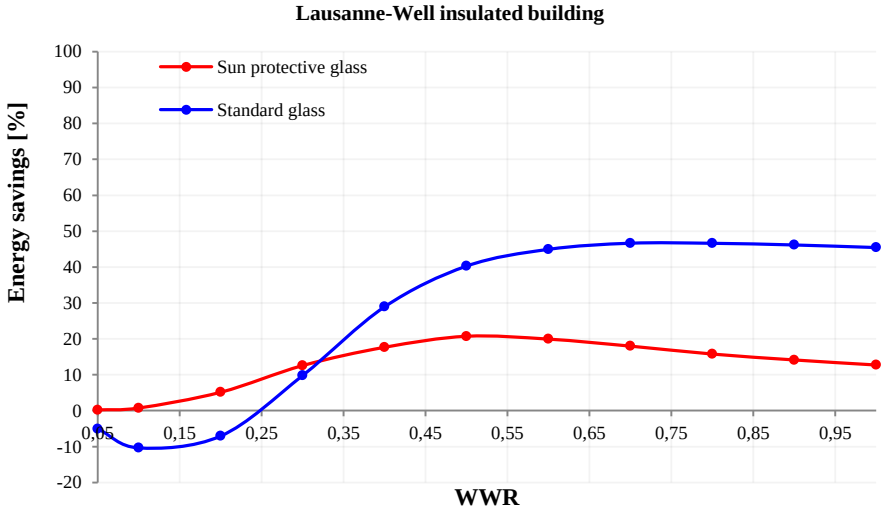

Fig. 6.11: relative energy savings in Lausanne, for a well-insulated building, comparing the microstructured glass with the reference glazing.

In Figure 6.12 relative savings are illustrated in Athens both for the well-insulated building and for the non-insulated one. If the exterior wall is well-insulated the trend of the relative savings is similar to that in Lausanne, reaching a saturation value. If the window to wall ratio is lower than 15% in comparison with the standard glass. Then energy savings start to increase until they achieve 80% (above a WWR of 0,5) in comparison with the double standard glass. When it is compared with the sun protective glass, energy is always saved for all the WWR values. In this case there is a peak when the glazed area is equal to 40%. If the building is not provided with insulation, the range of WWR for which the microstructured glass is not convenient is larger (until 30% when compared with the standard glass). After these values relative savings begin to increase until reaching 78% (related to the standard glass) and 20% (compared with the sun protective glass) when the façade is completely glazed. It can be noticed that, for the non-insulated building, energy savings are lower than in the well-insulated configuration. Varying the window size, energy savings are higher when the wall is provided with insulation. Therefore, also in southern European latitudes, the microstructured glass better performs, in comparison with the reference cases, if the building has an insulation layer

in the exterior wall. The difference between energy savings for the well-insulated configuration and the non-insulated one is less relevant with the increase of the WWR (around when the WWR is equal to 100%). Moreover, comparing the microstructured glazing with the sun protective glass, when the WWR is larger than 80%, the non-insulated building presents the lowest annual loads.

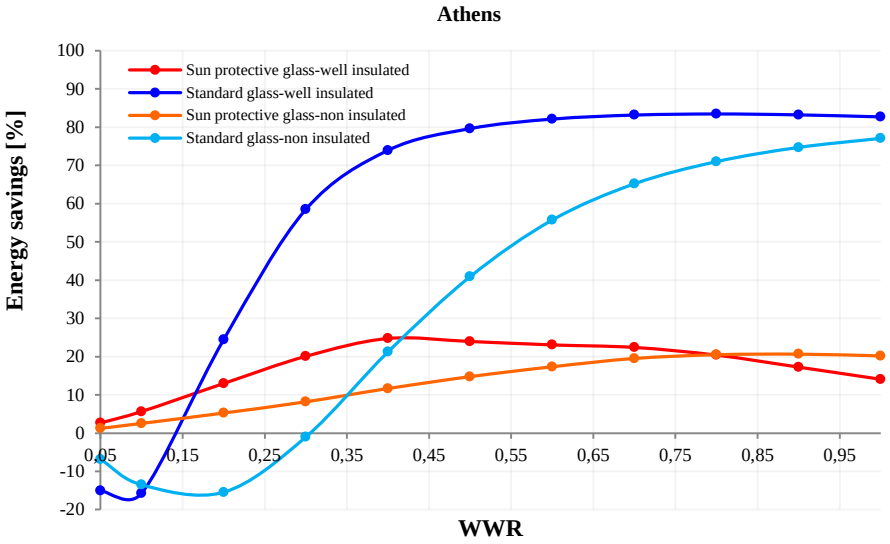

Fig. 6.12: relative energy savings in Athens, for a well-insulated building and a non-insulated building, comparing the microstructured glass with the reference glazing.

In general, this study confirms that the use of the embedded micro-mirrors in the glass can significantly reduce the energy consumption of the building when the glazed area is enough large, depending on the type of building and on the latitude. Increasing the WWR of the test room, energy savings become more and more important, reaching a value of saturation. Therefore, considering the growing spread of large glazed façades in the building constructions, the microstructured glass can give a relevant contribution to limit the annual loads, especially when the WWR is high. An angular dependent system, such as embedded micro-mirrors, able to manage a smart seasonal control of the thermal loads, performs better during the overall annual energy balance, especially if the glazed area is large.

In Figure 6.13 the obtained thermal loads in Lausanne varying the U-value of the window and the WWR of the façade are shown, for the microstructured glass (a), the sun protective glass (b) and the standard double glass (c). The microstructured glass leads to the lowest amount of thermal loads (around 16 kWh/m^2). Its best performance is when the glazed area is between 30%-40% of the wall surface and when the U-value of the window goes from 0,5 W/m^2K to 1,3 W/m^2K. However, increasing the WWR, the slope of the curve is not so significant, therefore embedded microstructures are the best solution. The minimum reachable thermal loads using the sun protective glass are around 19 kWh/m^2(Figure 6.13b) . The range of WWR in which the cumulated loads are enough low is always 30%-40%, with a U-value going from 0,5 W/m^2K to 0,9 W/m^2K. In this case, when the façade is completely glazed, the thermal loads amount between 55 kWh/m^2 and 71 kWh/m^2. The standard double glass (Figure 6.13c) is the glazing envelope that causes more thermal loads. In this case, cooling loads significantly increases as the WWR rises. The minimum value of thermal loads is around 20 kWh/m^2, when the U-value of the window is the lowest (0,5 W/m^2K) and the WWR is about 20%. When the façade is completely glazed thermal loads are very high, in the range between 70 kWh/m^2 and 115 kWh/m^2, depending on the thermal transmittance of the window.

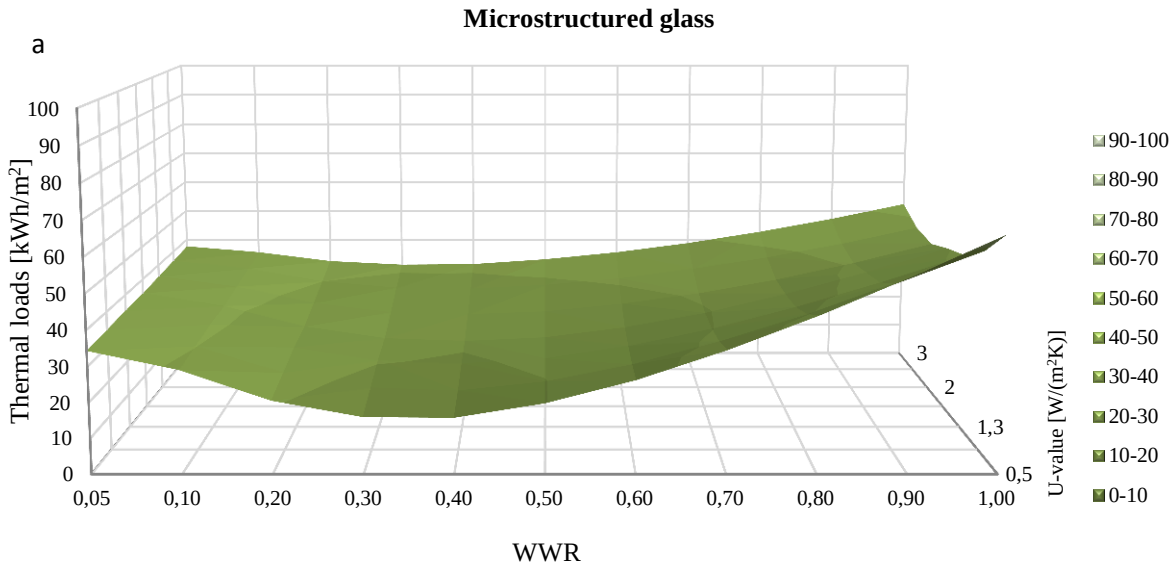
Microstructured glass
a
Thermal loads [kWh/m²]
100
90
80
70
60
50
40
30
20
10
0
0,05
0,10
0,20
0,30
0,40
0,50
0,60
0,70
0,80
0,90
1,00
WWR
3
2
1,3
0,5
U-value [W/(m²K)]
90-100
80-90
70-80
60-70
50-60
40-50
30-40
20-30
10-20
0-10

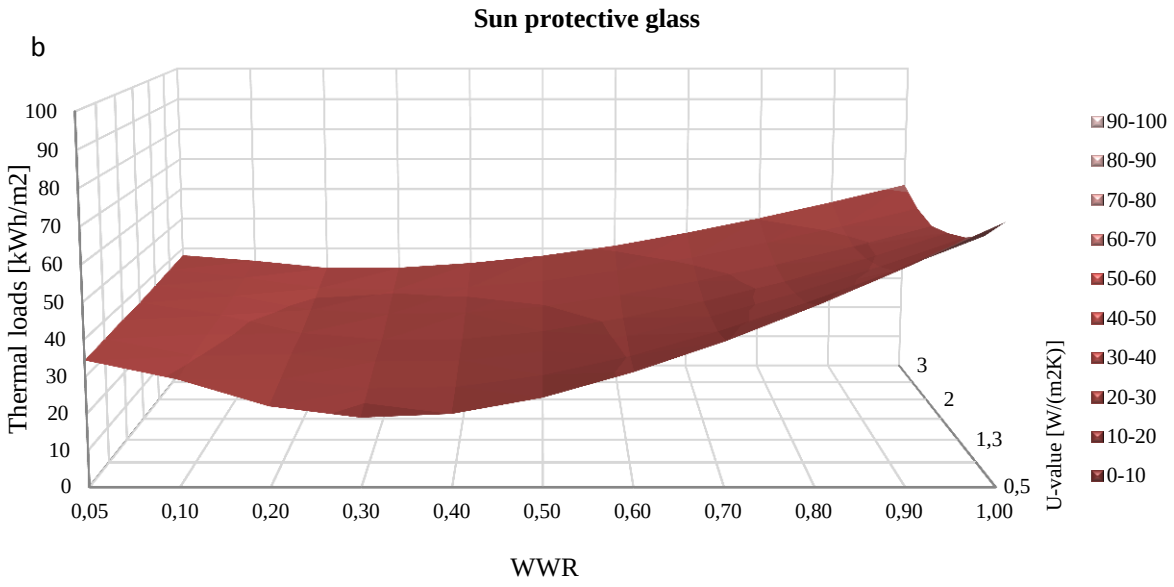
Sun protective glass
b
Thermal loads [kWh/m2]
100
90
80
70
60
50
40
30
20
10
0
0,05
0,10
0,20
0,30
0,40
0,50
0,60
0,70
0,80
0,90
1,00
WWR
3
2
1,3
0,5
U-value [W/(m2K)]
90-100
80-90
70-80
60-70
50-60
40-50
30-40
20-30
10-20
0-10

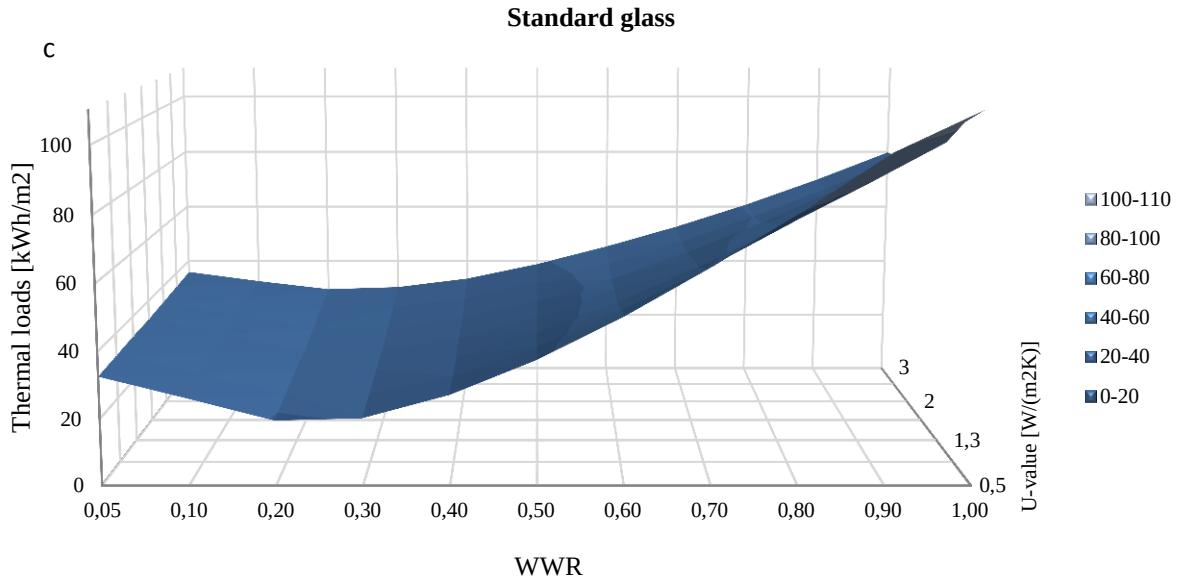

Fig. 6.13: 3D representation of the cumulated thermal loads in Lausanne, for a well-insulated building varying the U-value of the window and the WWR, considering the microstructured glass (a), the sun protective glass (b) and the double standard glass (c).

In conclusion, this study shows that a careful design of glazed façades for buildings should be considered for the thermal management of annual loads. Especially in highly or completely glazed buildings (with WWR equal to 100%), in which the façade is more sensitive to climatic conditions, a proper compromise between glazing and thermal properties of the building is crucial for the energy performance. Different types of constructions have a relevant impact on the energy efficiency, also depending on the U-value of the window and on the window to wall area.

Concerning the window properties, if the U-value is reasonably low (in the range between 0,5 W/m^2K and 1,5 W/m^2K), energy savings are relevant, in comparison with the reference glazing. When the building is provided with insulation and the WWR is 40%, the saved energy using the microstructured glazing amounts between 35% and 67% in Athens and between 42% and 16% in Lausanne.

When highly glazed office buildings are designed, the main aim should be to reduce the cooling demand, since it is the dominant part of the annual loads, both in southern locations and in higher range of latitudes. In Lausanne cooling loads using the embedded microstructures instead of a standard double glazing are reduced of 52%. In Athens the reduction is even higher with WWR equal to 1: cooling loads in comparison with the standard glass decrease of 83% and around 11% when compared with the sun protective glass.

A CFS, characterized by an angular dependence on the total solar transmittance, performs better in energy, considering the annual balance of the solar gains and thermal losses of the building. The PMMA film embedded in the glazing allows to have an higher transmittance when the solar altitude is low and it rejects the solar gains during the hot season, when the sun elevation is high.

7 Conclusions

In this chapter the achievements and the findings of this thesis are summarized. Considering today's energy challenges, the efficiency and the energy savings are considered the key element of the building system. Advanced façades are becoming more and more important for the building envelope. Especially in modern constructions, the glazed area is increasing and the need to reduce the overheating is growing up. Several typologies of glazing technologies have been presented in this thesis. The final aim was to evaluate the energetic performance of the glazing envelope. Of course, a compromise between the energy efficiency, the indoor comfort, the cost of the technology and the aesthetic point of view should always be found.

7.1 Summary

The first part of the thesis investigates the thermal performance of some glazing products. The optical and thermal characterization of the glazing samples is useful, in order to quantify the angular dependence of the transmitted and reflected energy. This was possible, thanks to the experimental set up available in the Solar Energy and Building Physics Laboratory at EPFL in Lausanne. Insulated glass units were analysed as the most common solution, currently. This glazing can reduce the overheating of the building. It is equipped with a low-e coating, that allow to reach low values of total energy transmittance (35%-38% at normal incidence angle) and higher values of the visible transmittance (around 60%-68% at normal incidence angle). Then, the potential application of the installation of the dye sensitized modules has been studied. The latter technology allows to obtained an integrated photovoltaic façade, providing a part of the electricity demand of the building. The aesthetic advantage is that dye-sensitized photovoltaic modules grant the architectural integration, thanks to their semi-transparency. From the measurements, a quite low visible transmittance (around 5%-6% for the opaque modules and 15%-23% for the transparent modules at normal incidence angle) indicates that these PV modules cannot be used for the whole façade. This is due to the fact that the PV modules should have a dominant part of absorbance, in order to not lose too much efficiency. For the analysed modules, the absorbance is around 60% for the transparent and 70% for the opaque. However, it is possible to combine these modules with standard double glazing, in order to have a clear vision towards outside. At the same time, in this way, the role of the façade becomes active, providing a part of the energy demand.

The second part of this work examines a particular type of Complex Fenestration System, not yet available in the market: embedded microstructures for glazing envelopes. The thermal performance of this glazing envelope has been investigated, in comparison with conventional glazing, such as a double standard glass and a sun protective glass. A proper ray tracing program, developed in research group of LESO, has been used to carry out thermal simulations. In general, results show that the novel CFS allows to reach a smart management of the thermal loads, all over the year. This is due to the geometric configuration of the micro-mirrors that can be suitably designed. The aim was to let the sun rays pass through the glass during winter time and to avoid them in summer, in order to reduce the risk of overheating. This design of the microstructured glass strictly depends on the location, the climatic conditions and on the geometric and thermal properties of the building. From the first parametric study, two possible geometric configurations of the embedded microstructures have been obtained. The first one adapted to Lausanne and the second one adapted to Athens. In Lausanne energy savings are significant, equalling 17%. It has been noticed that, with the optimized microstructured glass in Lausanne, energy savings in all the considered locations are achieved, even if they slightly decrease, as the latitude rises. The maximum of the saved energy is in Turin (45°N) and for southern locations, from Athens to Marseille, relative energy savings are between 6% and 14%, when compared with a sun protective glass. An optimization of the micro-mirrors geometry where the range of latitude is higher than 48°N is not able to significantly improve the energy savings. The reason is that the sky is mainly overcast during the year and temperatures are low. Consequently the annual cooling loads is not significant. The heating demand is not importantly reduced varying the embedded microstructures geometric configuration. However, a reduction of annual energy consumption is still reached (around 5%) with the optimized microstructured glass in Lausanne. The only exceptions are Glasgow and Bergen, where the irradiance is mainly diffuse all over the year.

However, concerning the southern locations, an improvement of the geometric configuration of microstructures can be obtained.

Higher energy savings can potentially be reached in southern locations, designing a suitable microstructured glass. The transmittance of the sun protective glass was properly adapted to a low range of latitude, in order to minimize thermal loads. The optimization of the micro-mirrors geometry, considering Athens as reference location, leads to a significant reduction in energy consumption. This new proposed geometric configuration is characterized by non-parabolic micro-mirrors and large vertical reflectors that allow to reflect outside most of the solar gains. The solar energy transmittance of the microstructured glass optimized in Athens comprises a blocking angle larger than the suitable microstructured glazing for Lausanne. Above an incidence angle of 50°, the transmitted energy through the new glazing envelope is below 3%. Energy savings in the building amount to 23% in the Greek location, if the sun protective glazing is replaced with the microstructured glass. Furthermore, this new design for the microstructured glass can potentially be suitable for a larger range of latitudes, in a perspective of climate change in the future years.

Finally, a discussion on the variation of the HVAC system efficiency was performed. A parametric study was carried out in Lausanne with the microstructured glass, varying the COP values for heating and cooling. Results confirmed that changing the value of COP of the reversible heat pump, thermal loads can significantly decrease. Increasing the COPs of the heat pump, thermal loads are significantly reduced. When both the COPs are equal to 1, thermal loads amount to 19,4 kWh/m^2. If the COPs for heating and cooling become equal to 4, the annual loads are reduced of 75%. Therefore, the choice of a reasonably efficient HVAC system is necessary, in order to diminish the annual energy consumption. In any case, energy savings are still relevant. Considering COPs values of 3 for heating and 3,5 for cooling, energy savings in Lausanne, in comparison with the sun protective glass, are equal to 16%.

The advantage of the microstructured glass has been confirmed studying the future scenario of the climate, in a perspective of global warming. Despite the predicted increase of temperature and global horizontal irradiance, the embedded microstructures turn out to be the best solutions in terms of energy consumption, in comparison with the conventional glazing. The saved energy is expected to slightly decrease in the future, especially in southern locations. However at high latitudes energy savings will slightly increase. The optimization of the microstructured glass in Athens can be a valid in a perspective of a future climate change.

The second parametric study is focused on influence of the geometric characteristic and of the thermal properties of the building. Three building configurations were assessed: the well-insulated, the moderately insulated and the non-insulated. Firstly, the variation of the performance of the microstructured glass varying the U-value of the window was performed both in Athens and in Lausanne. Considering that in Lausanne all the buildings are provided with a layer of insulation in the external wall, embedded microstructures perform better when the U-value is low (a reasonable range can be from 0,5 W/m^2K to 0,7 W/m^2K). In southern locations the insulation in the building is not so spread. However, the microstructured glass is advantageous for all the building configurations. However, in order to reach the highest energy savings using the embedded microstructures, it is necessary that the building is provided by insulation, even at low latitudes. In this way, the microstructured glass can reach around 10-20 kWh/m^2 of annual thermal loads, depending on the U-value and on the thickness of the insulated layer. Concerning the glazed area of the building, it is clear from simulations that in general, thermal loads significantly rise up, as the WWR increases. However, in case of high glazed building, the microstructured glass brings to important energy savings. In Lausanne they amount to 20% in comparison with the sun protective glass and almost 50% when compared with the standard glass, if the WWR is higher than 50%.

The purpose of embedded microstructures is to reach the best compromise between a good level of daylighting, glare protection, clear view and seasonal thermal control. In this study, the optimization of the novel CFS has been performed focusing on the thermal performance. The resulting energy consumption is significantly reduced. Consequently embedded microstructures could be a valid solution as glazing envelope that should be considered.

In conclusion, glazing envelopes with a seasonal dependence of the transmittance significantly contribute to a smart energy management, in particular when the heating and cooling loads can be balanced. The angular dependence of

the total transmitted energy induces the thermal control in the building. In general, overheating in summer can be reduced and during winter the heating consumption is maintained low by exploiting solar gains. Moreover, depending on the location and on the latitude, a suitable design of the microstructured glass can be realized, in order to minimize the energy consumption all over the year.

7.2 Future developments

Further research is required to improve some of the analysed novel glazing technologies. Especially concerning the application of the dye sensitized modules, they are at the start of their development. This kind of modules have not a high efficiency, compared with the efficiency of a silicon photovoltaic module. Another drawback is the lifetime of the modules, because of the early degradation of the dye. However, there are some commercial providers that are promising availability of the DSC modules in the near future. The analysed modules are already an example of production.

Regarding the embedded microstructures, this glazing technology has not yet penetrated the market and the field of work is research. The challenge now is to pass from the small scale production to the big scale, in order to obtain modules of the size of a normal window. In order to achieve this goal, fabrication techniques have to be improved [*Kostro, 2014*]. The cost for the production should be not to high, in comparison with other glazing envelope. The potential of this CFS is high, since it can significantly reduce energy consumption in the building (not only cooling and heating loads, but also electric lighting loads, better exploiting the daylight). However, it has to be considered that, concerning the designed embedded micro-mirrors for southern locations (optimization in Athens), the clear view through the glazing is not completely guaranteed. As future work, an improvement of this new proposed design should be performed, in order to assure the transparency through the glazed façade. This can be achieved by the use of selective coatings.

References

[*Andersen, 2011*] Andersen D., 2011 “Practical and policy relevant performance metrics for Complex Fenestration Systems”, ASHRAE.

[*Born et al., 1999*] Born M., Wolf E., 1999 “Principles of optics”, Cambridge University Press, 7edition.

[*Bouvard, 2015*] Bouvard O., Vanzo S., Schüler A., 2015 “Experimental determination of optical and thermal properties of semi-transparent photovoltaic modules based on dye-sensitized solar cells”, 6th International Building Physics Conference, Energy Procedia.

[*BPIE ,2011*] Atanasiu B., Despret C., Economidou M., Maio J., Nolte I., Rapf O., October 2011 “Europe’s buildings under the microscope – A country by country review of the energy performance of buildings”, Building Performance Institute Europe.

[*DATEC, 2011*] Dipartimento federale dell’ambiente, dei trasporti, dell’energia e delle comunicazioni DATEC, Ufficio federale dell’energia, Divisione Economica Energetica, june 2011 “Evoluzione dei prezzi dell’energia elettrica in Svizzera”, Rapporto del Consiglio Federale in adempimento del postulato 08.3208 Stähelin del 4 giugno 2008.

[*Edmonds, 1993*] Edmonds I. R., 1993 “Performance of laser cut light deflecting panels in daylighting applications” Solar energy materials and solar cells, vol. 29 pp. 1-26.

[*EN ISO 6946, 2008*] European Standard EN ISO 6946, 2008 “Componenti ed elementi per edilizia – Resistenza termica e trasmittanza termica – Metodo di calcolo”.

[*EnerGuide, 2004*] EnerGuide, 2004 “Heating and cooling with a heat pump” Natural Resources Canada’s office of Energy Efficiency.

[*Glass dBase*] http://glassdbase.unibas.ch.

[*Grätzel M., 2003*] Grätzel M. (2003) “Dye sensitized solar cells”, Journal of photochemistry and photobiology.

[*Grynning, 2011*] Grynning S., Time B., Uvsløkk S., 2011 “An overview and some reflections on energy saving potentials by heat loss reduction through the building envelope”. Project report to be published within the Research Centre on Zero Emission Buildings.

[*Gueymar et al., 2002*] Gueymar C.A., Myersand K. Eme D., December 2002 “Proposed reference irradiance spectra for solar energy systems testing” National Renewable Energy Laboratory, Golden, CO, USA.

[*Hassel, 2010*] Hegon P. Hassel, 2010 “Planck’s Radiation Law”, University Rostock, Germany.

[*IEA, 2013*] International Energy Agency, (2013) “Technology Roadmap – Energy efficient building envelopes” www.iea.org.

[*IPCC, 2000*] Intergovernmental Panel on Climate Change, 2000 “IPCC Special Report – Emissions scenarios”, Summary for Policymakers, Special Report of Working Group III.

[*ISO 10456, 2007*] European Standard ISO/10456, 2007 “Building materials and products – Hygrothermal properties – Tabulated designed values and procedures for determining declared and determined designed thermal values” pp. 9-12.

[*Kemmler et al, 2013*] Kemmler A., Piégsa A., Ley A., Wüthrich P., Keller M., Jakob M., Catenazzi G., September 2013 “Analyse des schweizerischen Energieverbrauchs 2000 – 2013 nach Verwendungszwecken”, Federal Department of Environment, Transport, Energy and Communications, Swiss Federal Office of Energy (BFE).

[*Klammt et al., 2012*] Klammt S., Müller H., Neyer A., 2012 “Microoptics for efficient redirection of sunlight”, Green Building R&D.

[*Kostro, 2014*] Kostro A., 2014 “Microstructured glazing for daylighting, glare protection, seasonal thermal control and clear view”, thesis n-1234, Solar Energy and Building Physics Laboratory, EPFL.

[*Kostro et al., 2011*] Kostro A., Scartezzini J.L., Schüler A., 2011 “Towards microstructured glazing for daylighting and thermal control” Solar Energy and Building Physics Laboratory (CISBAT 2011-EPFL).

[*Kostro et al., 2012*] Kostro A., Jeiger M., Jolissant N., Gonzalez Lazo M., Scartezzini J.L., Letterier Y., Schüler A., 2012 “Embedded microstructures for daylighting and seasonal thermal control” Solar Energy and Building Physics Laboratory (CISBAT 2012-EPFL).

[*Kostro et al., 2014*] Kostro A., Scartezzini J.L., Schüler A., 2014 “Radiance rendering and thermal modelling for the design of complex fenestration systems with optimized performances”, Status-Seminar, ETH Zurich; 18.

[*Le Treut, 2003*] Le Treut H., May 2003 “Les scénarios globaux de changement climatique et leurs incertitudes”, Geoscience 335, pp. 525-533.

[*Meteonorm, 2014*] Meteonorm Software version 7.1.2 2014, Meteotest, Berne (Switzerland).

[*Nazeeruddin, 2011*] Nazeeruddin Md.K., Baranoff E., Grätzel M., 2011 “”, Solar Energy vol.85 pp. 1172-1178.

[*NREL, 2014*] U.S. Department of Energy, NREL “National Renewable Energy Laboratory”.

[*paperblog.com, 2013*] http://en.paperblog.com/swisstech-convention-center-features-multicolored-solar-panel-facade-711293/.

[*Parisil M. L., 2014*] Parisi M. L., Maranghi S., Basosi R. (2014) “The evolution of the dye sensitized solar cells from Grätzel prototype to up-scaled solar applications: a life cycle assessment approach”, Renewable and sustainable Energy Reviews.

[*Perez et al., 1993*] Perez R., Seals R., Michalsky J., 1993 “All-weather model for sky luminance distribution-preliminary configuration and validation”, Solar Energy vol.50 pp. 235-245.

[*Ruck, 2000*] Ruck N., Aschehoug O., Aydinli S., Christoffersen J., Courret G., Edmonds I., Jakobiak R., Kischkoweit-Lopin M., Klinger M., Lee E., Michel L., Scartezzini J.L., Selkowitz S., 2000 “Daylight in buildings – a source book on daylighting systems and components”, IEA SHC Task 21, ECBCS Annex 29.

[*Scartezzini et al., 2002*] Scartezzini J.L., Courret G., 2002 “Anidolic daylighting systems” Solar Energy, vol. 73 pp. 123-135.

[*SINTEF, 2007*] Gustavsen A., Jelle B.P., Arasteh D., Kohler C., 2007 “State of the art highly insulated windows frame-Research and market review”, Project report 6, SINTEF Building and Infrastructure, Norwegian University of Science and Technology.

[*Steiner et al., 2005*] Steiner R., Oelhafen P., Reber G., Romanyuk A., 2005 “Angular dependent solar gain for insulating glasses from experimental optical and thermal data” pp. 173-178, “Experimental determination of spectral and angular dependent optical properties of insulating glasses” pp. 441-446, Institute of Physics, University of Basel (CISBAT 2005-EPFL).

[*Thanachareonkit, 2008*] Thanachareonkit A., 2008 “Comparing physical and virtual methods for daylight performance modelling including complex fenestration systems”, thesis n-4130, Solar Energy and Building Physics Laboratory, EPFL.

[*UNI EN 15242, 2006*] European Standard EN 15242, 2006 “Calculation methods for the determination of air flow rates in buildings including infiltration”.

[*UNI 7357/74*] UNI 7357/74, rispondenza con Legge 10/91 e DPR 412/93 “Calcolo del fabbisogno di Potenza termica dell’edificio per riscaldamento invernale”.

[*Urchueguìa, 2008*] Urchueguìa J.F., Zacarés M., Corberàn J.M., Montero A., Martos J., Witte H., October 2008 “Comparison between the energy performance of a ground coupled water to water heat pump system and a air to water heat pump system for heating and cooling In typical conditions of the European Mediterranean coast”, Energy Conversion and Management, vol.49, issue 10, pp. 2917-2923.

[*Van Den Bergh at al., 2013*] Van Den Bergh S., Hart R., Jelle B. P., Gustavsen A. (2013) “Windows spacers and edge seals in insulating glass units: a state of the art review and future perspectives”, Energy and Buildings.

[*Wolf, 1992*] Wolf, A.T. (1992) “Studies into the life expectancy of insulating glass units”, Building and Environment.

[*Zervos, 2013*] Zervos H. (2013) “Dye Sensitized Solar Cells (DSSC/DSC) 2013-2023: Technologies, Markets, Players”, IDTechEx.